# Orbitally Induced Peierls Mechanism for Charge-Orbital Orderings in Transition-Metal Compounds

**Takashi Mizokawa**
**Department of Applied Physics, Waseda University**

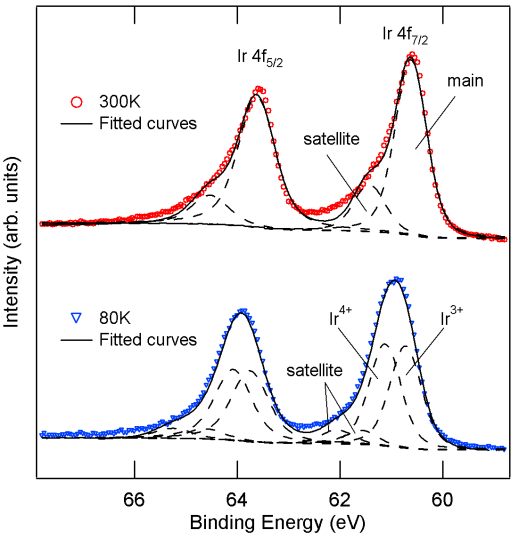


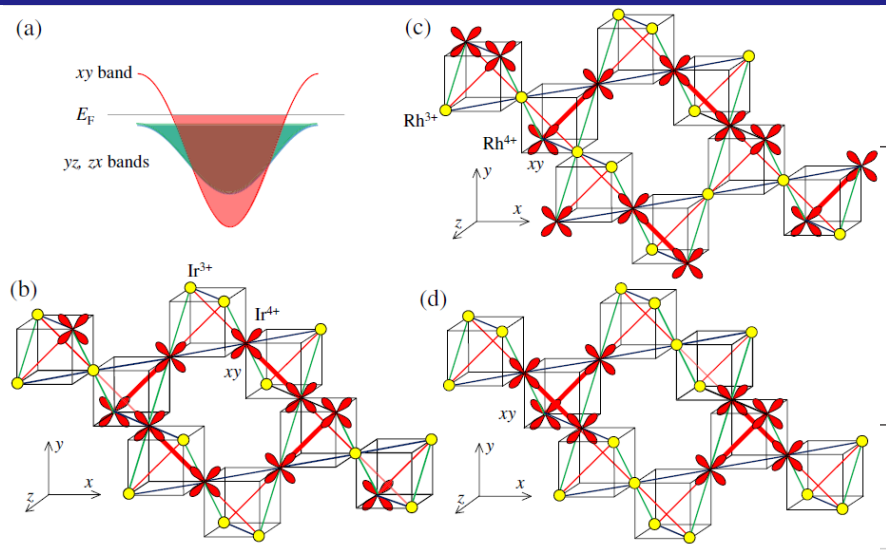

graduated from Prof. Fujimori's group in Tokyo, photoemission experiment

Interplay between orbital ordering and lattice distortions in $LaMnO_3$, $YVO_3$, and $YTiO_3$
T. Mizokawa, D. I. Khomskii, and G. A. Sawatzky, Phys. Rev. B 60, 7309 (1999)

Spin and charge ordering in self-doped Mott insulators
T. Mizokawa, D. I. Khomskii, and G. A. Sawatzky, Phys. Rev. B 61, 11263 (2000)

→ Orbitally Induced Peierls State in Spinels
D. I. Khomskii and T. Mizokawa, Phys. Rev. Lett. 94, 156402 (2005)

$VO_2PO_4$ XAS + HAXPES
Phys. Rev. B 101, 235159 (2020); Phys. Rev. B 101, 245106 (2020)

$Ba_3CuSb_2O_9$ HAXPES + Tr-REXS
Phys. Rev. Materials 5, 075002 (2021); Phys. Rev. B 104, 205110 (2021)

educated by Prof. Khomskii and Prof. Sawatzky
→ very aggressive, a tough reviewer

Regarding peer review, Mizokawa says,
"*npj Quantum Materials* is one of the most exciting journals in my research field. I always enjoy serving it as a reviewer."

https://www.nature.com/npjquantmats/for-authors-and-referees/reviewer-of-the-year

# Outline

1. Electron-phonon interaction and Peierls transition
   (not in the text, for undergraduate)

2. Orbitally induced Peierls transition: Case study on $CuIr_2S_4$ (section 2.1)

3. Toy models on square/triangular lattice (sections 2.2 and 2.3)

4. Application to Spinel and Pyrochlore materials (sections 3.1 and 3.2)

5. Application to triangular/honeycomb/kagome lattice systems (3.3/3.4/3.5)

6. Summary

# Electron-phonon interaction

Periodic potential $V(\vec{r}_i) = \sum_j v(\vec{r}_i - \vec{R}_j^0)$

Lattice vibration $\vec{R}_j = \vec{R}_j^0 + \vec{Q}_j$ $\vec{Q}_j$: displacement of the $j$-th ion

$$V(\vec{r}_i) = \sum_j v(\vec{r}_i - \vec{R}_j) = \sum_j \left[ v(\vec{r}_i - \vec{R}_j^0) - \vec{Q}_j \cdot \nabla v(\vec{r})|_{\vec{r}=\vec{r}_i - \vec{R}_j^0} + \cdots \right]$$

The displacement of the $j$-th ion can be expressed by phonons.

$$\sum_j \vec{Q}_j e^{-i\vec{q}\cdot\vec{R}_j^0} = \sqrt{N}\,\vec{Q}_{\vec{q}} = \sqrt{N} Q_{\vec{q}} \vec{e}_{\vec{q}} = \sqrt{\frac{N\hbar}{2m\omega_{\vec{q}}}} (a_{\vec{q}} + a_{-\vec{q}}^+) \vec{e}_{\vec{q}}$$

$$a_{\vec{q}} = \sqrt{\frac{m\omega_{\vec{q}}}{2\hbar}} \left( q_{\vec{q}} + \frac{i}{m\omega_{\vec{q}}} p_{-\vec{q}} \right) \qquad a_{\vec{q}}^+ = \sqrt{\frac{m\omega_{\vec{q}}}{2\hbar}} \left( q_{-\vec{q}} - \frac{i}{m\omega_{\vec{q}}} p_{\vec{q}} \right)$$

$$Q_{\vec{q}} = \frac{1}{\sqrt{N}} \sum_j Q_j e^{-i\vec{q}\cdot\vec{R}_j^0}$$

G. D. Mahan, Many particle physics

# Electron-phonon interaction

$$V(\vec{r}_i) = \sum_j v(\vec{r}_i - \vec{R}_j) = \sum_j \left[ v(\vec{r}_i - \vec{R}_j^0) - \vec{Q}_j \cdot \nabla v(\vec{r})|_{\vec{r}=\vec{r}_i-\vec{R}_j^0} + \cdots \right]$$

periodic potential

displacement of the $j$-th ion

$j$-th ion: $\vec{R}_j = \vec{R}_j^0 + \vec{Q}_j$

$$\nabla v(\vec{r})|_{\vec{r}=\vec{r}_i-\vec{R}_j^0} e^{i\vec{q}\cdot\vec{R}_j^0} = \frac{1}{\sqrt{N}} \sum_{\vec{q}} i\vec{q} v_{\vec{q}} e^{i\vec{q}\cdot\vec{r}_i} = \frac{1}{N\sqrt{N}} \sum_{\vec{k},\vec{q}} i\vec{q} v_{\vec{q}} \langle \vec{r}_i | c^+_{\vec{k}+\vec{q},\sigma} c_{\vec{k}\sigma} | \vec{r}_i \rangle$$

$$-\sum_j \vec{Q}_j e^{-i\vec{q}\cdot\vec{R}_j^0} \cdot \nabla v(\vec{r})|_{\vec{r}=\vec{r}_i-\vec{R}_j^0} e^{i\vec{q}\cdot\vec{R}_j^0} = -\frac{1}{N} \sum_{\vec{k},\vec{q}} i \sqrt{\frac{\hbar}{2m\omega_{\vec{q}}}} \vec{q} \cdot \vec{e}_{\vec{q}} v_{\vec{q}} \langle r_i | c^+_{\vec{k}+\vec{q},\sigma} c_{\vec{k}\sigma} (a_{\vec{q}} + a^+_{-\vec{q}}) | r_i \rangle$$

$v_q = (1/\varepsilon_\infty - 1/\varepsilon_0)\, 4\pi e^2/q^2$ : screened Coulomb interaction

$\omega_q = \omega_0$ : optical phonon

longitudinal $\vec{q} \cdot \vec{e}_{\vec{q}} = |q|$, transverse $\vec{q} \cdot \vec{e}_{\vec{q}} = 0$

Electron-phonon interaction term

$$H_{ep} = \frac{1}{N} \sum_{k,q} \frac{M}{|q|} c^+_{k+q,\sigma} c_{k,\sigma} (a_q + a^+_{-q}) = \frac{1}{N} \sum_{k,q} V_q c^+_{k+q,\sigma} c_{k,\sigma} (a_q + a^+_{-q})$$

G. D. Mahan, Many particle physics

# Peierls transition and superstructure

Peierls transition (2D/3D material with 1D Fermi surface)
Charge density wave is formed by the electron-phonon interaction.

Mean-field approximation

$$H_{ep} = \frac{1}{N}\sum_{k,q} V_q c^{+}_{k+q,\sigma} c_{k,\sigma} \langle a_q + a^{+}_{-q} \rangle$$

analogous to e × E Jahn-Teller effect

electron-lattice interaction

elastic energy

$$H = -Aq \begin{pmatrix} 1 & 0 \\ 0 & -1 \end{pmatrix} + \frac{1}{2} M\omega^2 q^2 \begin{pmatrix} 1 & 0 \\ 0 & 1 \end{pmatrix}$$

One dimensional Fermi surface:
perfect nesting with $Q = 2k_F$

$$\langle a_Q + a^{+}_{-Q} \rangle = q_Q \neq 0$$ ➡ superstructure

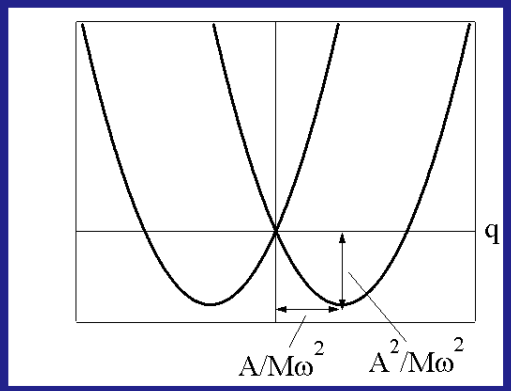


Mean-field Hamiltonian

$$H_e + H_{ep} = \sum_k \varepsilon_k c^{+}_{k,\sigma} c_{k,\sigma} + \sum_k V_Q c^{+}_{k+Q,\sigma} c_{k,\sigma} \langle a_Q + a^{+}_{-Q} \rangle$$

$$\rho_{Q,\uparrow} = \frac{1}{N}\sum_k \langle c^{+}_{k+Q,\uparrow} c_{k,\uparrow} \rangle \neq 0$$ ➡ charge density wave

# Peierls transition and metal-insulator transition

$(E-\varepsilon_k)(E-\varepsilon_{k+Q})+(V_Q q_Q)^2=0$ has two solutions $E=E_k^+, E_k^-$

$$\rho_{Q,\uparrow}=\frac{1}{N}\sum_k\langle c_{k+Q,\uparrow}^+ c_{k,\uparrow}\rangle=\frac{1}{N}\sum_k\frac{1}{\beta}\sum_n\frac{V_Q q_Q}{(i\omega_n-\varepsilon_k)(i\omega_n-\varepsilon_{k+Q})-(V_Q q_Q)^2}$$

$$=\frac{1}{N}\sum_k\frac{1}{\beta}\sum_n\frac{V_Q q_Q}{(i\omega_n-E_k^+)(i\omega_n-E_k^-)}=\frac{1}{N}\sum_k\frac{V_Q q_Q}{E_k^+-E_k^-}\frac{1}{\beta}\sum_n\left(\frac{1}{i\omega_n-E_k^+}-\frac{1}{i\omega_n-E_k^-}\right)$$

$$=\frac{1}{v}\sum_k V_Q q_Q\frac{n(E_k^+)-n(E_k^-)}{E_k^+-E_k^-}$$

$$n(E)=\frac{1}{e^{\beta E}+1}$$

$$\omega_0 q_Q+4V_Q\rho_{Q,\uparrow}=0$$

Order parameter $\langle a_Q+a_{-Q}^+\rangle$

$$\rho_{Q,\uparrow}=\frac{1}{N}\sum_k\langle c_{k+Q,\uparrow}^+ c_{k,\uparrow}\rangle$$

Gap equation

$$1=-\frac{4{V_Q}^2}{\omega_0}\frac{1}{N}\sum_k\frac{n(E_k^+)-n(E_k^-)}{E_k^+-E_k^-}$$

$$1=\frac{4{V_Q}^2}{\omega_0}\int d\varepsilon g(\varepsilon)\frac{\tanh\left(\frac{\beta\sqrt{\varepsilon^2+\Delta^2}}{2}\right)}{2\sqrt{\varepsilon^2+\Delta^2}}$$

density of states

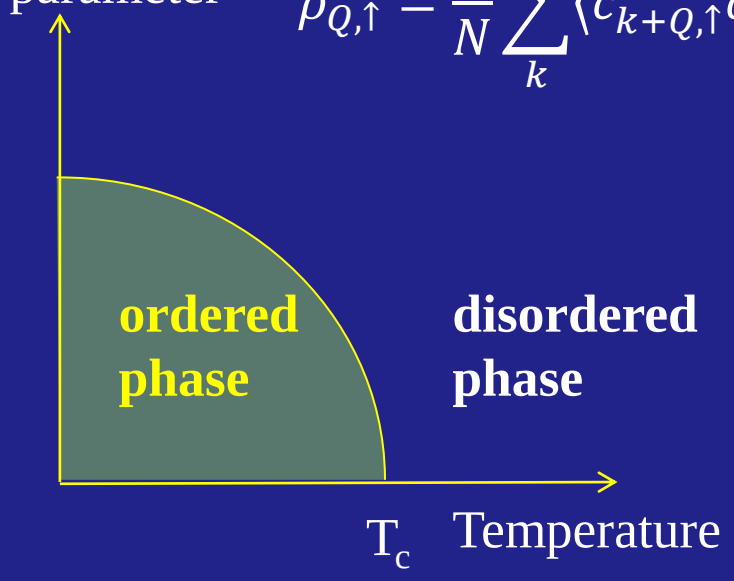

# Fermi surface nesting and Peierls transition

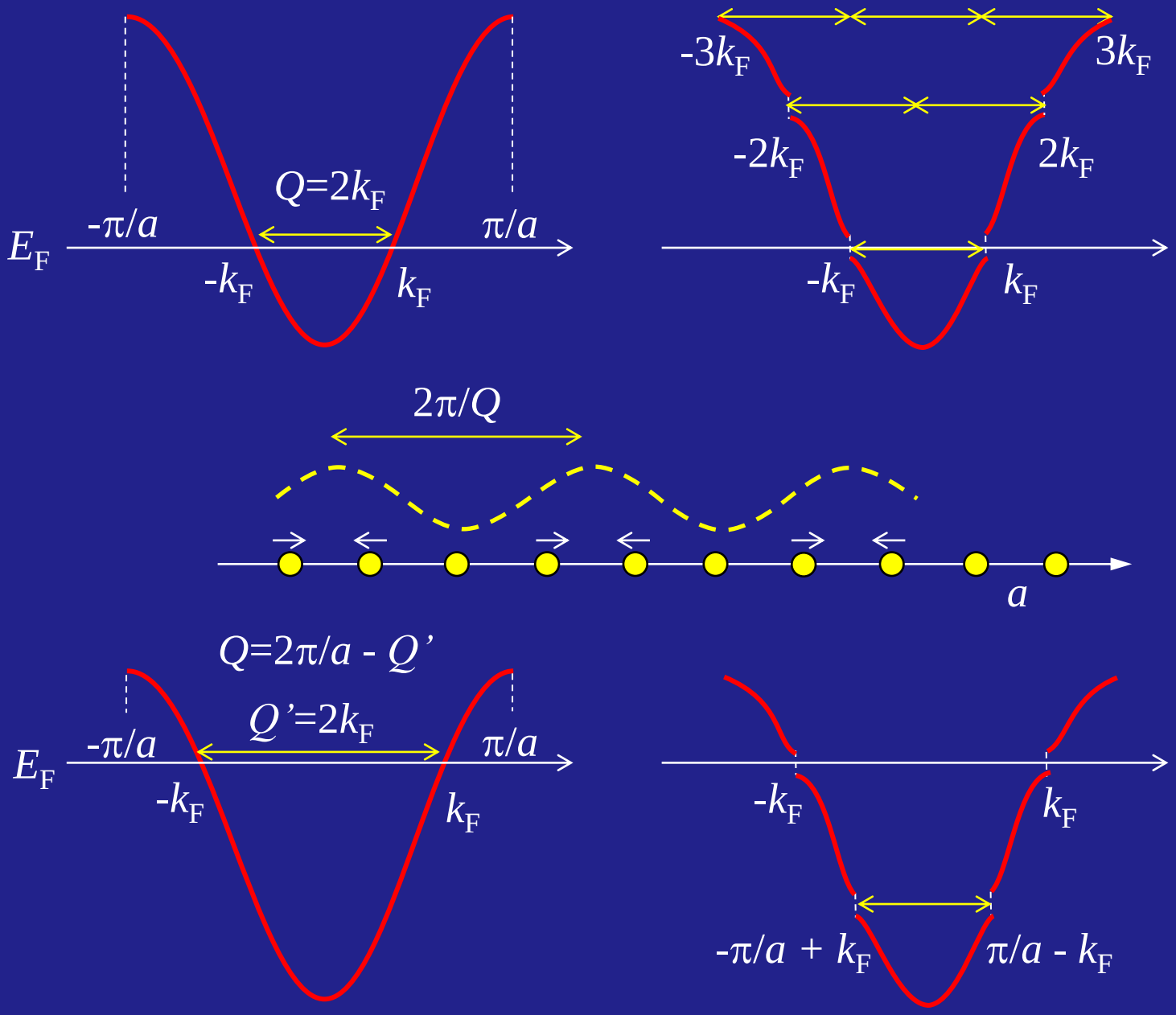

# Half-filled band

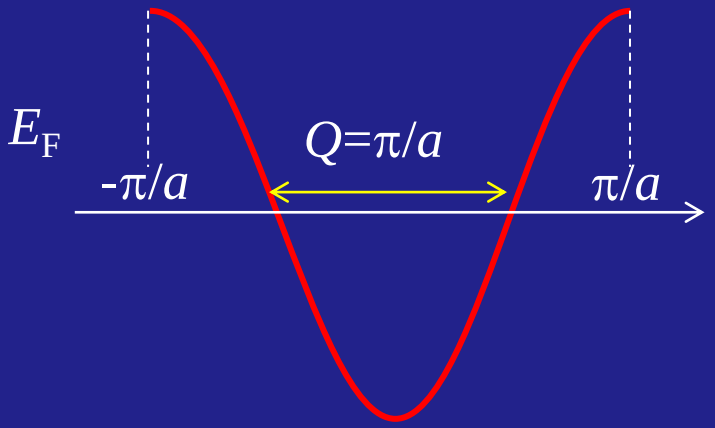


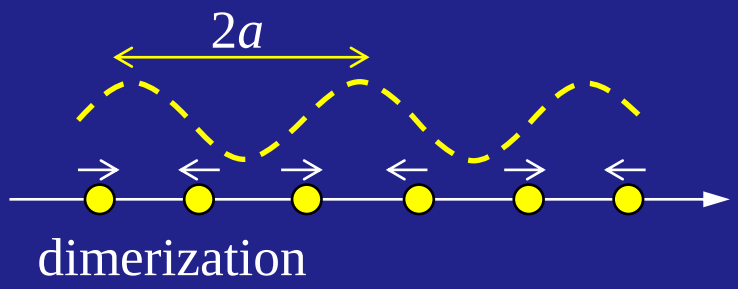


no charge ordering

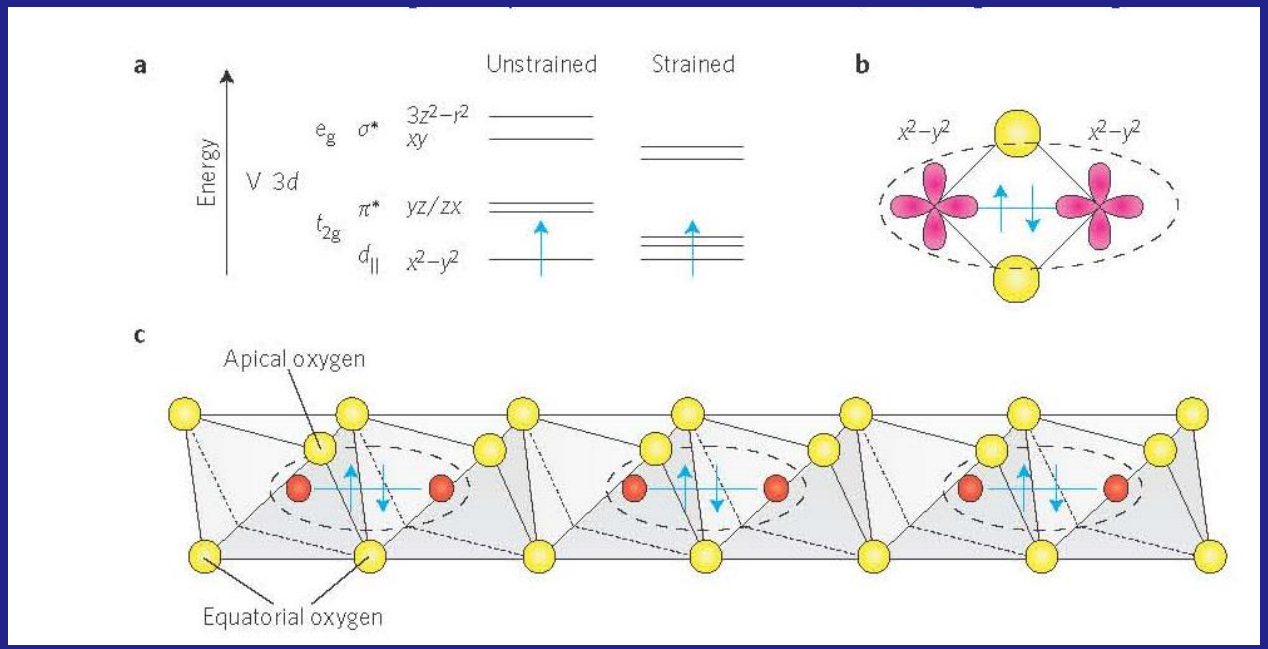


Nature Phys. **9**, 612 (2013)

# Quarter filled band

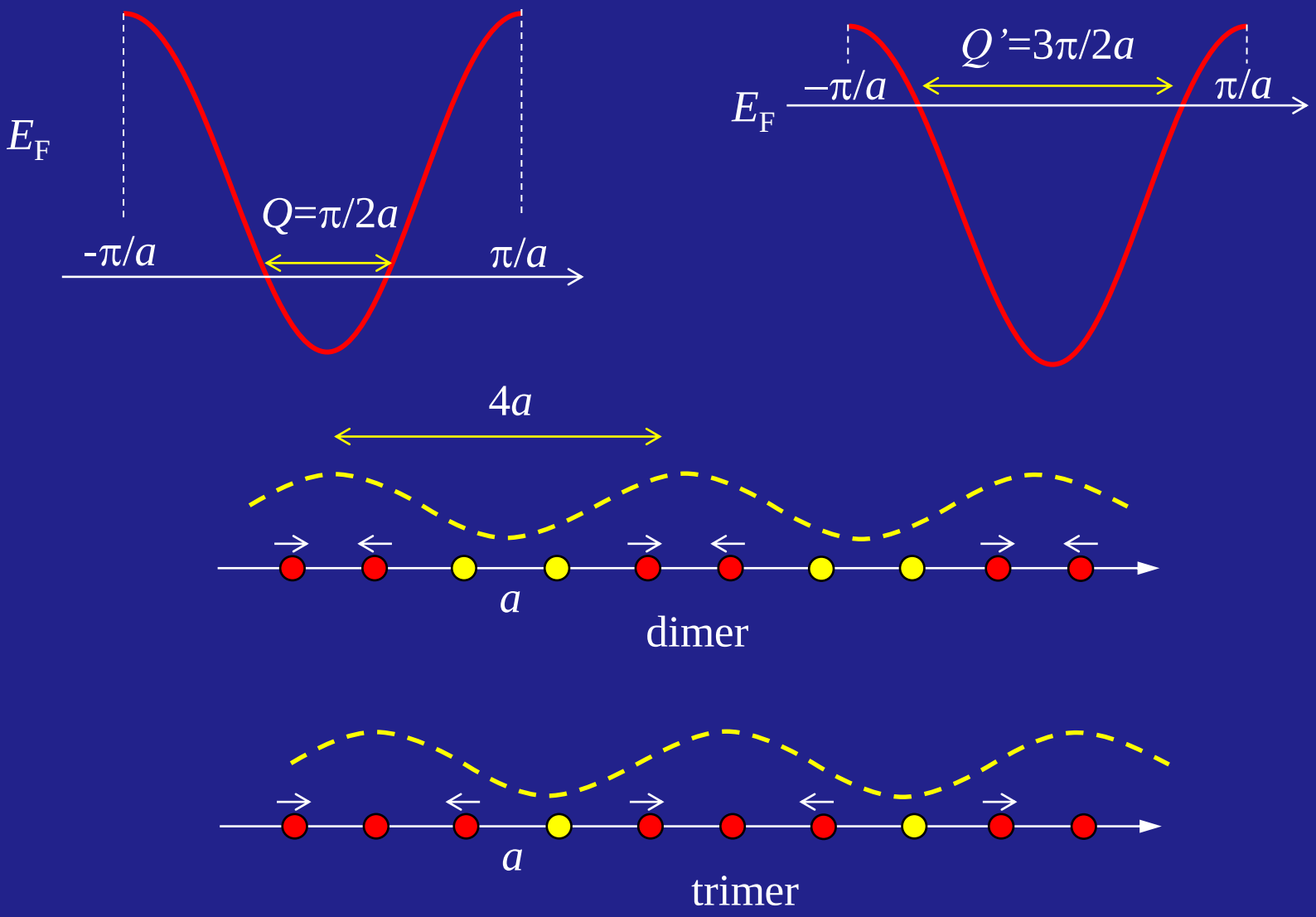

# Strong electron-phonon interaction

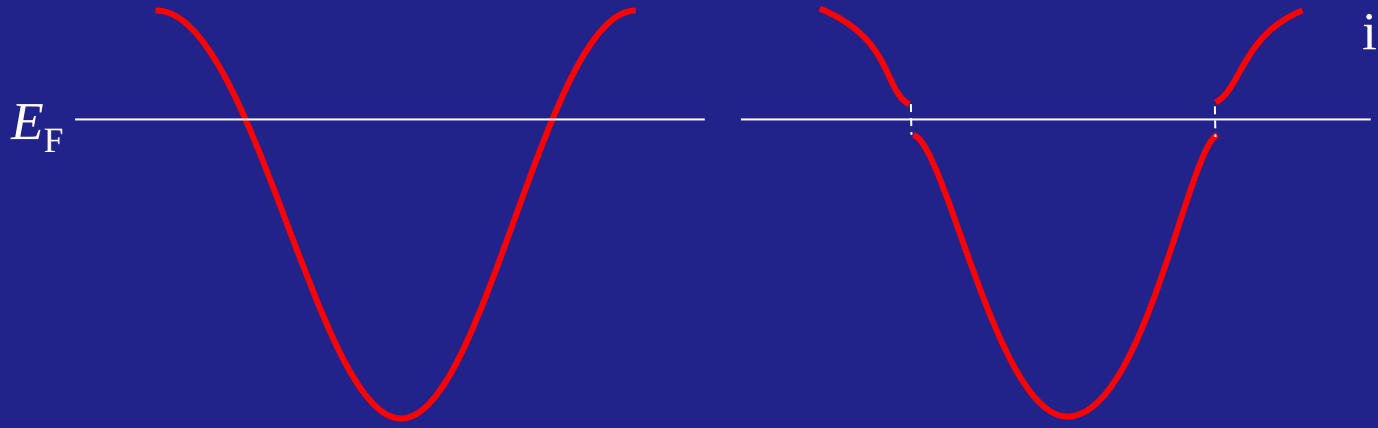


interaction gap

$$\frac{4V_Q{}^2}{\omega_0} \gg E_G$$

**weak coupling**

charge density wave

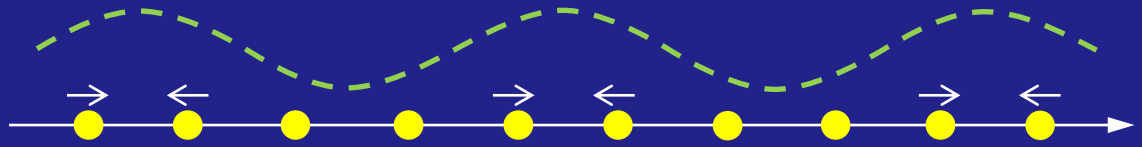

$$\frac{4V_Q{}^2}{\omega_0} \sim E_G$$

**strong coupling**

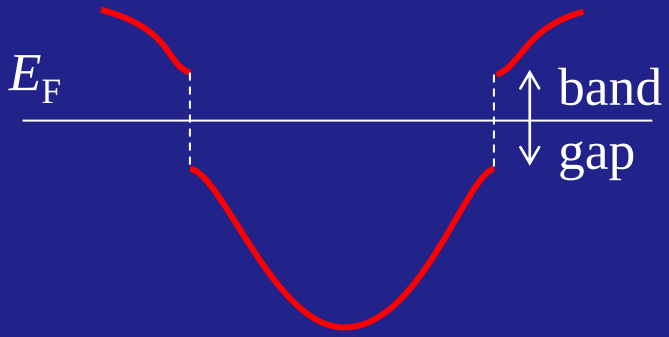


charge order

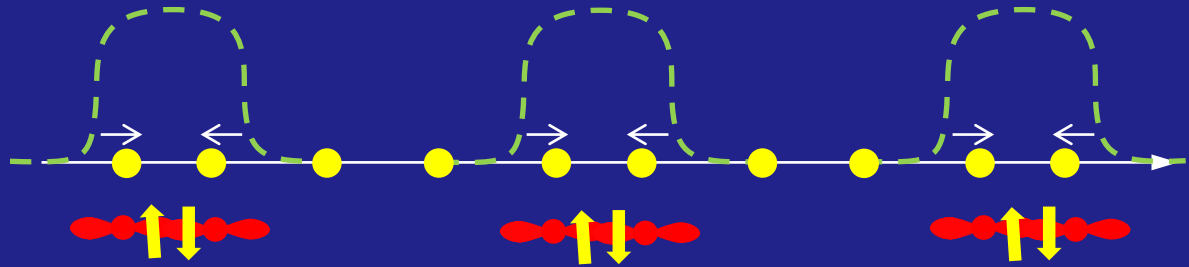

dimer
(singlet bond)

# Outline

1. Electron-phonon interaction and Peierls transition
   (not in the text, for undergraduate)

2. Orbitally induced Peierls transition: Case study on $CuIr_2S_4$ (section 2.1)

3. Toy models on square/triangular lattice (sections 2.2 and 2.3)

4. Application to Spinel and Pyrochlore materials (sections 3.1 and 3.2)

5. Application to triangular/honeycomb/kagome lattice systems (3.3/3.4/3.5)

6. Summary

# Transition-metal oxides with edge-sharing octahedra

**Rutile(1D)**

$VO_2$: $V^{4+}$ $d^1$ $T_{MI}$=340 K M-NMI

**Hollandite(1D)**

$K_2V_8O_{16}$: $V^{4+}$,$V^{3+}$ $d^1$,$d^2$ $T_{MI}$=210 K M-NMI

$K_2Cr_8O_{16}$: $Cr^{4+}$,$Cr^{3+}$ $d^2$,$d^3$ $T_{MI}$=95 K FM-FMI

**triangular lattice (2D)**

$NaTiO_2$ $Ti^{3+}$ $d^1$ $T_{NM}$ = 260 K I-NMI

$LiVO_2$ $V^{3+}$ $d^2$ $T_{NM}$ = 500 K I-NMI

$BaV_{10}O_{15}$ $V^{3+}$ ,$V^{2+}$ $d^2$,$d^3$ $T_{MI}$=130 K M-AFI

$Na_xCoO_2$ $Co^{4+}$,$Co^{3+}$ $d^5$,$d^6$

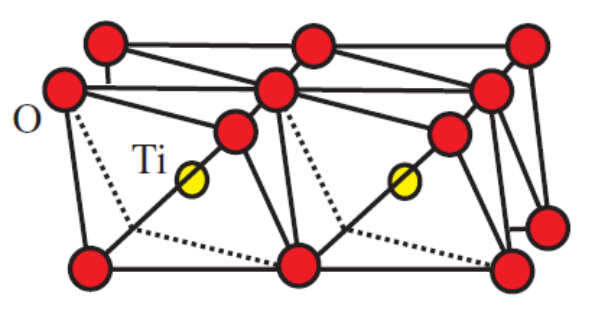


**honeycomb lattice (2D)**

$Li_2RuO_3$ $Ru^{4+}$ $d^4$ $T_{MI}$ = 540 K M-NMI

$Na_2IrO_3$ $Ir^{4+}$ $d^5$

**Spinel (3D)**

$MgTi_2O_4$ $Ti^{3+}$ $d^1$ $T_{MI}$ = 260 K M-NMI

$ZnV_2O_4$ $V^{3+}$ $d^2$

$AlV_2O_4$ $V^{3+}$, $V^{2+}$ $d^2$,$d^3$

$LiRh_2O_4$ $Rh^{4+}$,$Rh^{3+}$ $d^5$,$d^6$ $T_{MI}$=170 K M-NMI

M: (paramagnetic) metal
AFM: antiferromagnetic metal
NMI: nonmagnetic insulator
AFI: antiferromagnetic ins.

# Transition-metal chalcogenides/pnictides

**q-1D**

| | | | | |
|---|---|---|---|---|
| $(TaSe_4)_2I$ | $Ta^{5+}$, $Ta^{4+}$ | $d^0$, $d^1$ | $T_{MI}$=260 K | M-NMI |
| $BaVS_3$ | $V^{4+}$ | $d^1$ | $T_{MI}$=74 K, $T_N$=35 K | |
| $BaFe_2S_3$ | $Fe^{2+}$ | $d^6$ | $T_S$=200 K, $T_N$=120 K | |
| $Ta_2NiSe_5$ | $Ni^{0+}$, $Ta^{5+}$ | $d^{10}$ , $d^0$ | $T_S$=328 K | NMI-NMI |

**q-2D**

| | | | | |
|---|---|---|---|---|
| $TiSe_2$ | $Ti^{4+}$ | $d^0$ | $T_S$=200 K | M-M |
| $VSe_2$ | $V^{4+}$ | $d^1$ | $T_S$=110 K | M-M |
| $TaS_2$ | $Ta^{4+}$ | $d^1$ | $T_S$=200-350 K | M-M |
| $LiVS_2$ | $V^{3+}$ | $d^2$ | $T_{MI}$=305 K | M-NMI |
| $CrSe_2$ | $Cr^{4+}$ | $d^2$ | $T_{MI}$=165-180 K | M-AFI |
| $IrTe_2$ | $Ir^{4+}$ | $d^5$ | $T_S$=180-280 K | M-M |
| FeSe | $Fe^{2+}$ | $d^6$ | $T_S$=90 K | M-M |
| $BaFe_2As_2$ | $Fe^{2+}$ | $d^6$ | $T_S$=$T_N$=143 K | M-AFM |
| $BaNi_2As_2$ | $Ni^{2+}$ | $d^8$ | $T_S$=130 K | M-M |

**3D**

| | | | | |
|---|---|---|---|---|
| RuP | $Ru^{3+}$ | $d^5$ | $T_{MI}$=270 K | M-NMI |
| $CuIr_2S_4$ | $Ir^{4+}$, $Ir^{3+}$ | $d^5$, $d^6$ | $T_{MI}$=226 K | M-NMI |
| NiS | $Ni^{2+}$ | $d^8$ | $T_S$=$T_N$=200 K | M-AFM |

M: (paramagnetic) metal
AFM: antiferromagnetic metal
NMI: nonmagnetic insulator
AFI: antiferromagnetic ins.

**Many unsolved mysteries!**

# Without Fermi surface nesting

The phase transitions are always driven by Fermi surface instability?

Fermi surface nesting → Peierls transition

No Fermi surface nesting → ??

(1) Mott/Wigner localization + spin/orbital

(2) Excitonic instability →

(3) Orbital instability + Peierls

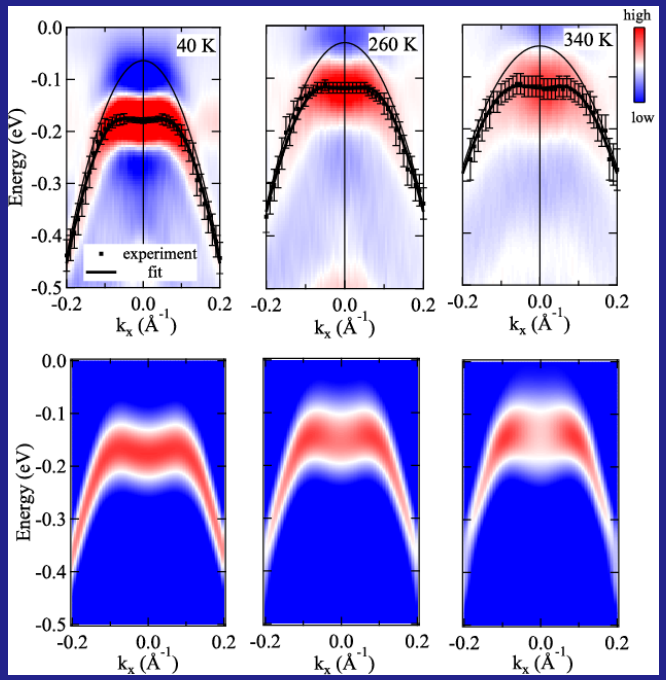


$Ta_2NiSe_5$ transition around 328 K

Y. Wakisaka *et al*., Phys. Rev. Lett. **103**, 026402 (2009).

K. Seki *et al*., Phys. Rev. B 90, 155116 (2014).

# Case study : spinel-type $CuIr_2S_4$

**$Ir^{3+}$ : $Ir^{4+}$ = 1:1**

**Charge frustration on a pyrochlore lattice ?**

S. Nagata *et al*, Physica B **194-196**, 1077 (1994).

**1st order metal-insulator transition at 226 K with tetragonal distortion (c > a)**

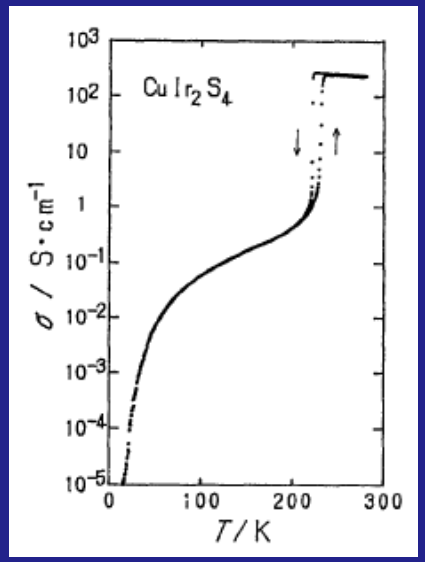


P. G. Radaelli *et al.*, Nature **416**, 155 (2002).

**triclinic distortion with octamer charge ordering**

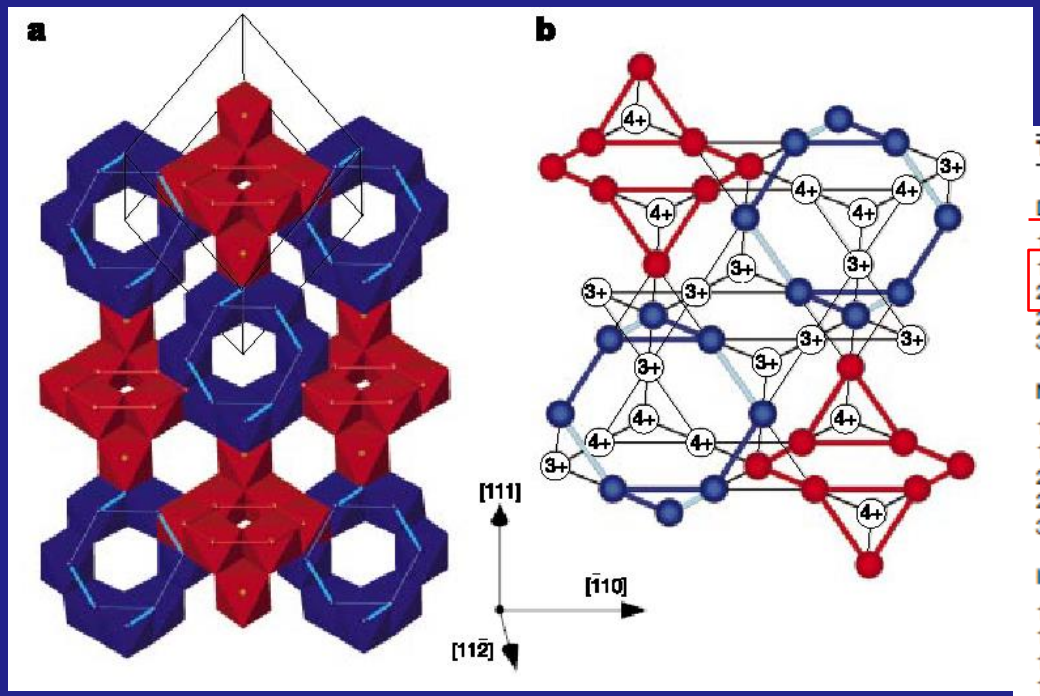


**$Ir^{4+}$ octamers (four dimers)**

$Ir^{4+}$

$Ir^{3+}$

**Table 1 Ir–Ir bond lengths of $CuIr_2S_4$ at 50 K**

Dimerized rings ($Ir^{4+}$)

| | |
|---|---|
| 1:3 | 3.464(7) |
| 1:4 | 3.012(5) |
| 2:3 | 2.956(5) |
| 2:4 | 3.582(7) |
| 3:4 | 3.490(8) |

**$Ir^{4+}$ $t_{2g}^5$**

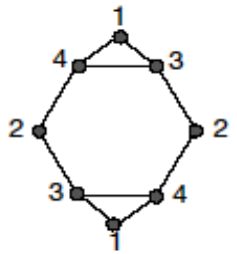


Non-dimerized rings ($Ir^{3+}$)

| | |
|---|---|
| 1:3 | 3.478(7) |
| 1:4 | 3.493(5) |
| 2:3 | 3.602(5) |
| 2:4 | 3.487(7) |
| 3:4 | 3.470(9) |

$Ir^{4+}$–$Ir^{3+}$ bonds across rings ($Ir^{4+}$:$Ir^{3+}$)

| | | | |
|---|---|---|---|
| 1:1 | 3.551(7) | 2:4 | 3.605(7) |
| 1:1 | 3.437(7) | 3:1 | 3.658(5) |
| 1:3 | 3.540(7) | 3:2 | 3.458(8) |
| 1:4 | 3.554(7) | 3:3 | 3.458(7) |
| 2:2 | 3.507(6) | 4:1 | 3.486(7) |
| 2:2 | 3.483(6) | 4:2 | 3.581(5) |
| 2:3 | 3.432(7) | 4:4 | 3.554(8) |

Data determined from Rietveld refinements of X-ray and neutron powder diffraction data. All bond lengths are given in Å.

# 1D $t_{2g}$ bands in the pyrochlore lattice?

Ir 5d $t_{2g}$ orbitals: triply degenerate *xy*, *zx*, and *yz*

d-d transfer

*xy* : 1D band along (1,1,0) and (1,-1,0)
*zx* : 1D band along (1,0,1) and (1,0,-1)
*yz* : 1D band along (0,1,1) and (0,1,-1)

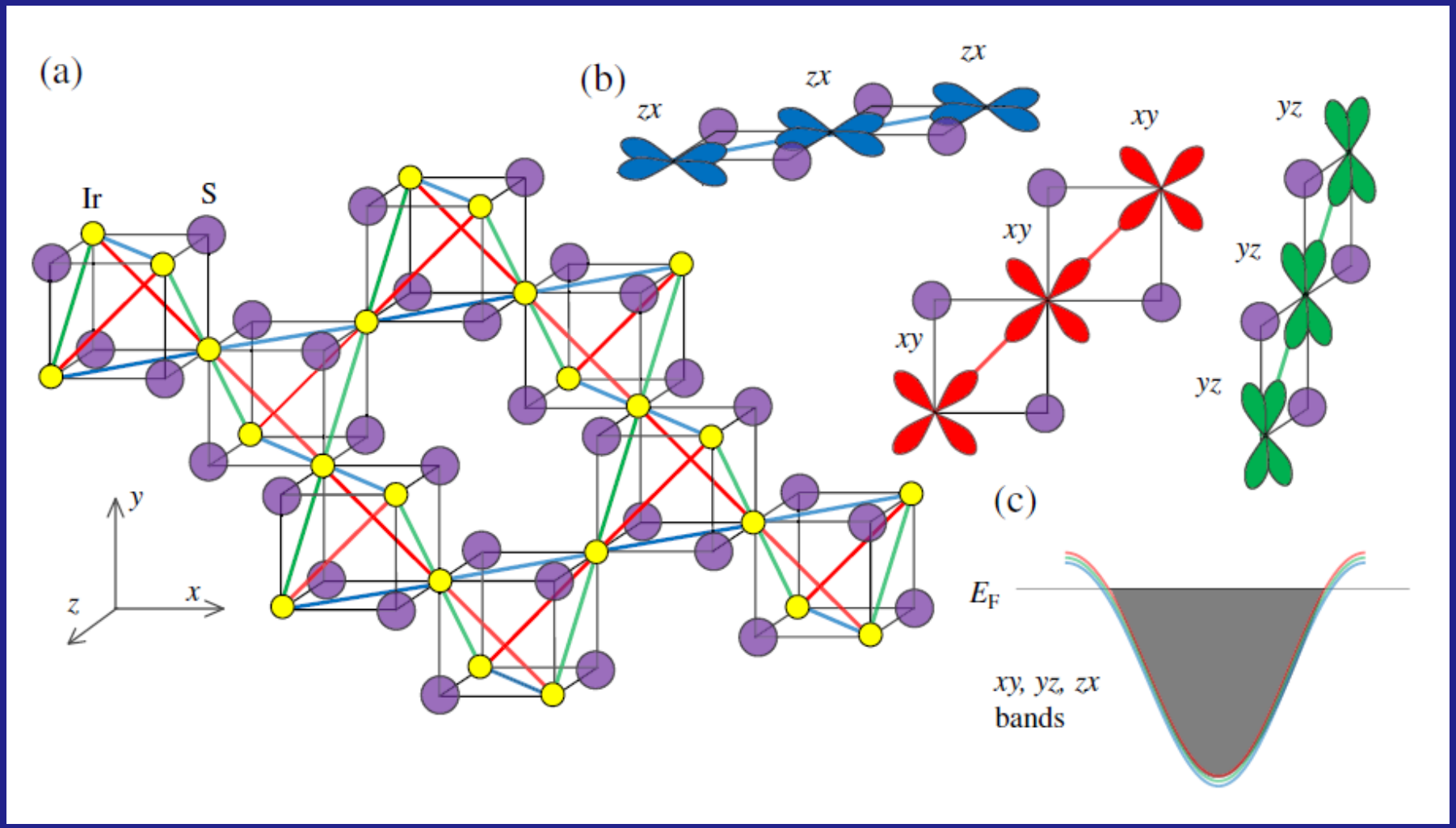

# d-d transfer *versus* d-p-d transfer

d-p-d transfer provides hybridization between the *xy* and *yz* and *zx* bands.

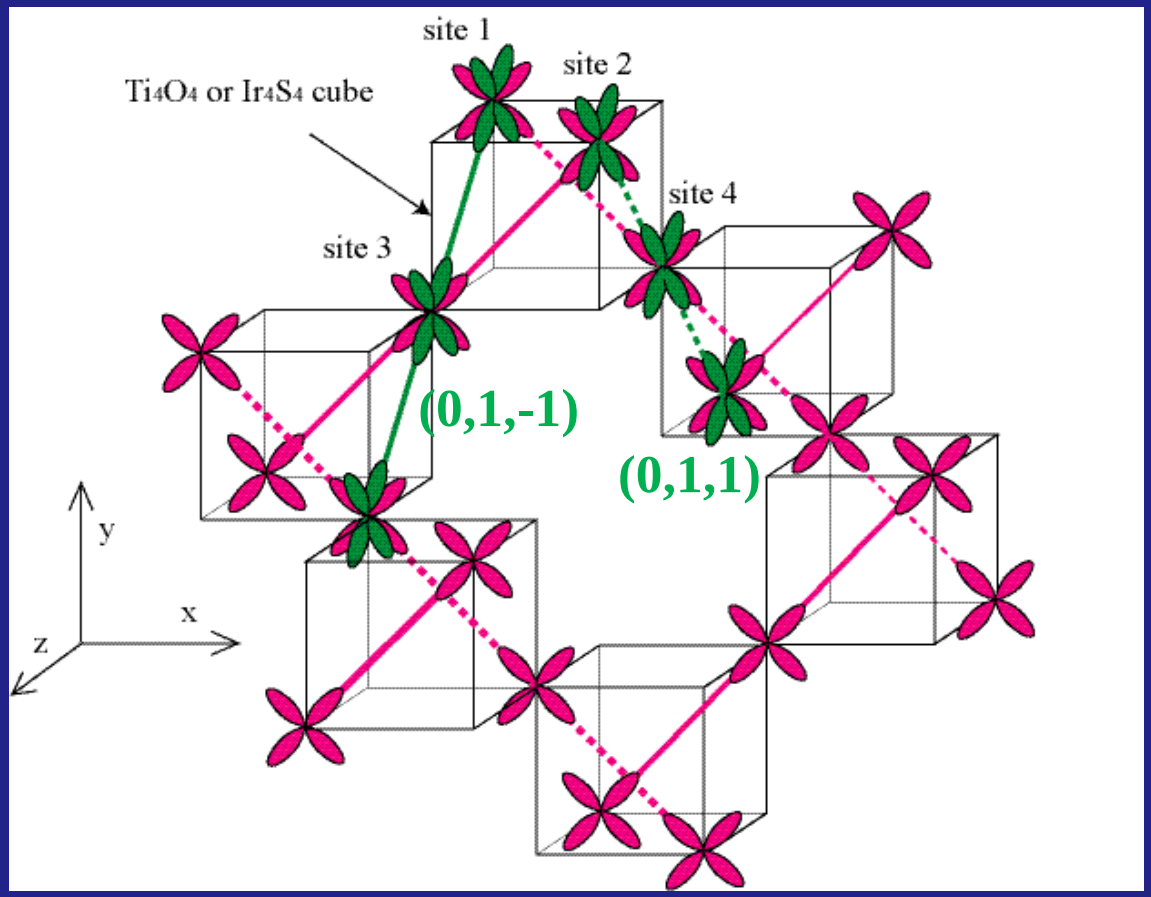


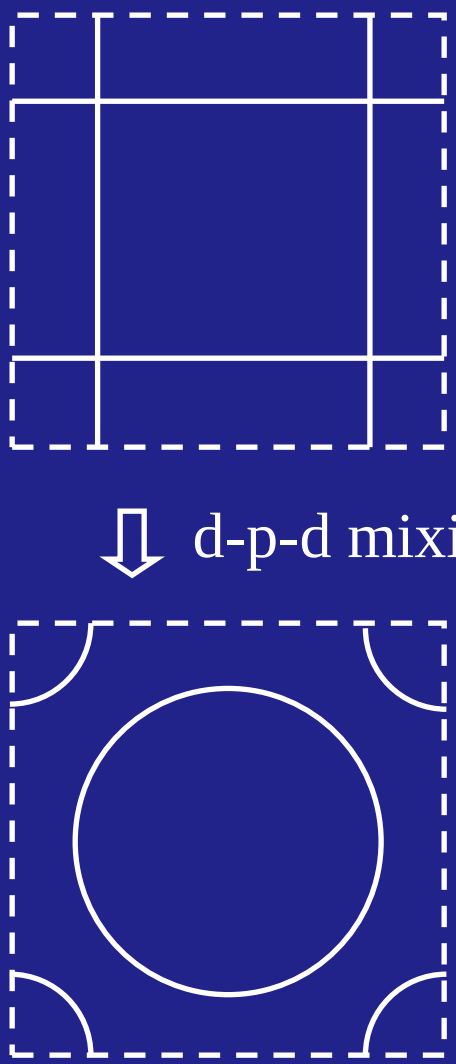

# 3D Fermi surface of $CuIr_2S_4$

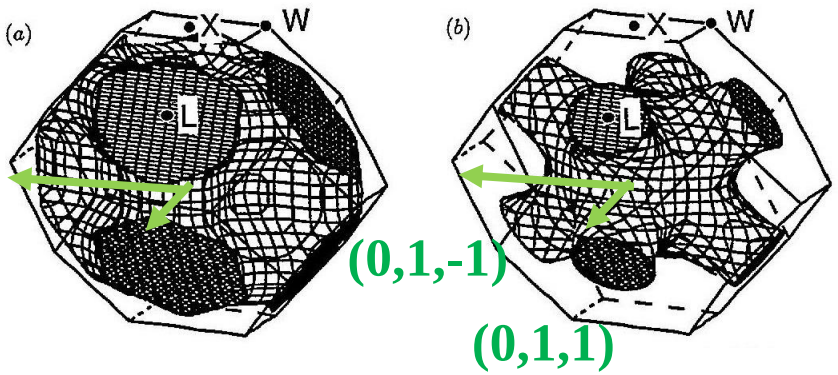


T. Oda, M. Shirai, N. Suzuki, K. Mochizuki, J. Phys. Condens. Matter **7**, 4433 (1995).

**high temperature cubic phase:**
**Ir 5d $t_{2g}$ and S 3p orbitals form the 3D Fermi surfaces.**

**No FS nesting**

T. Sasaki *et al.*, J. Phys. Soc. Jpn. **73**, 1875 (2004).

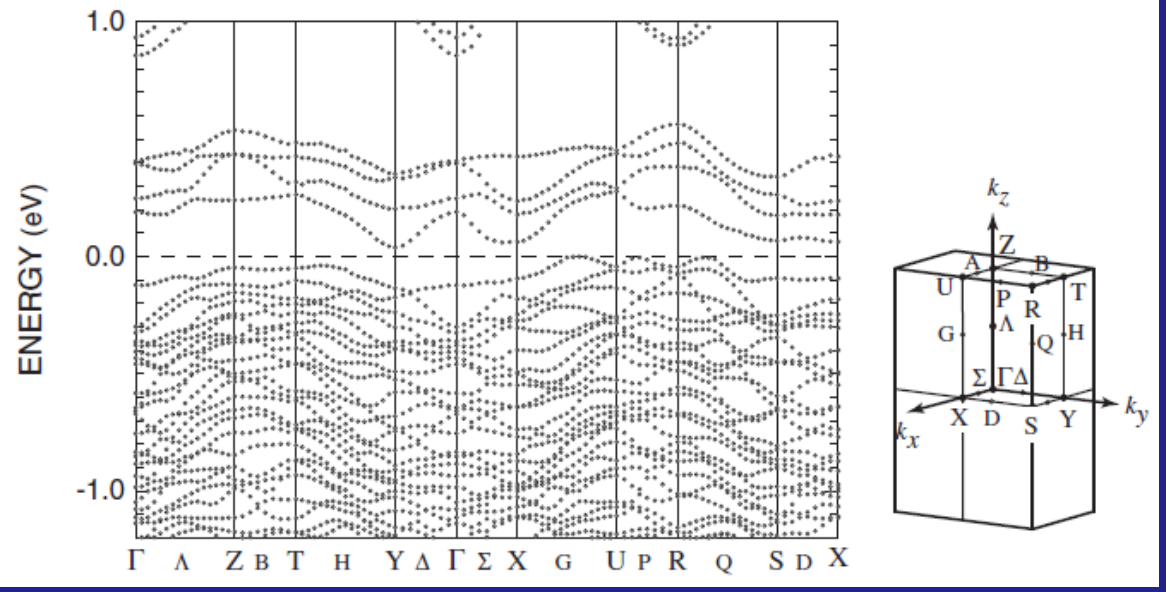


**low temperature triclinic phase:**
**LDA calculation predicts indirect small band gap of ~ 0.03 eV.**
**Strong electron-lattice coupling**
**The magnitude of band gap is underestimated.**
**Experiment: ~ 0.2 eV**

# Jahn-Teller effect in $t_{2g}^{1}$ configuration

$d^1$ configuration ($t_{2g}$ system)

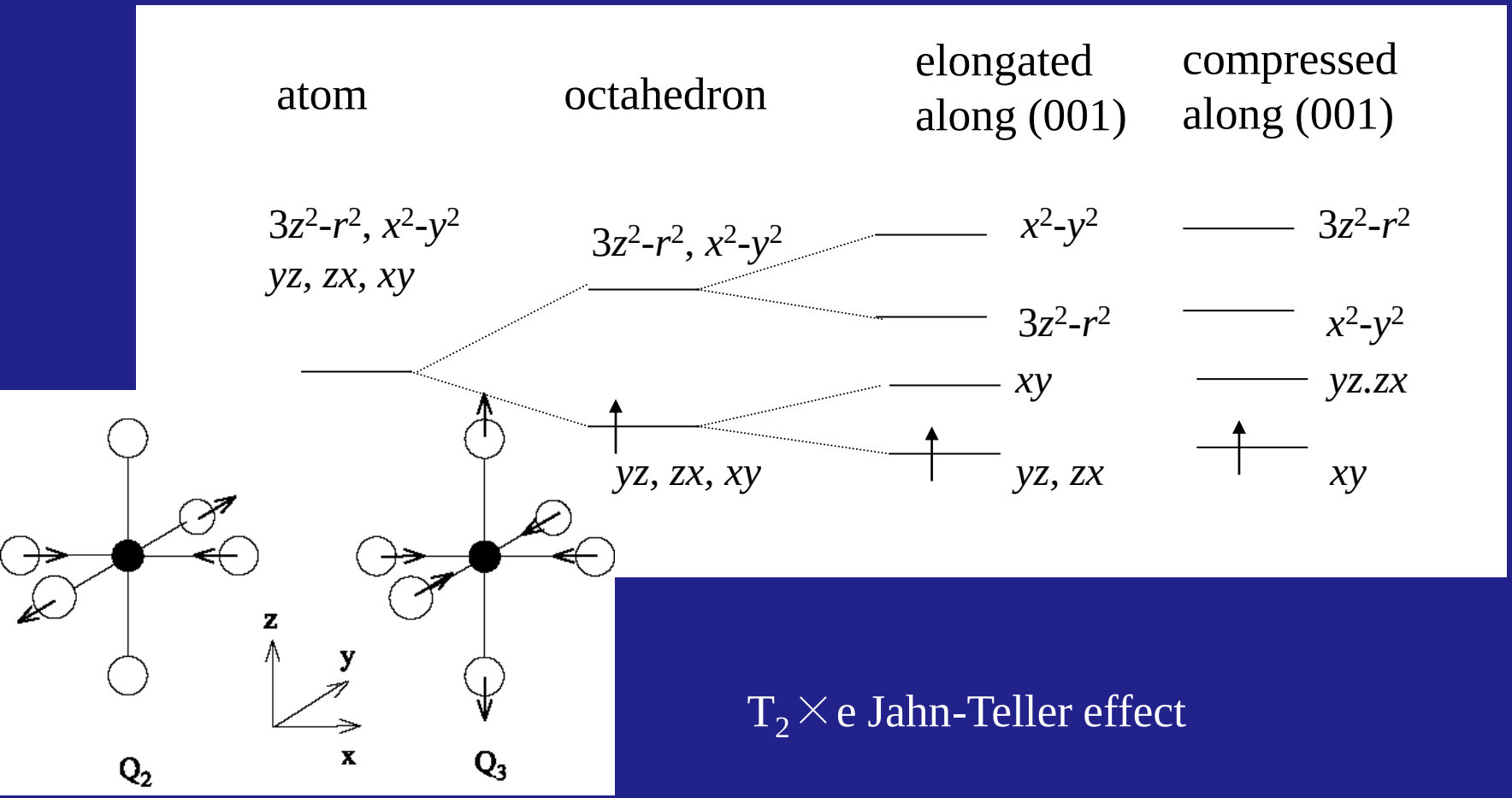


$T_2 \times e$ Jahn-Teller effect

$$H = -Aq\sin\theta\begin{pmatrix}0 & 0 & 0\\ 0 & \sqrt{3}/2 & 0\\ 0 & 0 & -\sqrt{3}/2\end{pmatrix} - Aq\cos\theta\begin{pmatrix}-1 & 0 & 0\\ 0 & 1/2 & 0\\ 0 & 0 & 1/2\end{pmatrix} + \frac{1}{2}M\omega^2q^2$$

# Band Jahn-Teller effect

band Jahn-Teller effect : Jahn-Teller distortion due to itinerant electrons

In a cubic lattice,
the *xy*, *yz*, *zx* orbitals can form triply degenerate bands.

Under tetragonal elongation along the z-axis,
the *xy* band becomes wider than the *yz*, *zx* bands.
→ The *yz*, *zx* bands can be fully (un)occupied in order to gain kinetic energy.

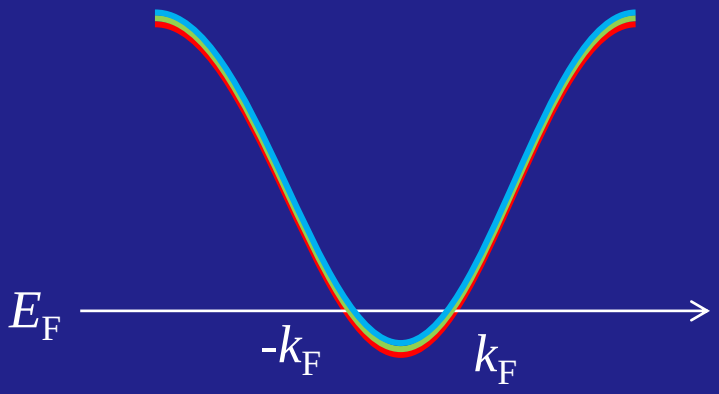


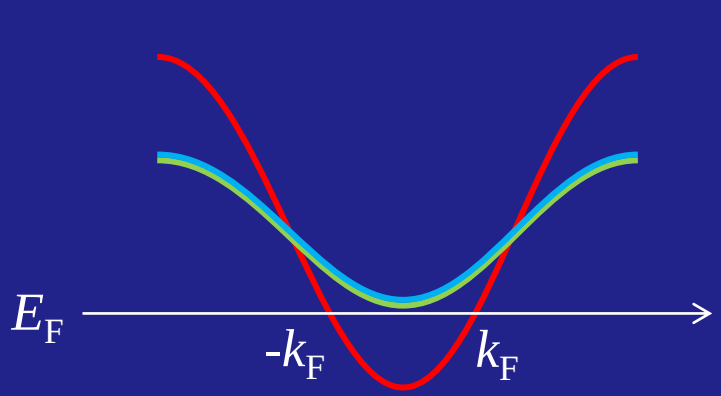


In contrast to the localized electron case, it is not so easy to overcome
the elatic energy loss by the band Jahn-Teller effect alone.

# Jahn-Teller effect in $t_{2g}^{1}$ configuration

$d^1$ configuration ($t_{2g}$ system)

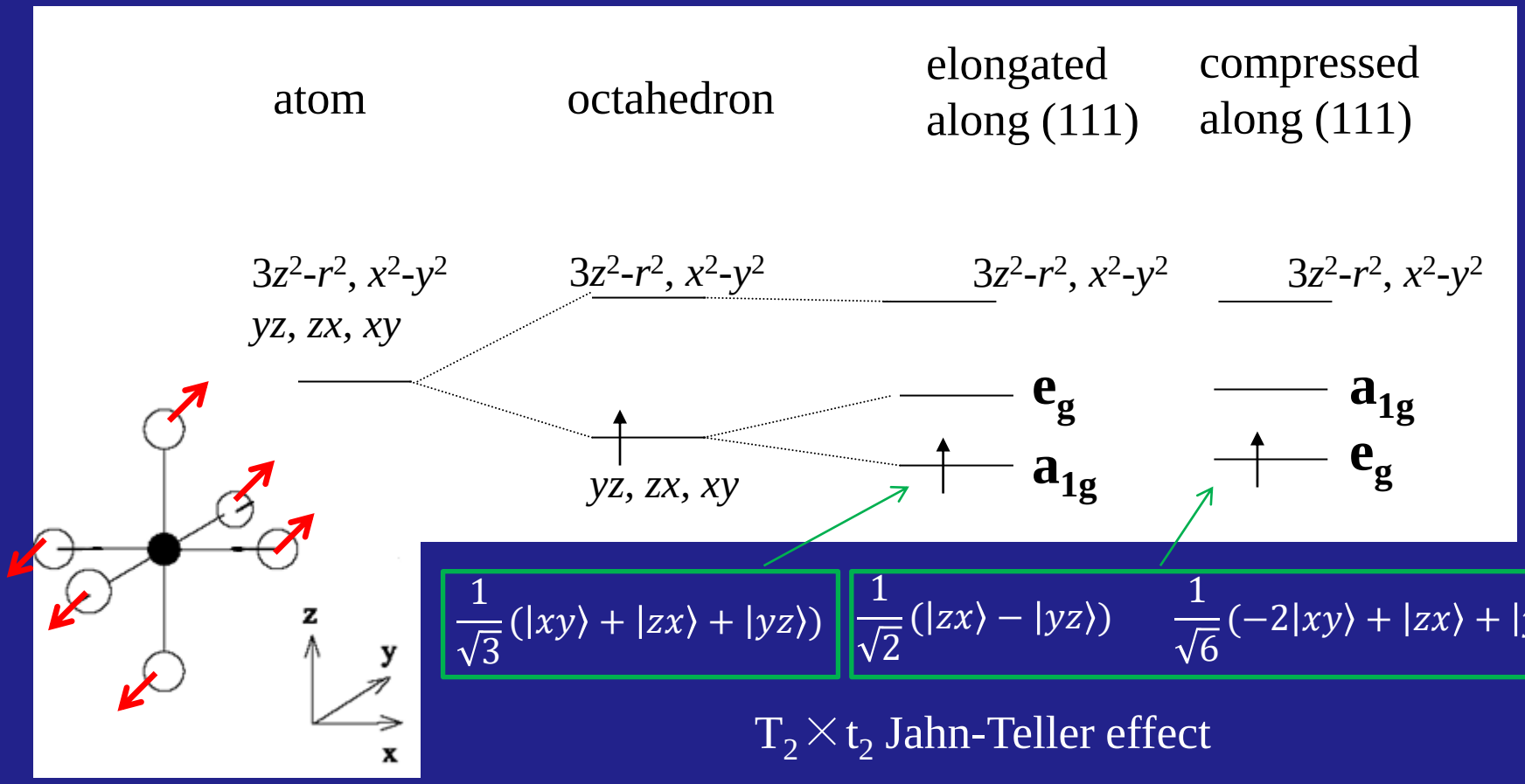


$$\frac{1}{\sqrt{3}}(|xy\rangle + |zx\rangle + |yz\rangle) \qquad \frac{1}{\sqrt{2}}(|zx\rangle - |yz\rangle) \qquad \frac{1}{\sqrt{6}}(-2|xy\rangle + |zx\rangle + |yz\rangle)$$

$T_2 \times t_2$ Jahn-Teller effect

$$H = -Aq_x \begin{pmatrix} 0 & 0 & 0 \\ 0 & 0 & 1/\sqrt{2} \\ 0 & 1/\sqrt{2} & 0 \end{pmatrix} - Aq_y \begin{pmatrix} 0 & 0 & 1/\sqrt{2} \\ 0 & 0 & 0 \\ 1/\sqrt{2} & 0 & 0 \end{pmatrix} - Aq_z \begin{pmatrix} 0 & 1/\sqrt{2} & 0 \\ 1/\sqrt{2} & 0 & 0 \\ 0 & 0 & 0 \end{pmatrix} + \frac{1}{2}M\omega^2 q^2$$

# Band Jahn-Teller effect

band Jahn-Teller effect : Jahn-Teller distortion due to itinerant electrons

In a cubic lattice,
the *xy*, *yz*, *zx* orbitals can form triply degenerate bands.

Under trigonal elongation along the 111-axis,
the $e_g$ bands become wider than the $a_{1g}$ band.
→ The $a_{1g}$ band can be fully (un)occupied in order to gain kinetic energy.

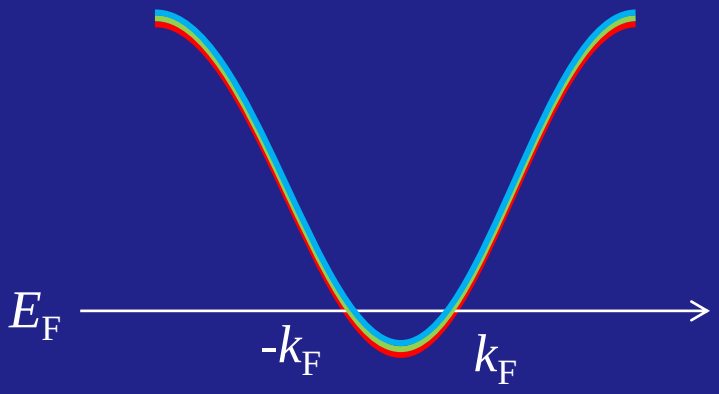


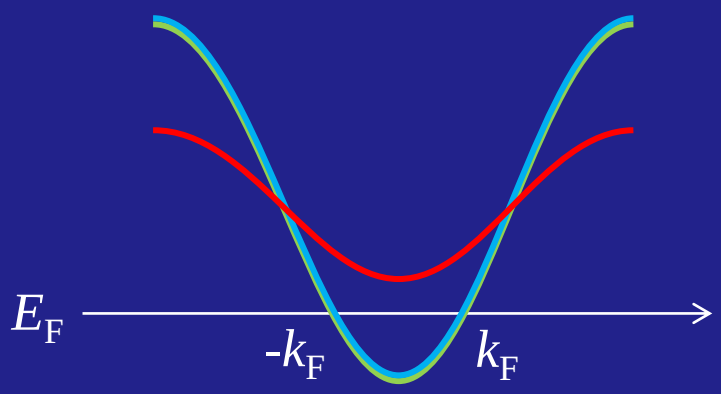


In contrast to the localized electron case, it is not so easy to overcome
the elatic energy loss by the band Jahn-Teller effect alone.

# Band Jahn-Teller effect and Peierls instability

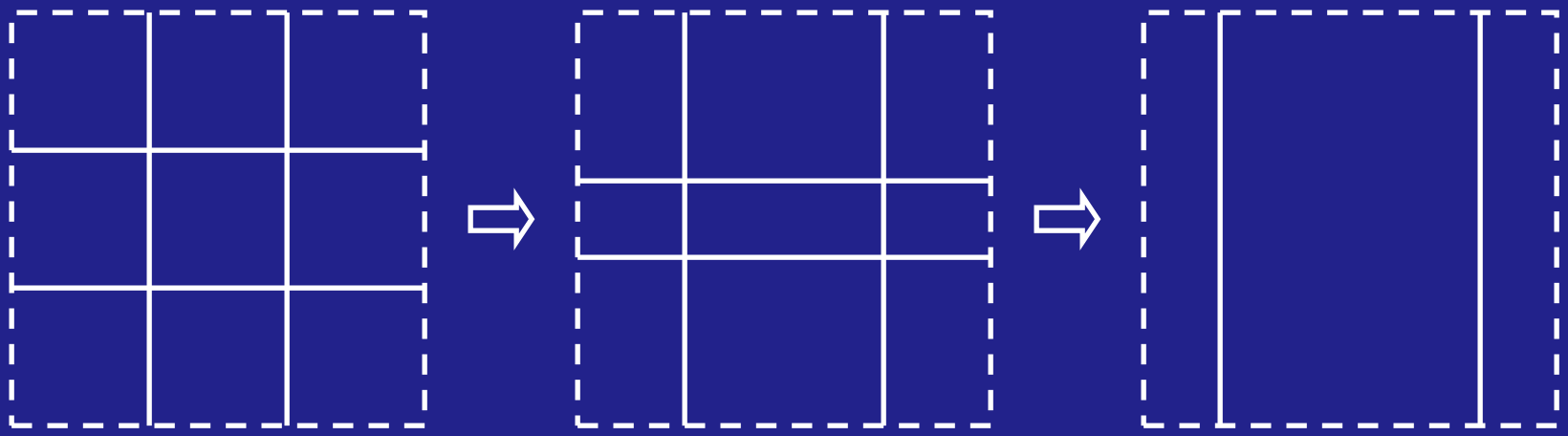

Band Jahn-Teller effect

⇩ d-p-d mixing

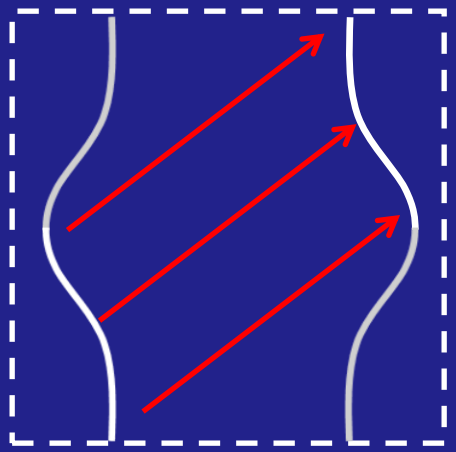

nesting wave vector $Q$

One-dimensional character is partially recovered by the band Jahn-Teller effect.

# Orbitally induced Peierls transition (dimer)

**xy holes → 3/4 filled 1D band along (1,1,0) and (1,-1,0)**

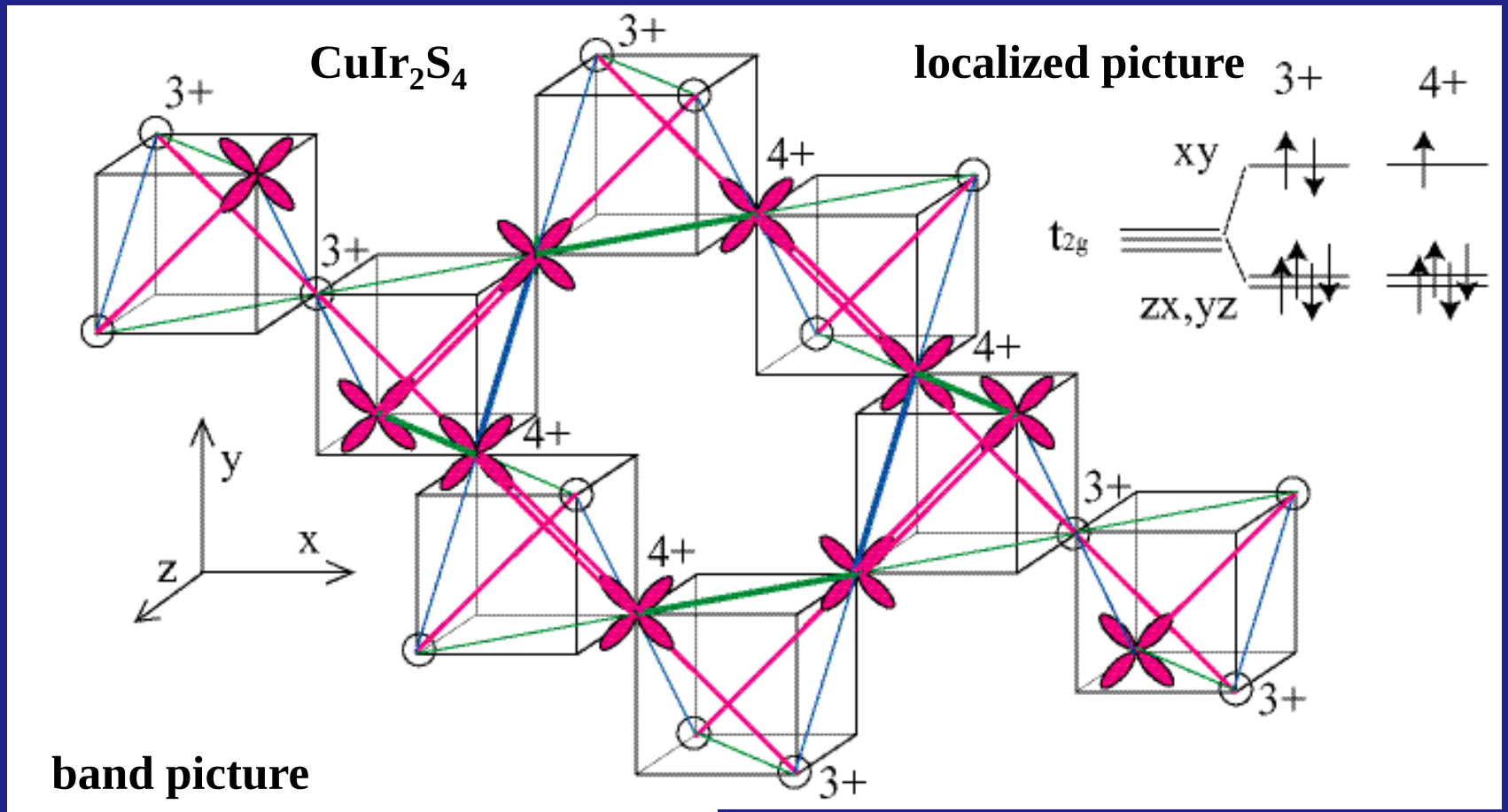


D. I. Khomskii and TM,
Phys. Rev. Lett. **94**, 156402 (2005).

# Ir 5d charge order in $CuIr_2S_4$

## Ir 4f core level XPS

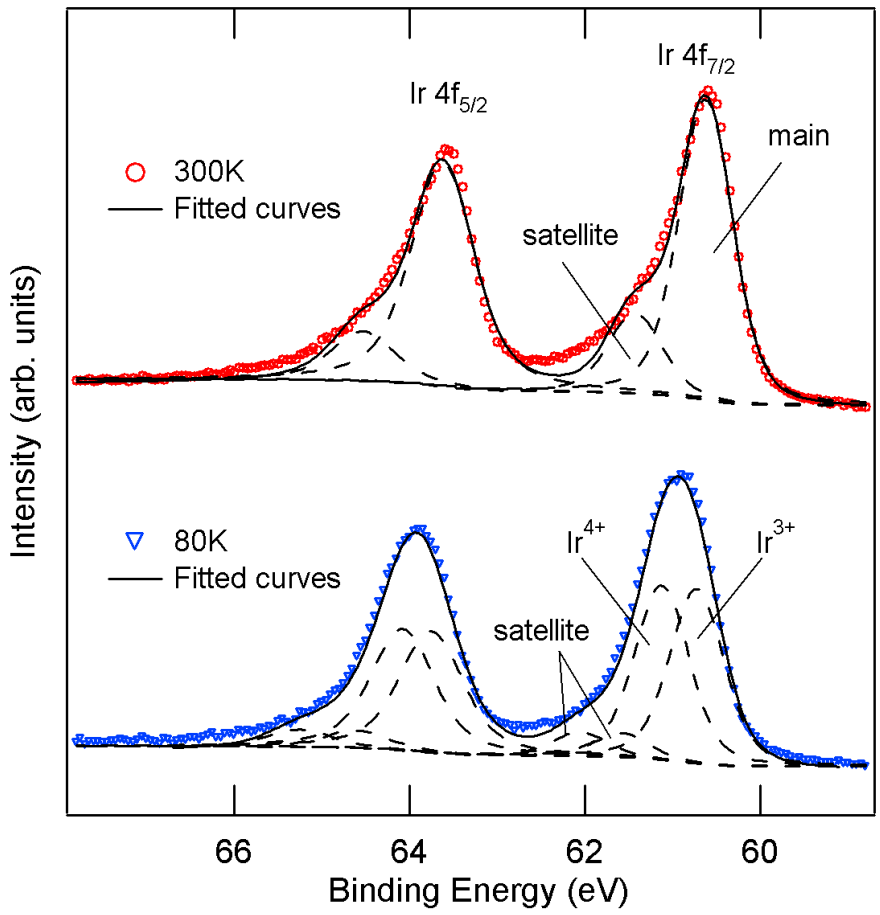


K. Takubo *et al.*, Phys. Rev. Lett. **95**, 246401 (2005).

**$Ir^{4+}$ and $Ir^{3+}$ charge modulation manifests in the Ir 4f core level.**

**Ir 4f core level spectrum of insulating phase can be decomposed into the $Ir^{3+}$ and $Ir^{4+}$ peaks.**

**$Ir^{3+}$ : $Ir^{4+}$ = 1 : 1**

**charge modulation predicted by LDA**

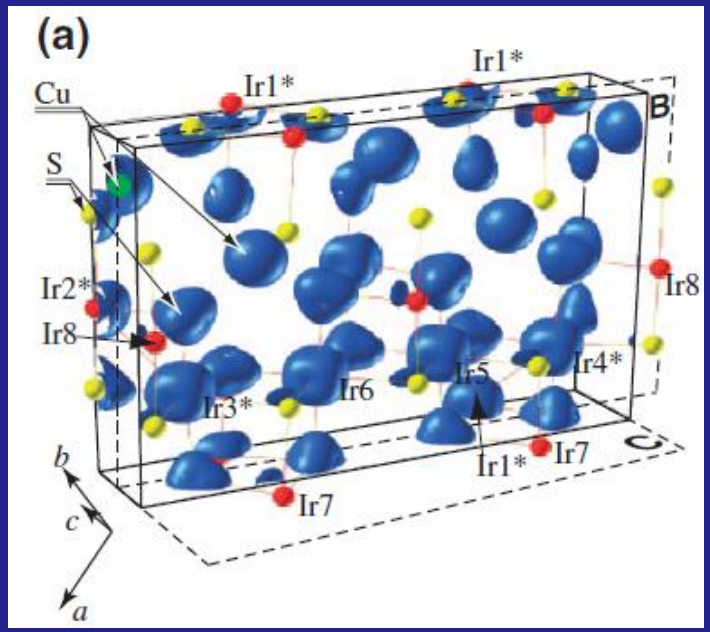


T. Sasaki *et al.*, J. Phys. Soc. Jpn. **73**, 1875 (2004).

# Outline

1. Electron-phonon interaction and Peierls transition
   (not in the text, for undergraduate)

2. Orbitally induced Peierls transition: Case study on $CuIr_2S_4$ (section 2.1)

3. Toy models on square/triangular lattice (sections 2.2 and 2.3)

4. Application to Spinel and Pyrochlore materials (sections 3.1 and 3.2)

5. Application to triangular/honeycomb/kagome lattice systems (3.3/3.4/3.5)

6. Summary

# two-band model on a square lattice

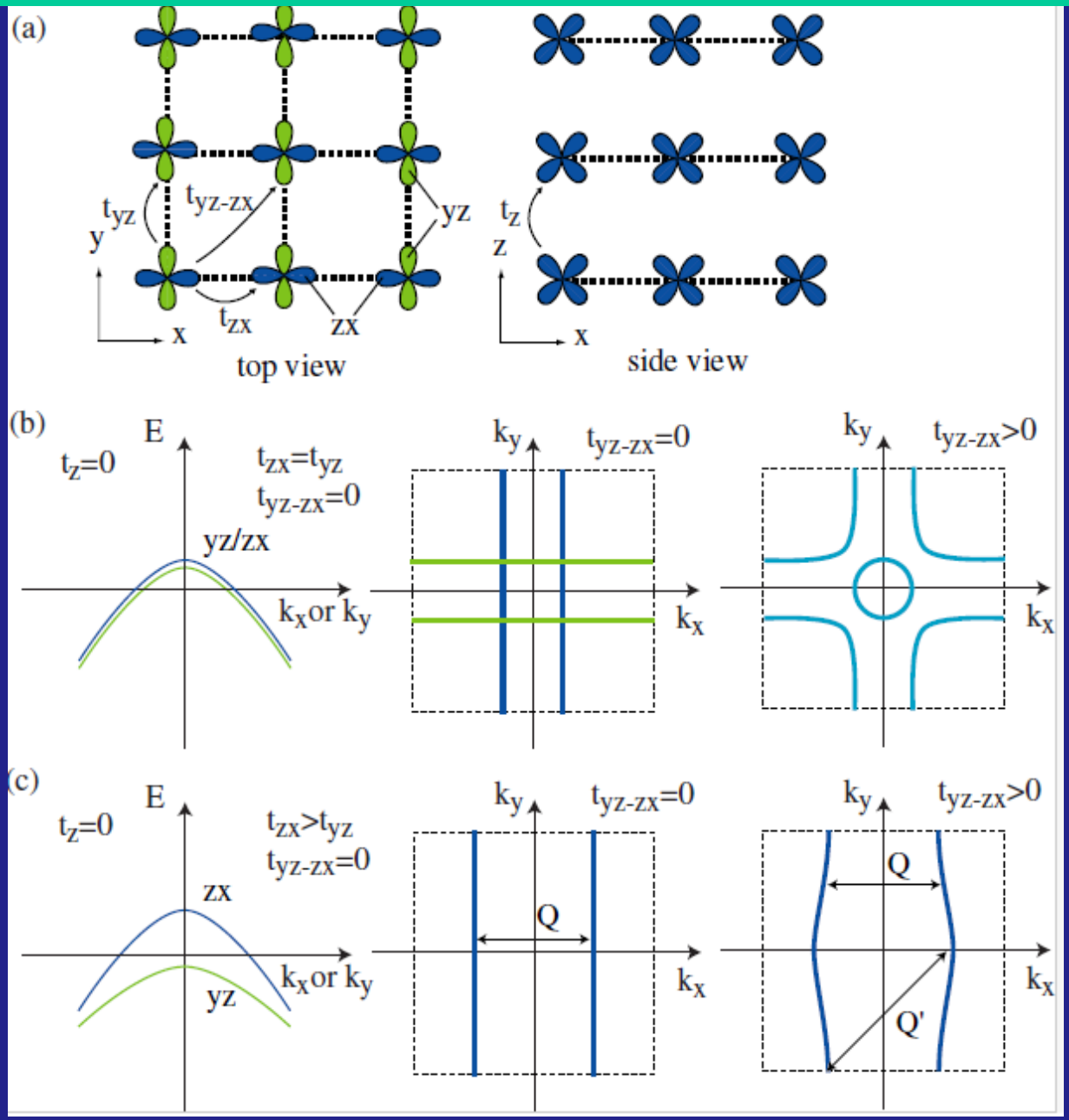


$t_z = 0$ **purely 2D**

$$E_1 = 2t_{zx}\cos k_x$$

$$E_2 = 2t_{yz}\cos k_y$$

$$t_{zx} = t_{yz} > 0$$

$$E_{12} = 2t_{yz\cdot zx}\cos(k_x + k_y) - 2t_{yz\cdot zx}\cos(k_x - k_y)$$

$$E_1 = \Delta + 2t_{zx}\cos k_x$$

$$E_2 = -\Delta + 2t_{yz}\cos k_y$$

$$t_{zx} > t_{yz} > 0$$

# Effect of interlayer coupling

$t_z > 0$ **quasi 2D**

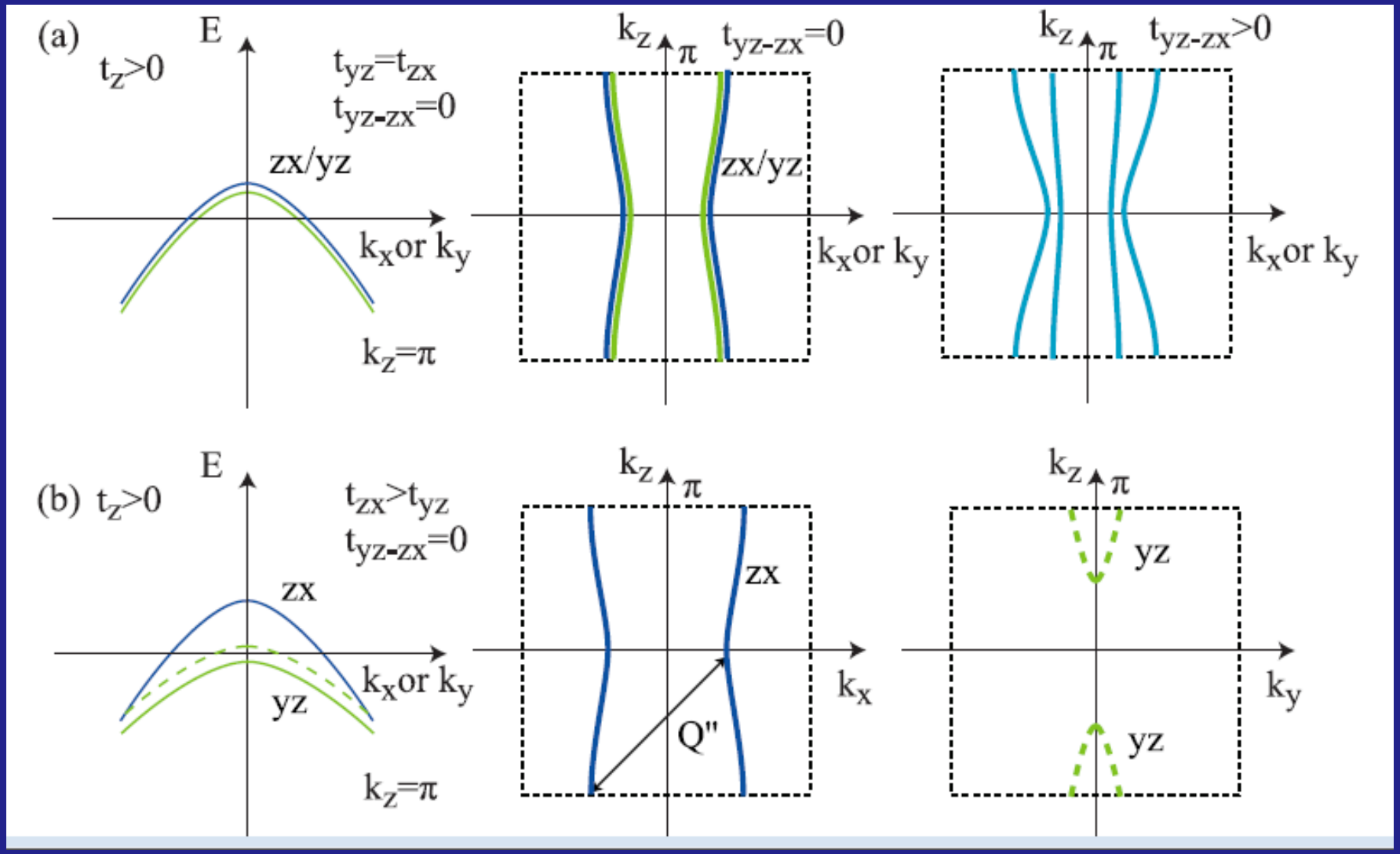

# Three-band model on a square lattice

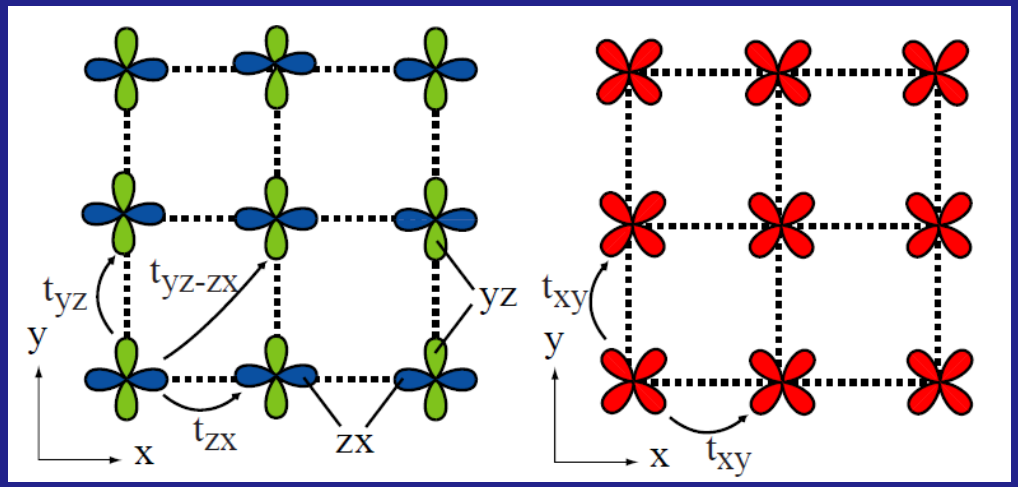


$$t_{xy} = t_{zx} = t_{yz} > 0$$

$$E_1 = 2t_{zx}\cos k_x$$

$$E_2 = 2t_{yz}\cos k_y$$

$$E_3 = 2t_{xy}(\cos k_x + \cos k_y) + 2t_{xy\cdot xy}\cos(k_x + k_y) + 2t_{xy\cdot xy}\cos(k_x - k_y)$$

$$t_{xy\cdot xy} > 0$$

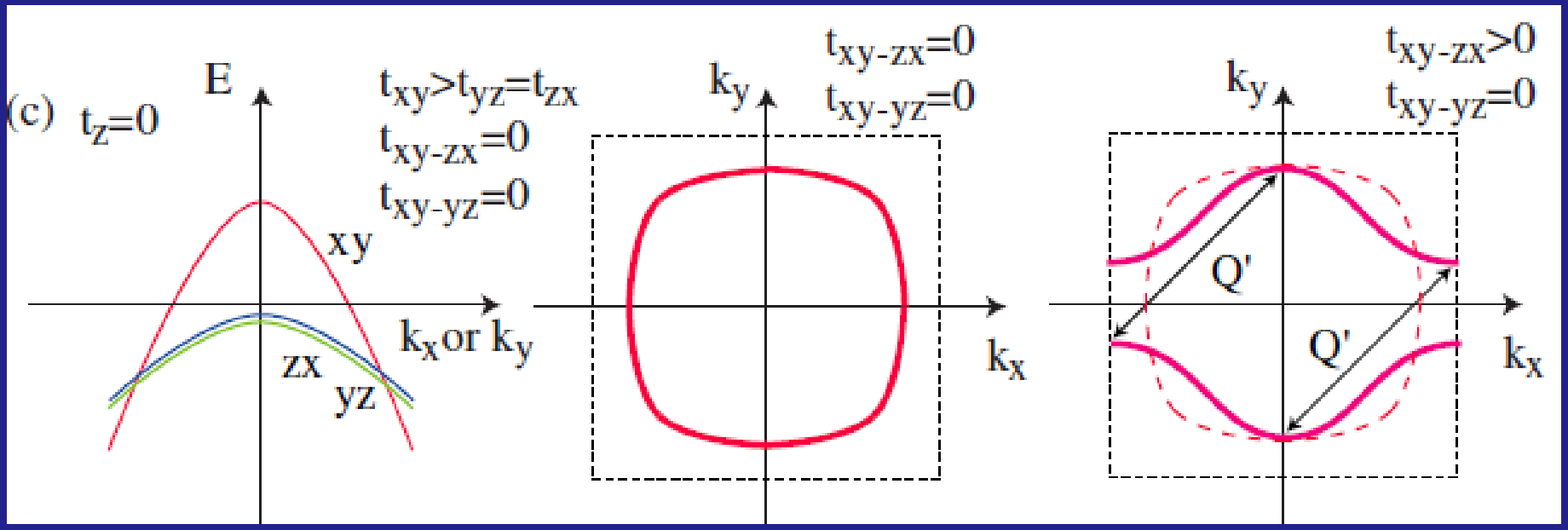

# triangular lattice model

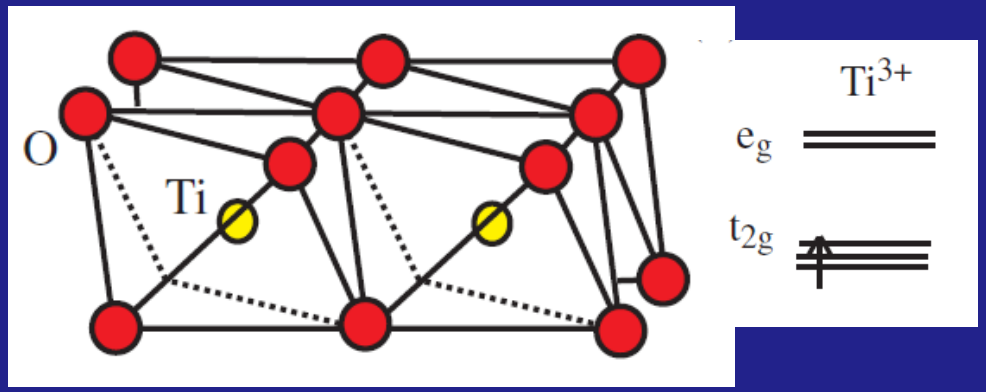


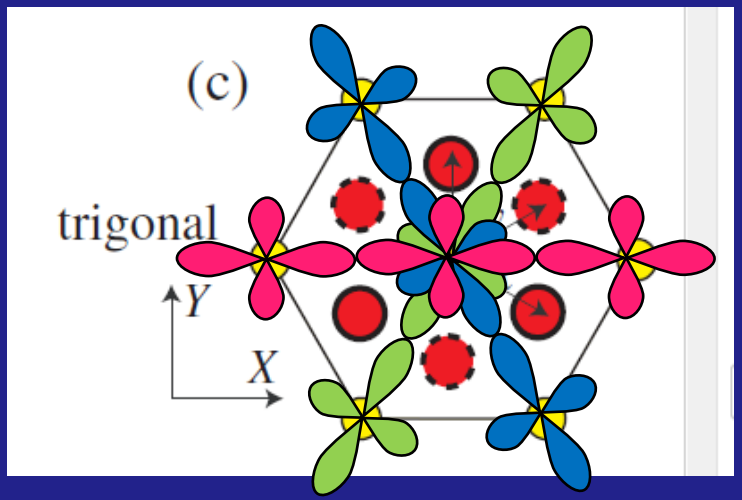


$$E_1 = 2t_{yz}\cos(k_x/2 + \sqrt{3}k_y/2)$$

$$E_2 = 2t_{zx}\cos(k_x/2 - \sqrt{3}k_y/2) \qquad E_3 = 2t_{xy}\cos k_x$$

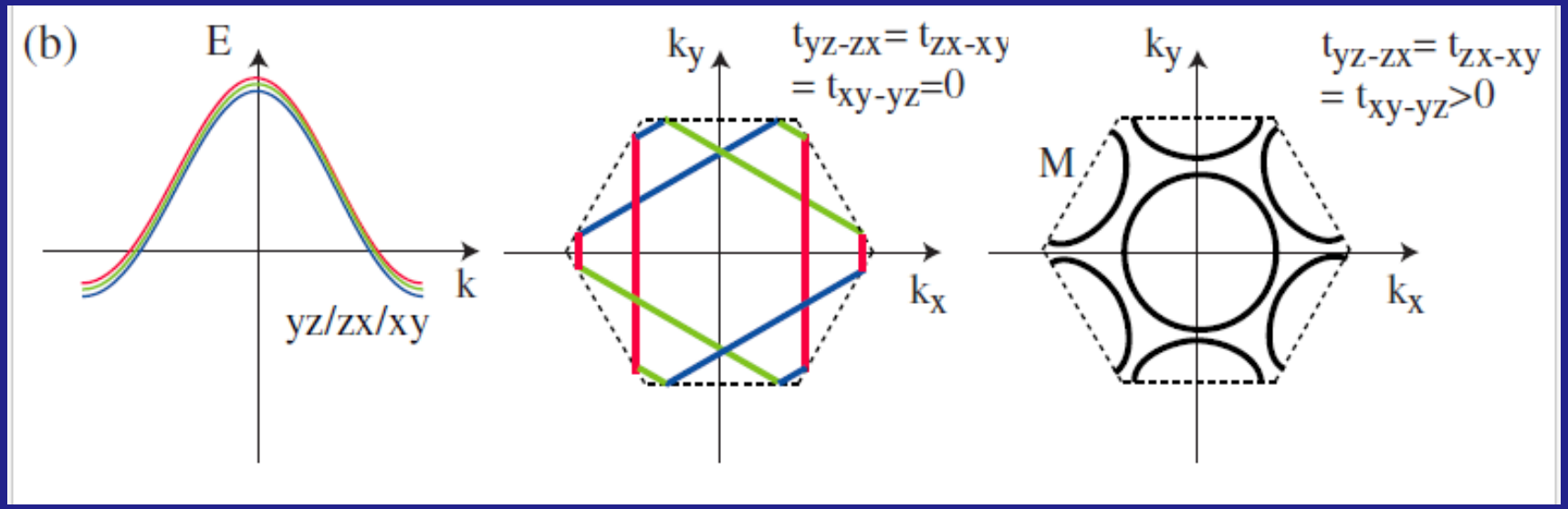

# triangular lattice model

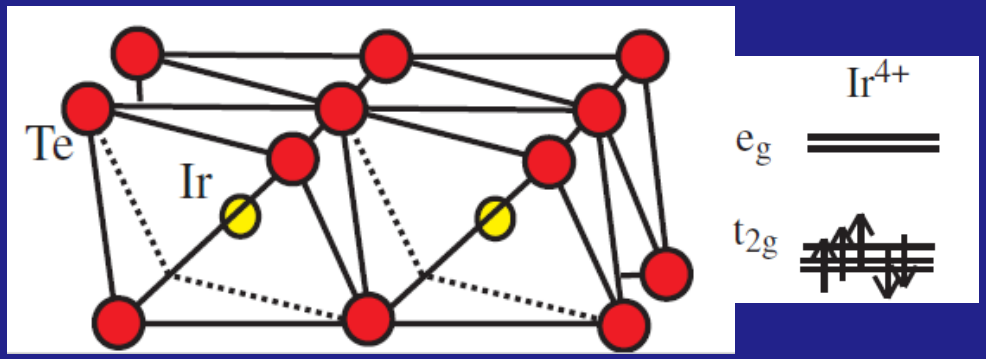


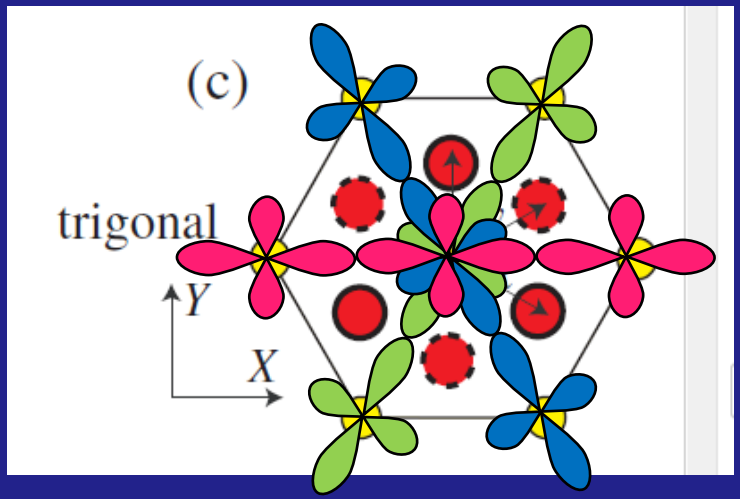


$$E_1 = 2t_{yz}\cos(k_x/2 + \sqrt{3}k_y/2)$$

$$E_2 = 2t_{zx}\cos(k_x/2 - \sqrt{3}k_y/2) \qquad E_3 = 2t_{xy}\cos k_x$$

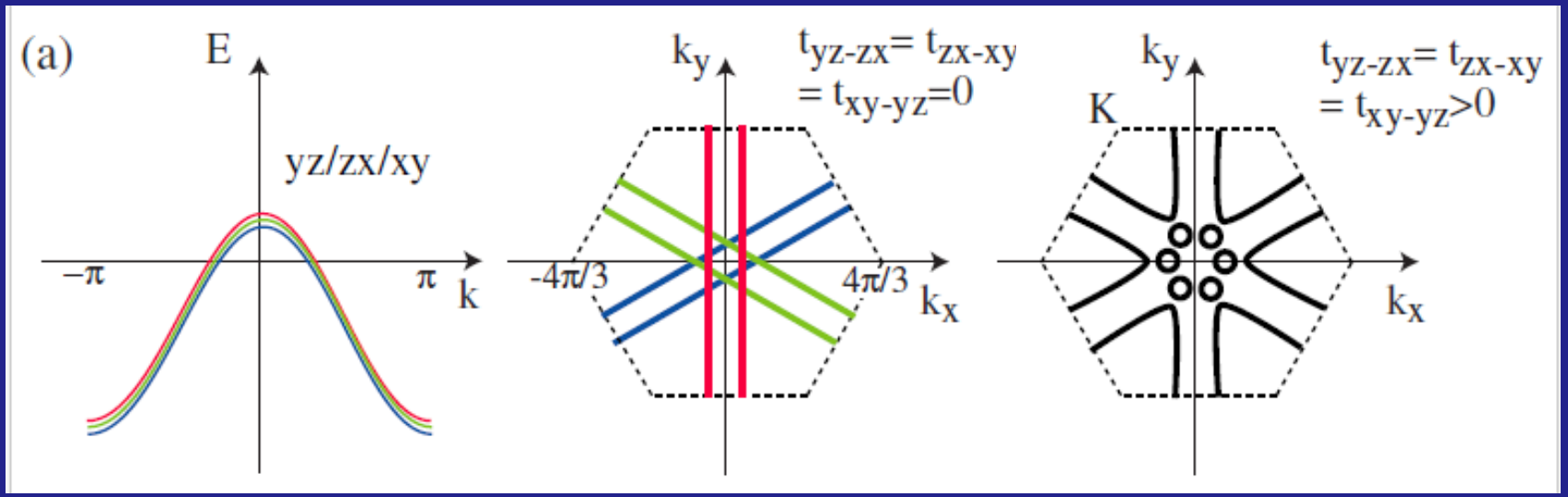

# Orbitally induced Peierls mechanism

When the triangular lattice is compressed along (1,0)

the *xy* band becomes wider than the *yz*, *zx* bands.

→ *yz*, *zx*: fully (un)occupied

***xy* : 1/2 filled 1D band along (1,0)**

→ **dimerization along (1,0)**

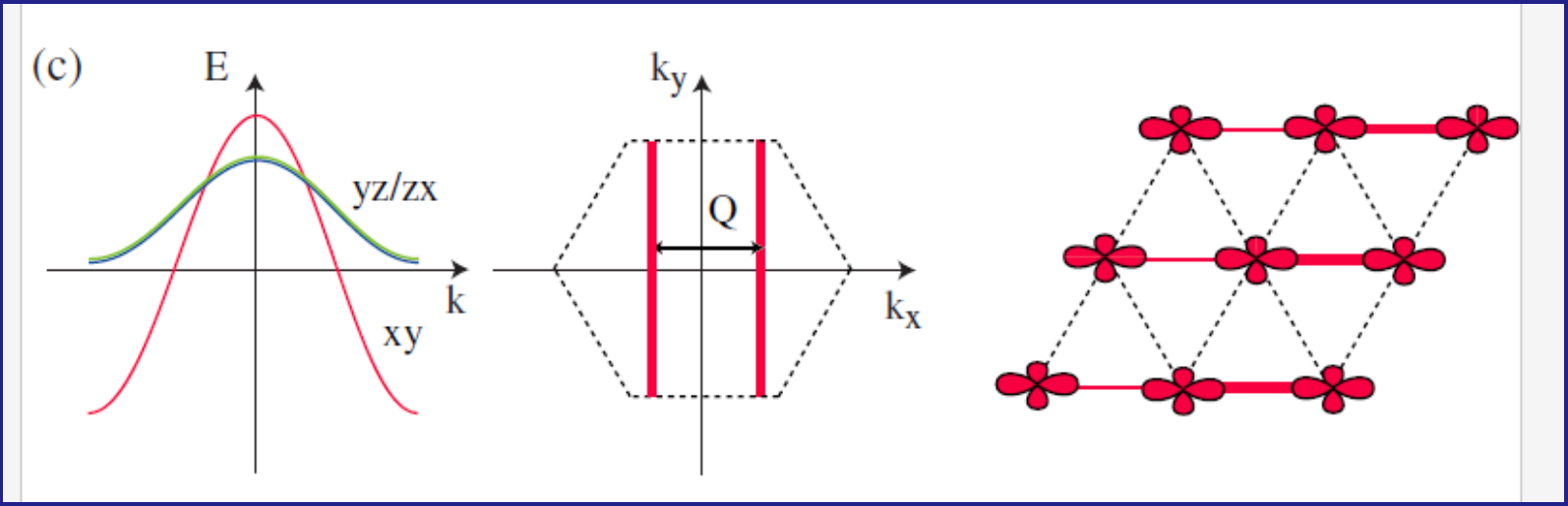


However, such dimerization for $d^1$ was not observed in actual triangular lattice systems.

# $Na_xCoO_2$

**close to low spin $Co^{3+}$**

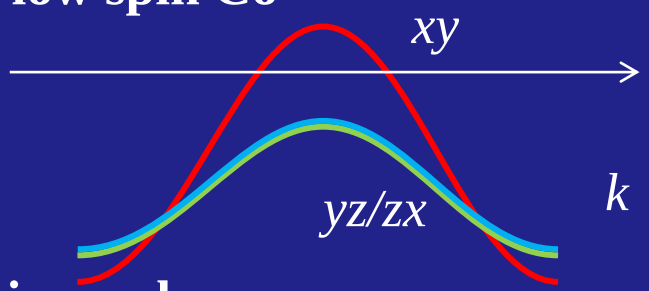


**Na ion order →**
**Anisotropic $a_{1g}$-$e_g^{\pi}$ hybrizization**
**→ Fermi surface nesting**

K. Ikedo *et al.*,
J. Phys. Soc. Jpn. 78, 063707 (2009)

D.N. Argyriou, O. Prokhnenko, K. Kiefer, and C.J. Milne, Phys. Rev. B 76, 134506 (2007)

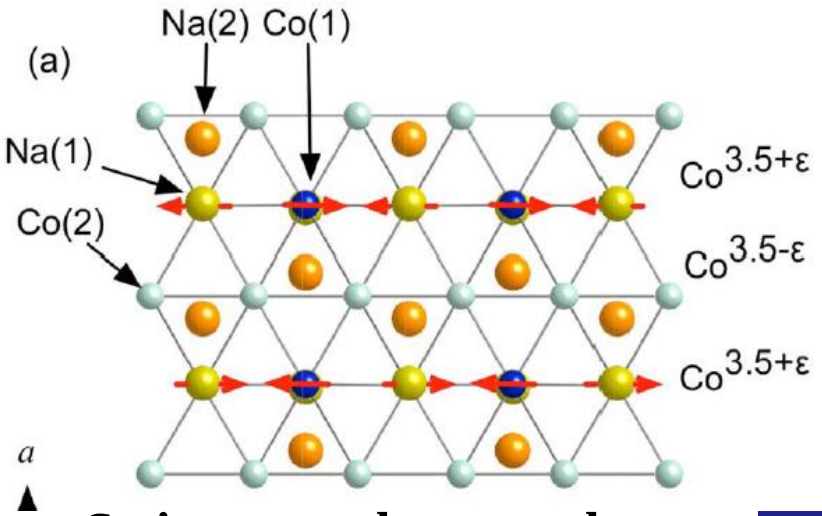


**Stripe-type charge order**

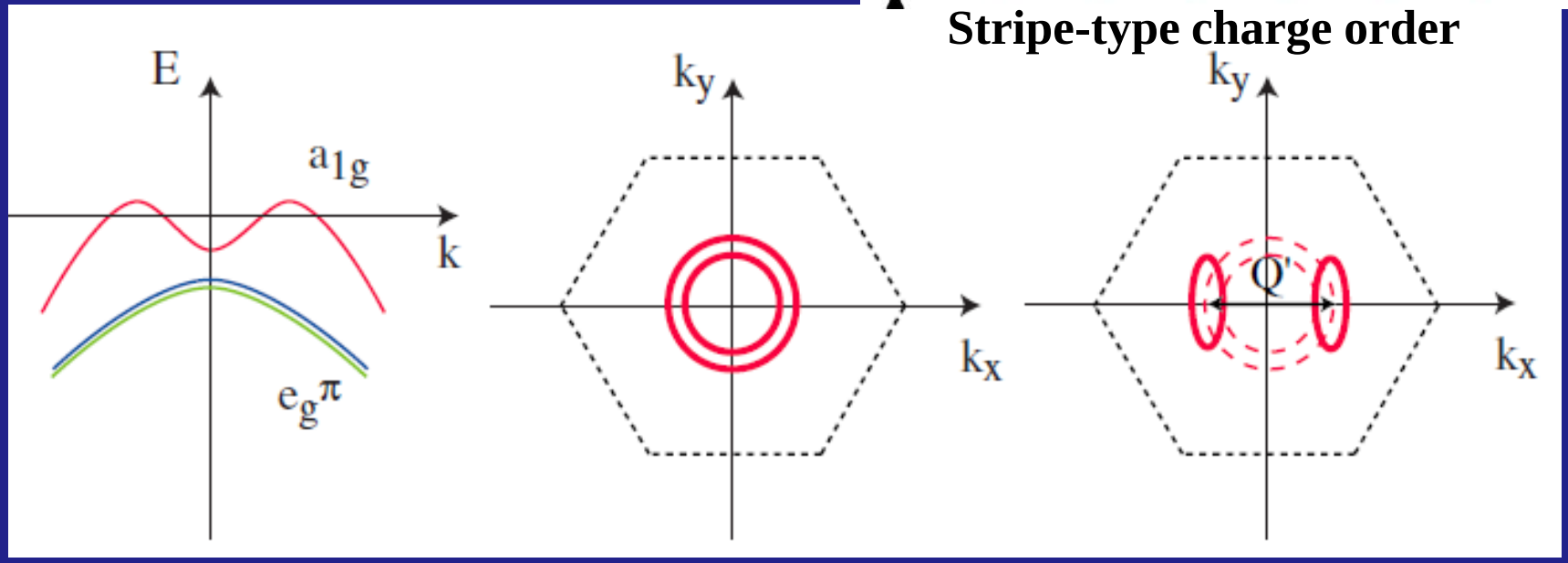

# Outline

1. Electron-phonon interaction and Peierls transition
   (not in the text, for undergraduate)

2. Orbitally induced Peierls transition: Case study on $CuIr_2S_4$ (section 2.1)

3. Toy models on square/triangular lattice (sections 2.2 and 2.3)

4. Application to Spinel and Pyrochlore materials (sections 3.1 and 3.2)

5. Application to triangular/honeycomb/kagome lattice systems (3.3/3.4/3.5)

6. Summary

# Transition-metal oxides with edge-sharing octahedra

**Rutile(1D)**

$VO_2$: $V^{4+}$ $d^1$ $T_{MI}$=340 K M-NMI

**Hollandite(1D)**

$K_2V_8O_{16}$: $V^{4+}$,$V^{3+}$ $d^1$,$d^2$ $T_{MI}$=210 K M-NMI

$K_2Cr_8O_{16}$: $Cr^{4+}$,$Cr^{3+}$ $d^2$,$d^3$ $T_{MI}$=95 K FM-FMI

**triangular lattice (2D)**

$NaTiO_2$ $Ti^{3+}$ $d^1$ $T_{NM}$ = 260 K I-NMI

$LiVO_2$ $V^{3+}$ $d^2$ $T_{NM}$ = 500 K I-NMI

$BaV_{10}O_{15}$ $V^{3+}$ ,$V^{2+}$ $d^2$,$d^3$ $T_{MI}$=130 K M-AFI

$Na_xCoO_2$ $Co^{4+}$,$Co^{3+}$ $d^5$,$d^6$

**honeycomb lattice (2D)**

$Li_2RuO_3$ $Ru^{4+}$ $d^4$ $T_{MI}$ = 540 K M-NMI

$Na_2IrO_3$ $Ir^{4+}$ $d^5$

**Spinel (3D)**

$MgTi_2O_4$ $Ti^{3+}$ $d^1$ $T_{MI}$ = 260 K M-NMI

$ZnV_2O_4$ $V^{3+}$ $d^2$

$AlV_2O_4$ $V^{3+}$, $V^{2+}$ $d^2$,$d^3$

$LiRh_2O_4$ $Rh^{4+}$,$Rh^{3+}$ $d^5$,$d^6$ $T_{MI}$=170 K M-NMI

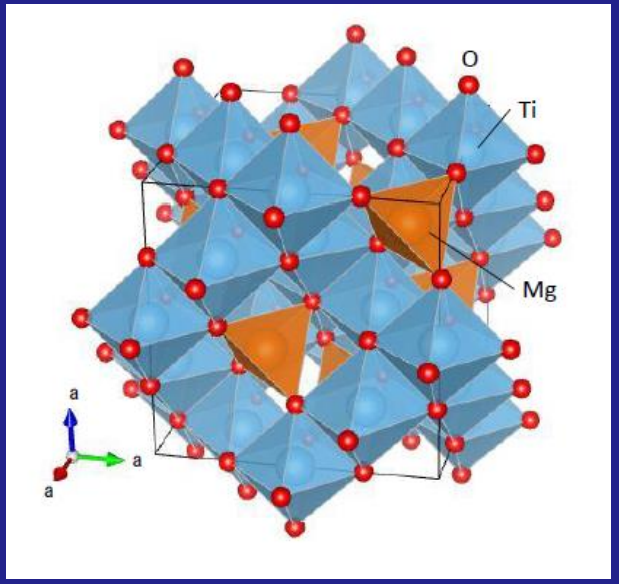

# Rh 4d charge order in $LiRh_2O_4$

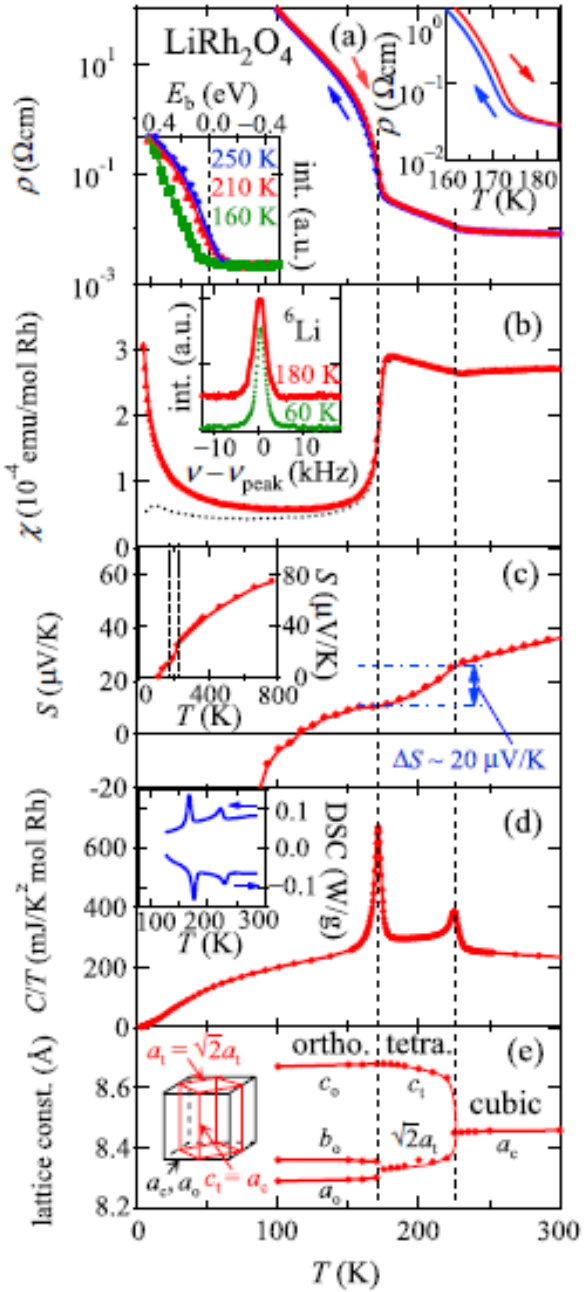


Y. Okamoto et al., Phys. Rev. Lett. **101**, 086404 (2008).

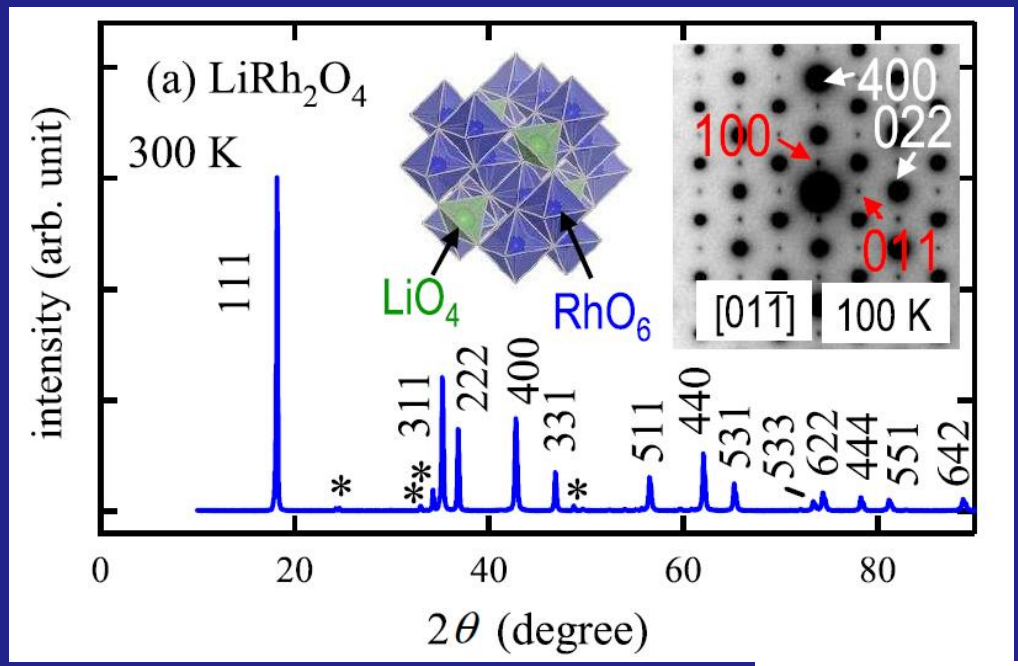


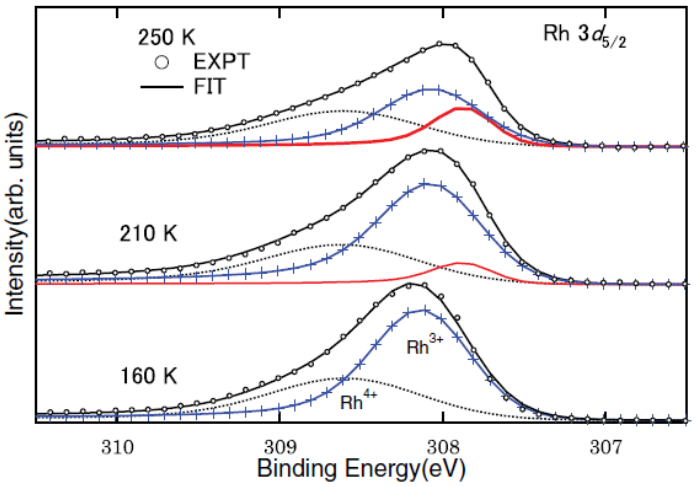


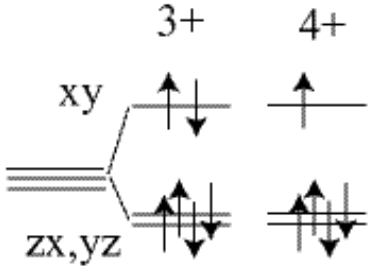


**$Rh^{3+}$ : $Rh^{4+}$ = 1 : 1**

Y. Nakatsu et al., Phys. Rev. B **83**, 115120 (2011).

# Charge ordering and Anderson's condition

repulsion between dimers

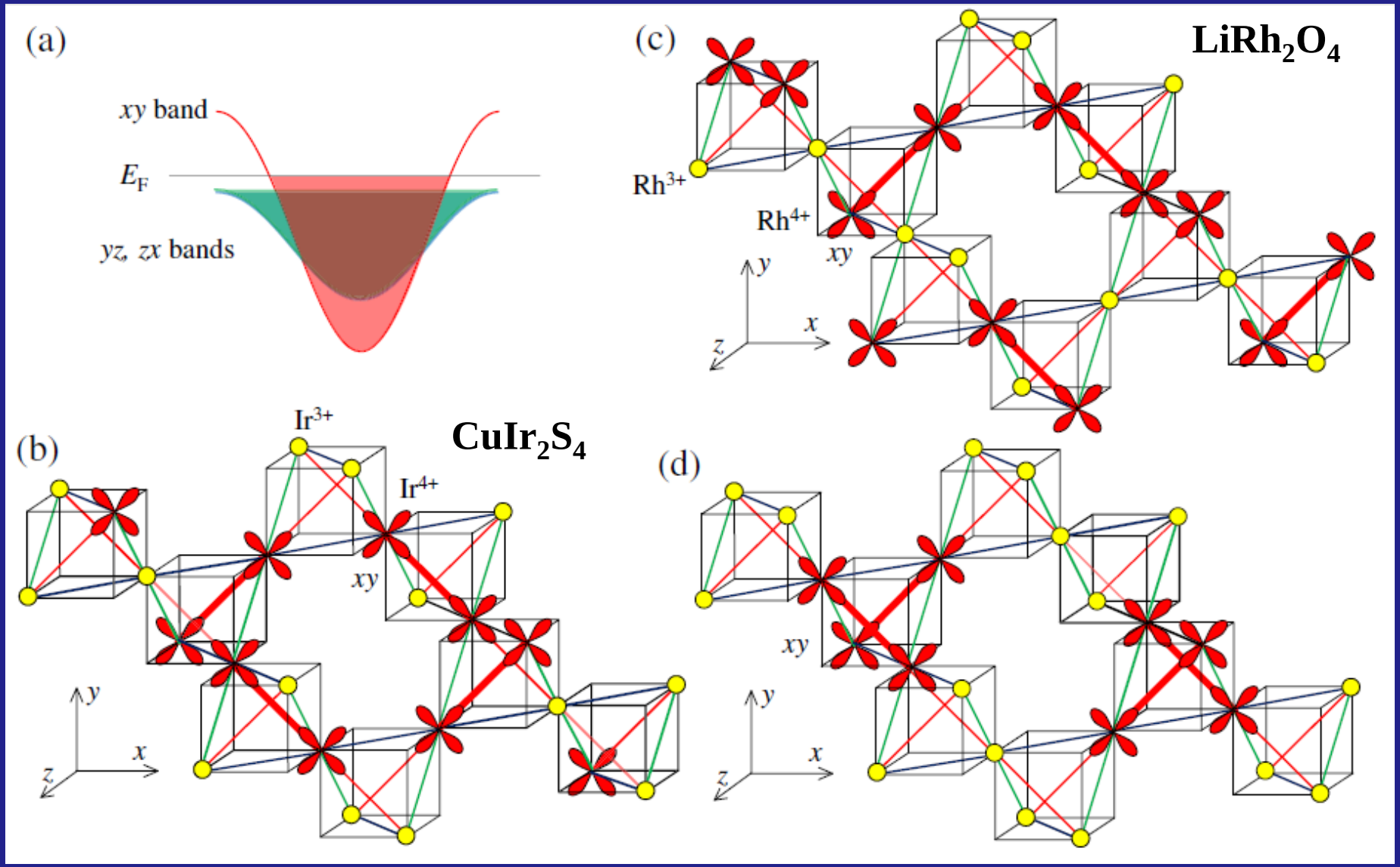


attraction between dimers

# Helical dimerization in $MgTi_2O_4$

M.Schmidt *et al.*, Phys. Rev. Lett. **92**, 056402 (2004).

| Bond (A) | Cubic, 275 K | | Tetragonal, 200 K |
|---|---|---|---|
| Ti-Ti | 3:00843 1 | 6 | 2:853 7 1 |
| | | | 3:007 5 2, 3:0147 3 2 |
| | | | 3:157 7 1 |
| Ti-O | 2.0520(2) | 6 | 2.031(5), 2.026(5), 2.024(5) |
| | | | 2.083(5), 2.138(4), 2.020(4) |

Ti-Ti dimerization

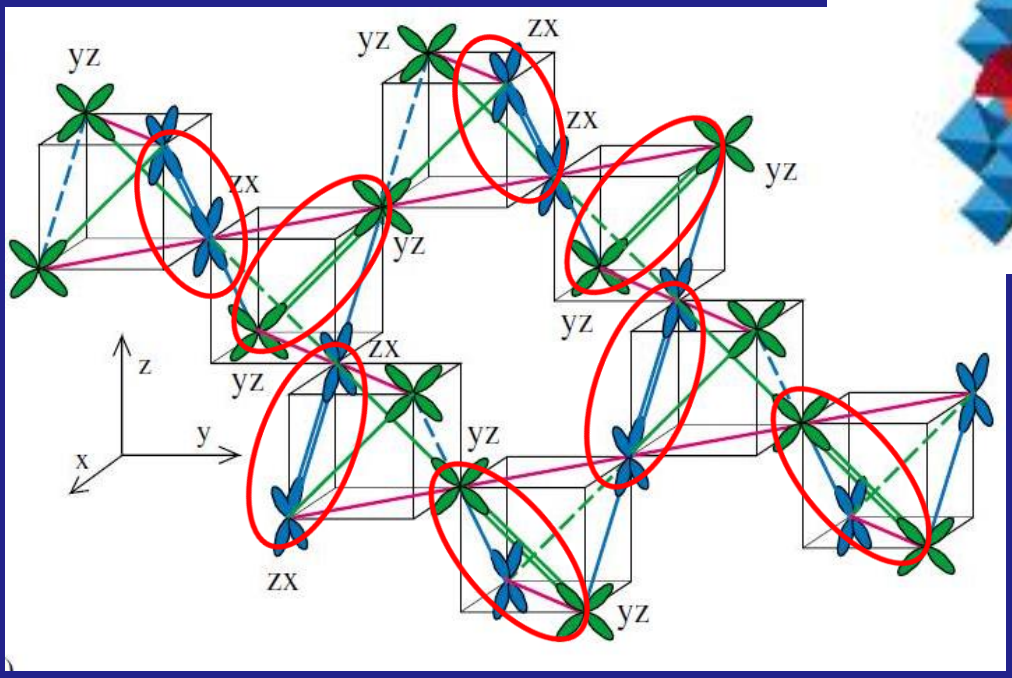


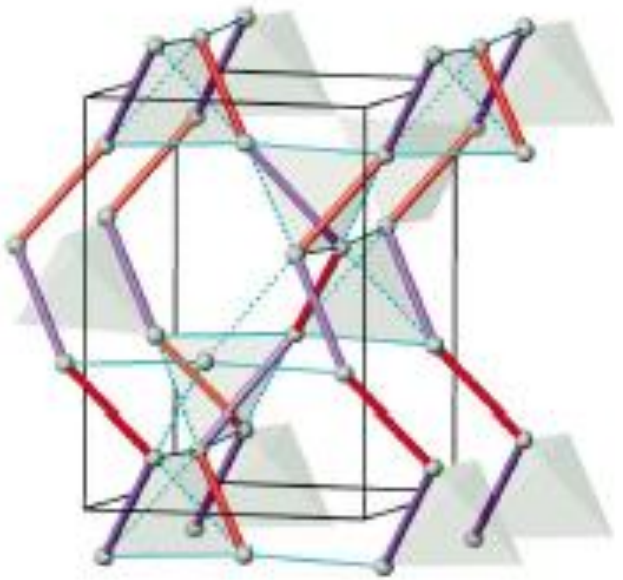

Mott transition + spin singlet ?

Orbitally-induced Peierls transition?

# Orbitally induced Peierls transition (dimer + dimer)

$MgTi_2O_4$

**yz → 1/4 fillled 1D band along (0,1,1) and (0,1,-1)**

**zx → 1/4 fillled 1D band along (1,0,1) and (1,0,-1)**

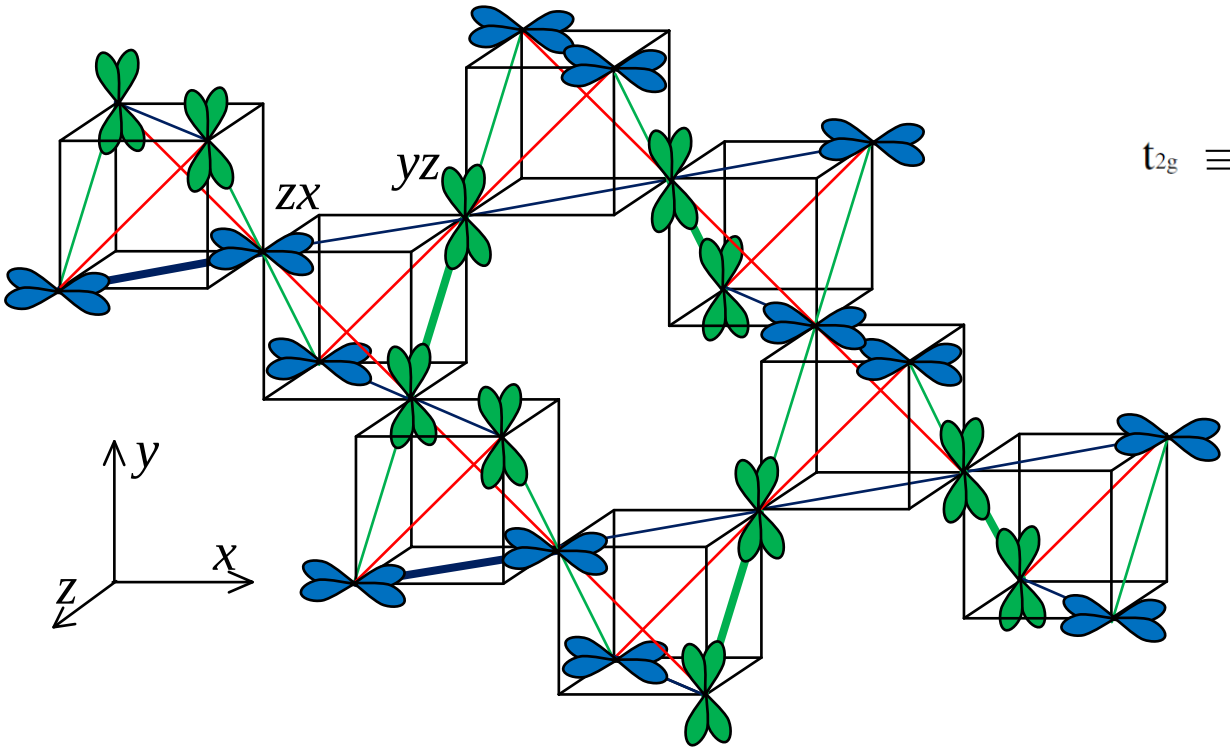


**band picture**

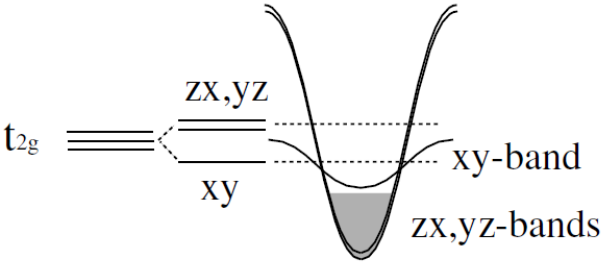


**localized picture**

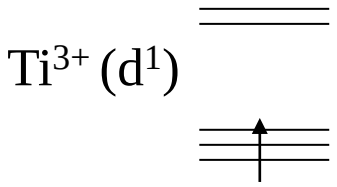

# Heptamer (tetramer +trimer) in $AlV_2O_4$

Heptamer : Y. Horibe *et al*., Phys. Rev. Lett. 96, 086406 (2006).

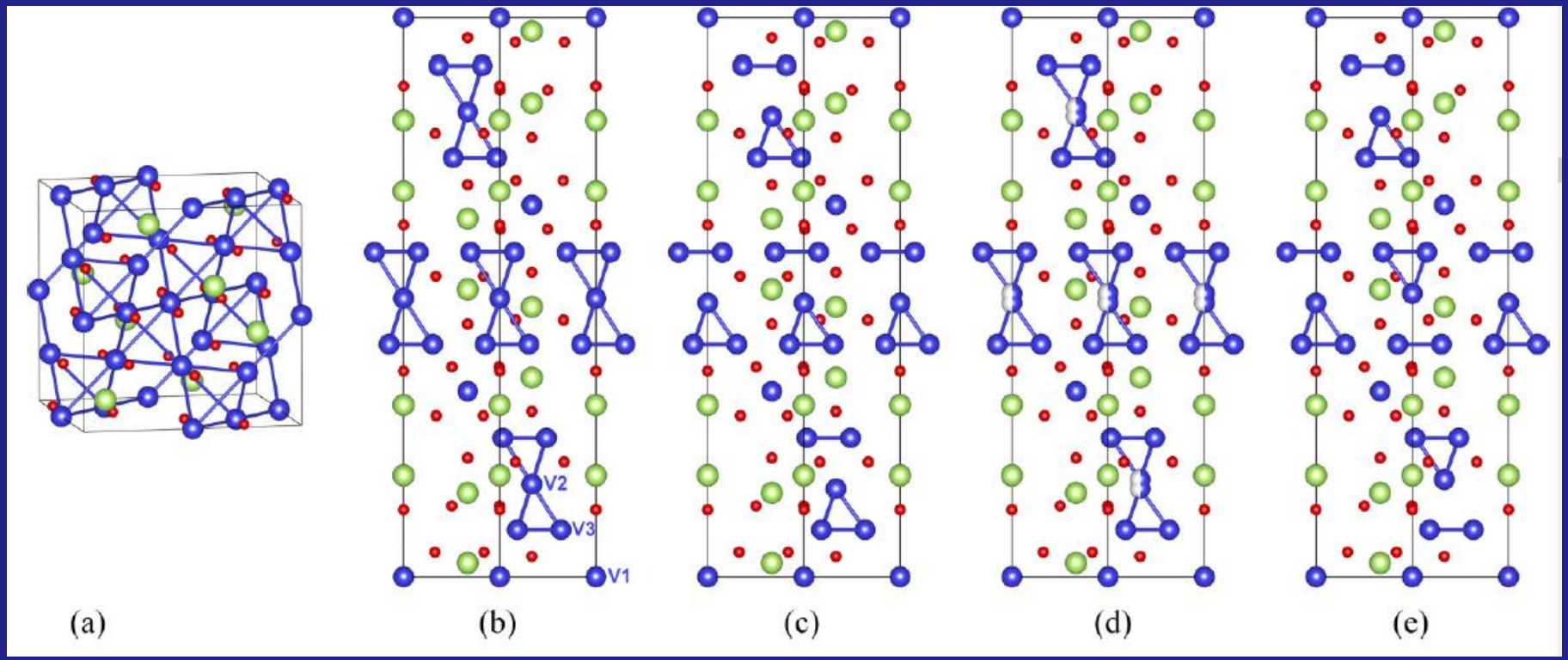


Tetramer + trimer : A. J. Browne, S. A. J. Kimber, and J. P. Attfield, Phys. Rev. Mater. **1**, 052003(R) (2017).

# Orbitally induced Peierls transition (tetramer + trimer)

$AlV_2O_4$

kagome layer (1,-1,0) (0,1,-1) (1,0,-1)

yz:1/4 filled band along (0,1,1)
1/2 filled band along (0,1,-1)

xy:1/4 filled band along (1,1,0)
1/2 filled band along (1,-1,0)

zx:1/4 filled band along (1,0,1)
1/2 filled band along (1,0,-1)

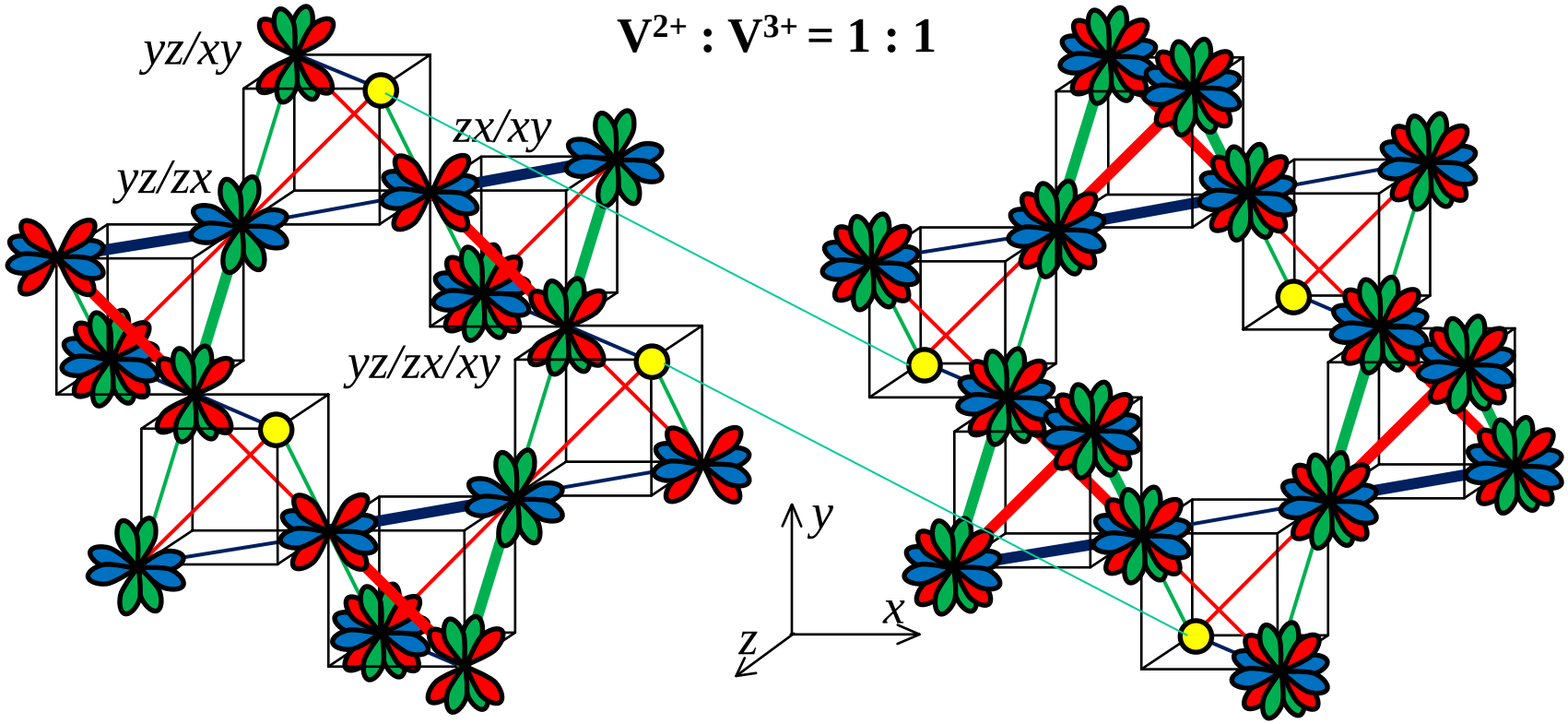

# β-pyrochlore $CsW_2O_6$

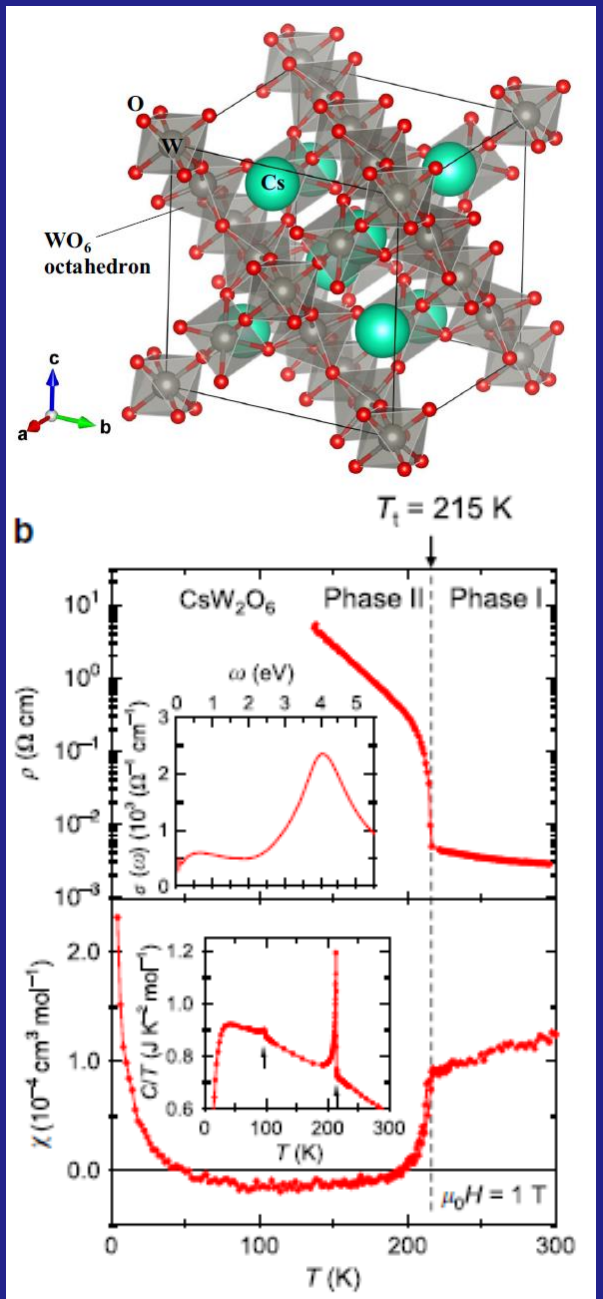


corner-sharing $WO_6$
metal-insulator transition
at 215 K

D. Hirai *et al.*,
Phys. Rev. Lett. 110,
166402 (2013)

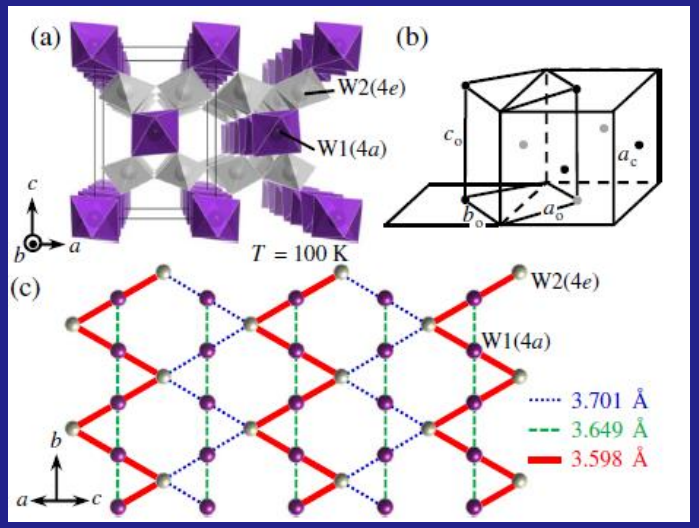


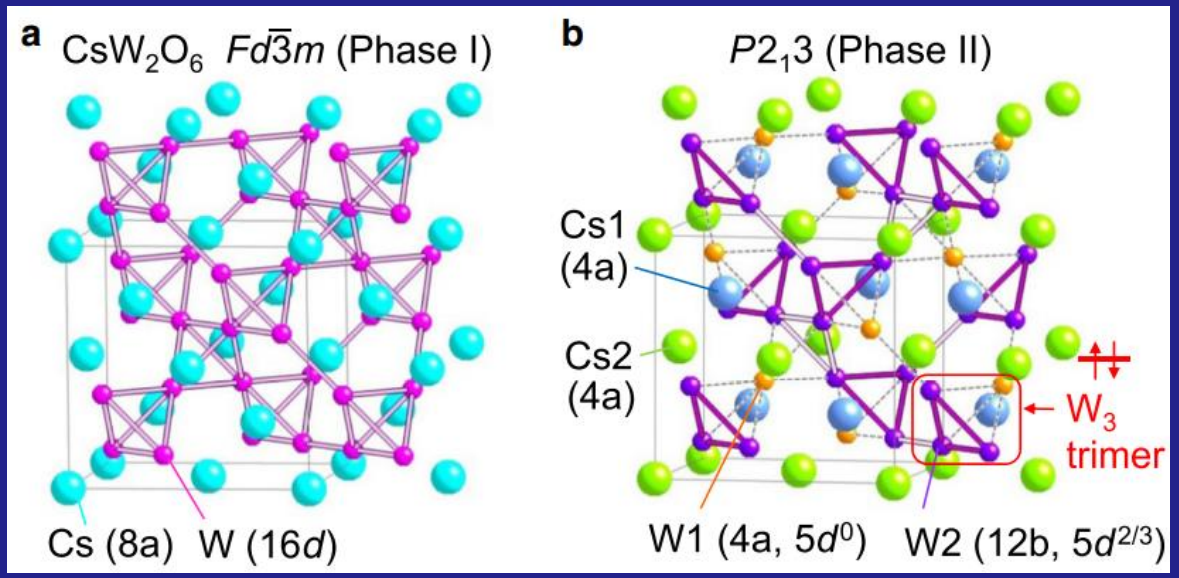


W trimers are formed below 215 K.
Y. Okamoto *et al.*, Nat. Commun. **11**, 3144 (2020).

# β-pyrochlore $CsW_2O_6$

**Why the behavior of β-pyrochlore $CsW_2O_6$ (0.5 $t_{2g}$ electron per W) is different from those of spinel $CuIr_2S_4$ and $LiRh_2O_4$ (0.5 $t_{2g}$ hole per Ir/Rh) ?**

**→ corner sharing *versus* edge sharing**

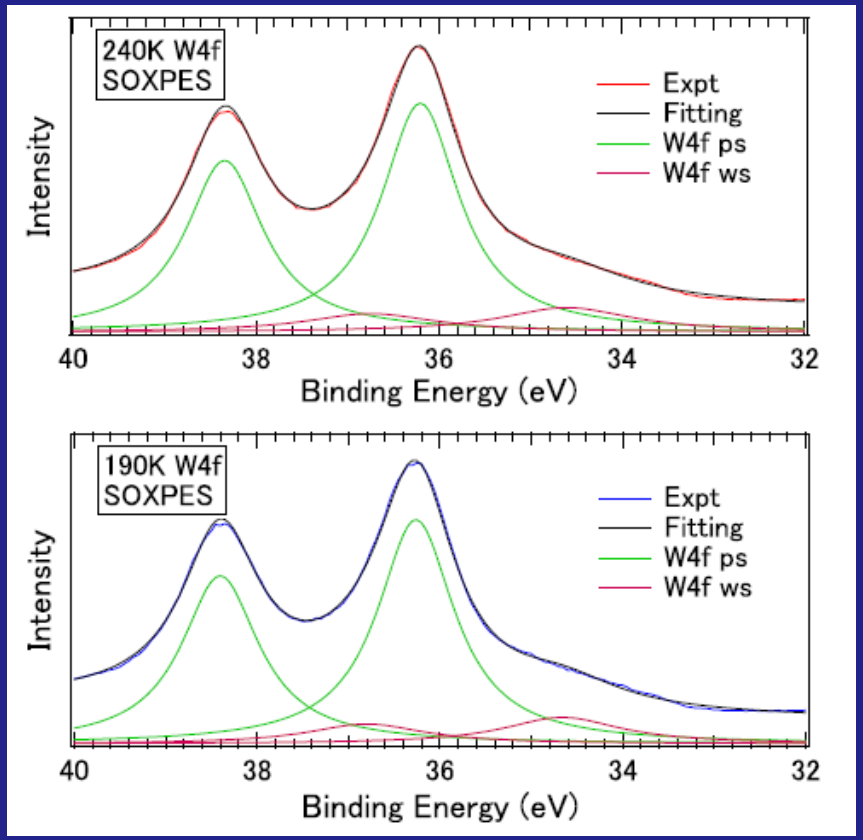


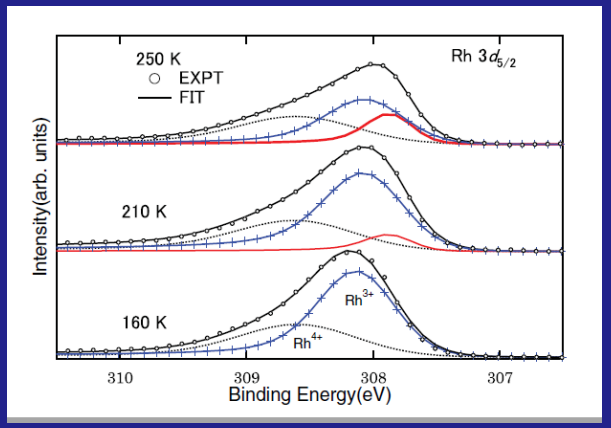


**$Rh^{3+}$ : $Rh^{4+}$ = 1 : 1**

Y. Nakatsu et al., Phys. Rev. B **83**, 115120 (2011).

**$W^{5+}$ : $W^{6+}$ is expected to be 1 : 1 inconsistent with the XPS result**

**W 5d electrons are highly itinerant.**

**→ well- and poorly-screened peaks**

R. Nakamura *et al.*, Phys. Rev. B **106**, 195104 (2022).

Theory

Peierls mechanism: S. V. Streltsov *et al.*, Phys. Rev. B, 94, 241101(R) (2016)

Flat band+spin-orbit interaction: H. Nakai and C. Hotta, Nat. Commun. **13**, 579 (2022)

# β-pyrochlore $CsW_2O_6$

Theory

Peierls mechanism: S. V. Streltsov *et al*., Phys. Rev. B 94, 241101(R) (2016)

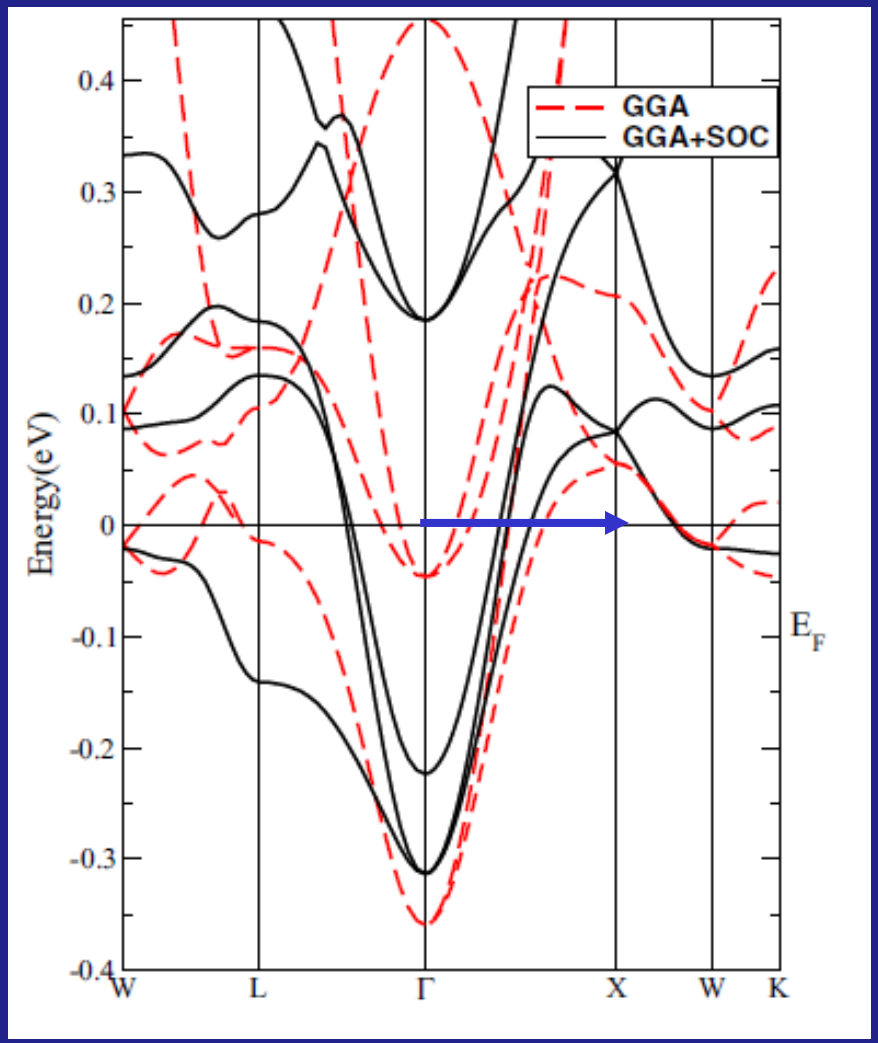


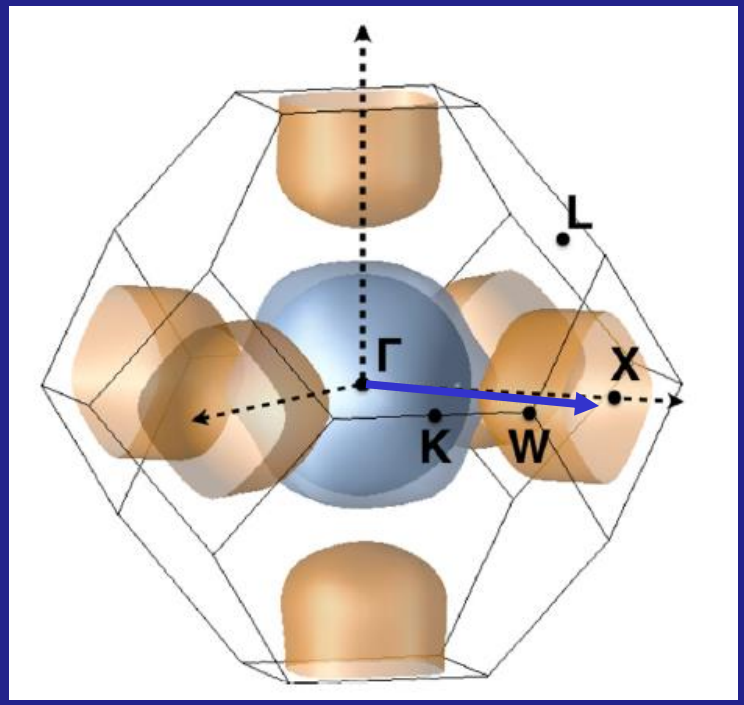

# Effect of spin-orbit interaction in $t_{2g}^{1}$ configuration

$$-\frac{i}{\sqrt{2}}[\Psi_{322}(r,\theta,\phi)-\Psi_{32-2}(r,\theta,\phi)]=\frac{r^2}{81\sqrt{2\pi}a_0^{\frac{7}{2}}}e^{-\frac{r}{3a_0}}\sin^2\theta\sin 2\phi \qquad xy$$

Corresponding to $m$=0

$$\frac{1}{\sqrt{2}}[\Psi_{321}(r,\theta,\phi)+\Psi_{32-1}(r,\theta,\phi)]=\frac{2r^2}{81\sqrt{2\pi}a_0^{\frac{7}{2}}}e^{-\frac{r}{3a_0}}\sin\theta\cos\theta\cos\phi \qquad zx$$

$$\frac{i}{\sqrt{2}}[\Psi_{321}(r,\theta,\phi)-\Psi_{32-1}(r,\theta,\phi)]=\frac{2r^2}{81\sqrt{2\pi}a_0^{\frac{7}{2}}}e^{-\frac{r}{3a_0}}\sin\theta\cos\theta\sin\phi \qquad yz$$

$yz+izx$ $m$=1

$yz-izx$ $m$=-1

$$H_{SO,\uparrow\uparrow}=\begin{pmatrix}0 & 0 & 0\\ 0 & 0 & -i\lambda/2\\ 0 & i\lambda/2 & 0\end{pmatrix} \qquad H_{SO,\uparrow\downarrow}=\begin{pmatrix}0 & -i\lambda/2 & \lambda/2\\ i\lambda/2 & 0 & 0\\ -\lambda/2 & 0 & 0\end{pmatrix}$$

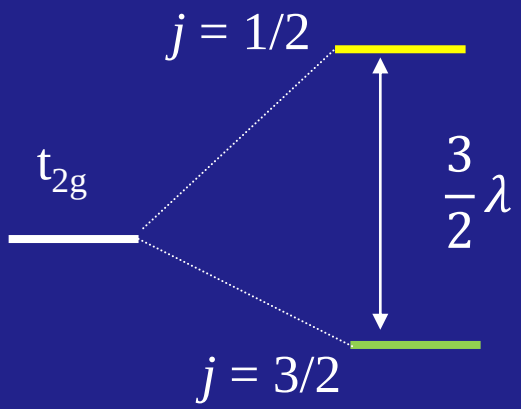


$$\frac{1}{\sqrt{3}}xy\uparrow+\frac{1}{\sqrt{3}}[yz+izx]\downarrow \qquad \frac{1}{\sqrt{3}}xy\downarrow-\frac{1}{\sqrt{3}}[yz-izx]\uparrow$$

$$\frac{1}{\sqrt{2}}[yz+izx]\uparrow \qquad \frac{2}{\sqrt{6}}xy\uparrow-\frac{1}{\sqrt{6}}[yz+izx]\downarrow$$

$$\frac{2}{\sqrt{6}}xy\downarrow+\frac{1}{\sqrt{6}}[yz-izx]\uparrow \qquad \frac{1}{\sqrt{2}}[yz-izx]\downarrow$$

S. Sugano, Y. Tanabe, A. Kamimura, *Multiplets of Transition-Metal Ions in Crystals*

# β-pyrochlore $CsW_2O_6$

**triangle of corner sharing $WO_6$ octahedra**

**spin-orbit interaction becomes more important**

$$\frac{1}{\sqrt{2}}[y'z' + iz'x'] \uparrow \qquad \frac{1}{\sqrt{2}}[y'z' - iz'x'] \downarrow$$

**Assuming straight W-O-W bond,**
**1/4 filled band along (1,0,1) and (1,0,-1)**

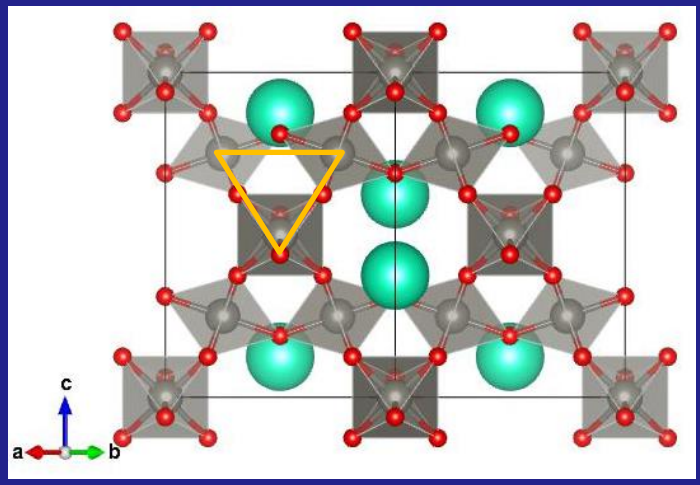


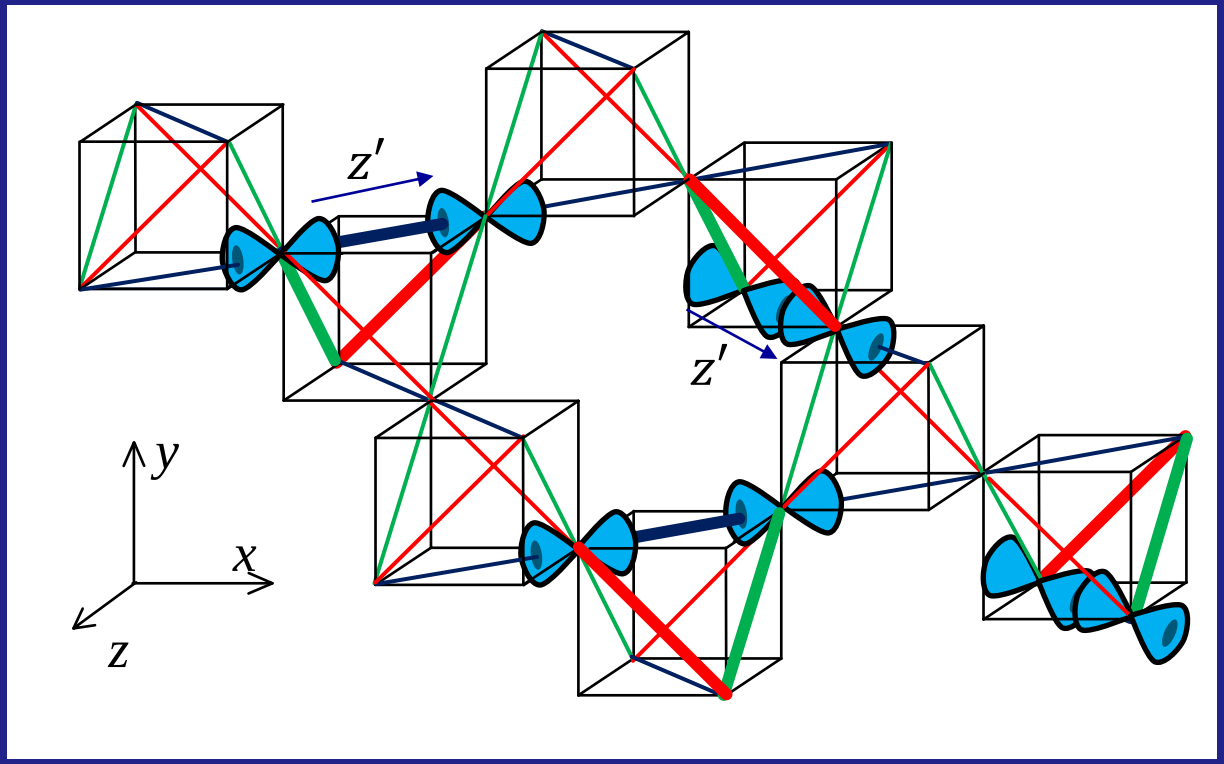

# β-pyrochlore $CsW_2O_6$

**zig-zag structure**

$$\frac{1}{\sqrt{2}}[y'z' + iz'x'] \uparrow \quad \frac{1}{\sqrt{2}}[y'z' - iz'x'] \downarrow$$

**“half-filled” zig-zag**

D. Hirai *et al.*, Phys. Rev. Lett. 110, 166402 (2013)

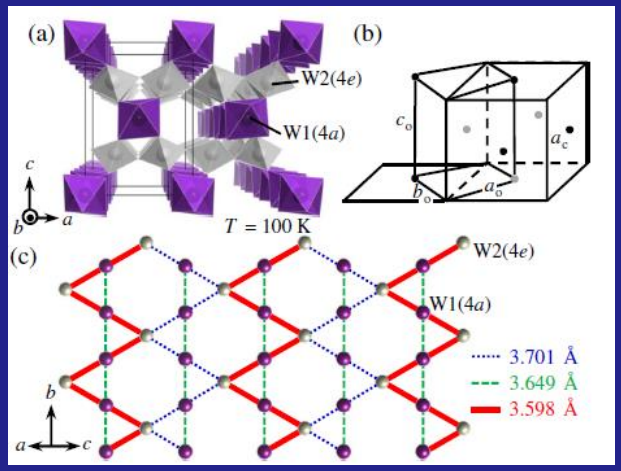


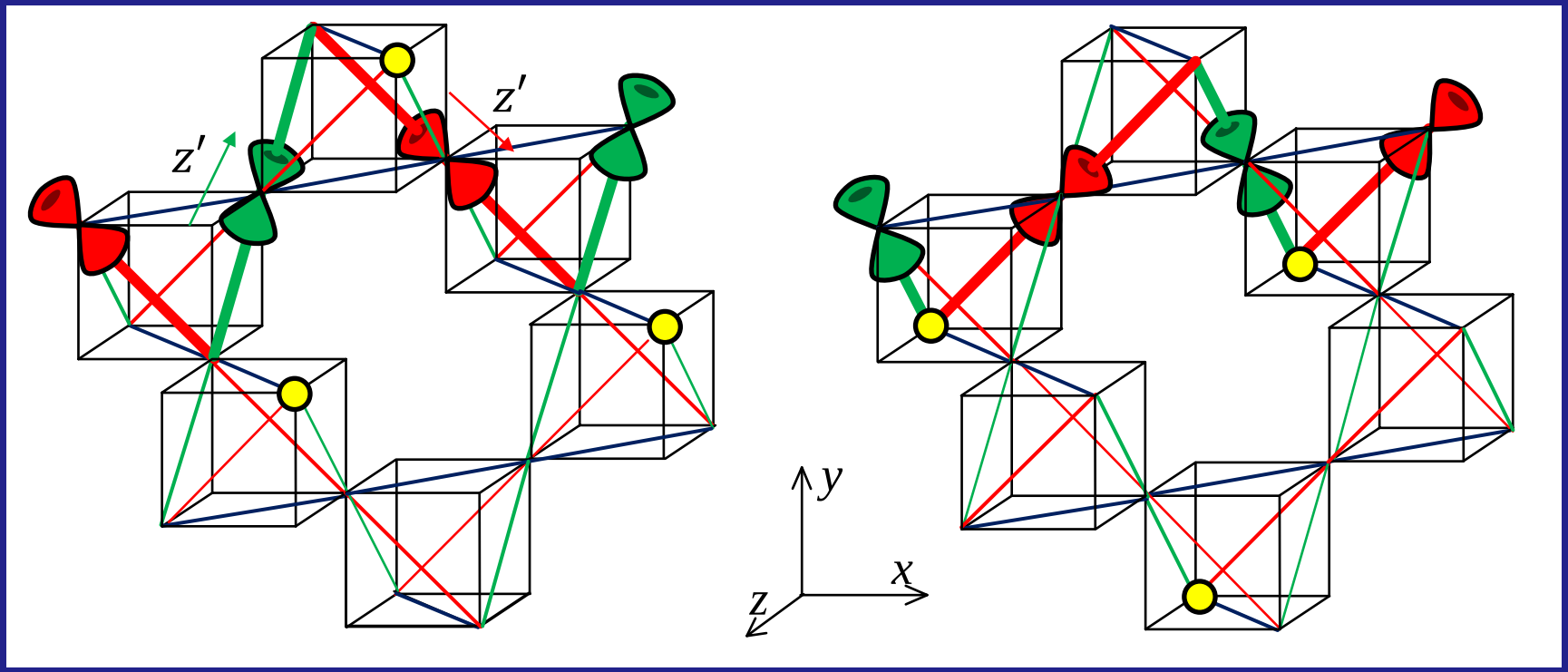

# α-pyrochlore $Tl_2Ru_2O_7$

**zig-zag structure for $Ru^{4+}$ (S=1)**

S. Lee, J.-G. Park, D. I. Khomskii *et al.*, Nat. Mater. 5, 471 (2006)

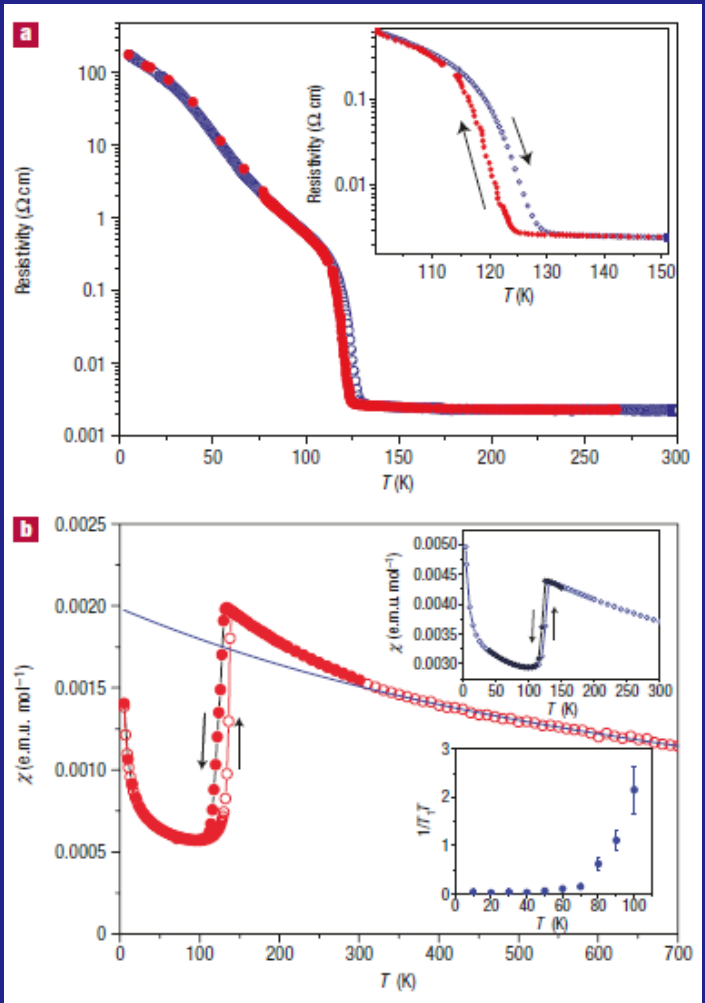


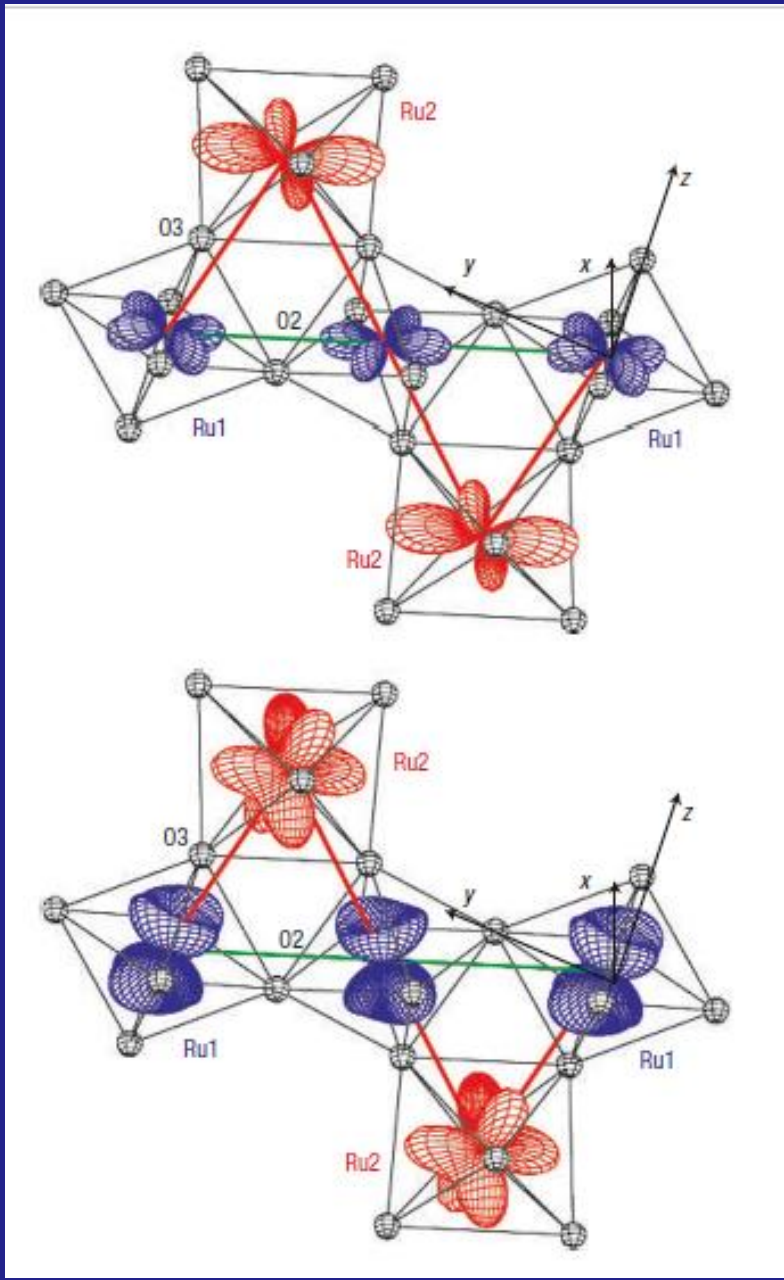

# α-pyrochlore $Tl_2Ru_2O_7$

**two holes per Ru**

$Ru^{4+}$ ($d^4$)

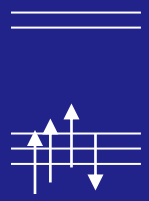

$$\frac{1}{\sqrt{2}}[y'z' + iz'x'] \uparrow \qquad x'y' \uparrow$$

$$\frac{1}{\sqrt{2}}[y'z' - iz'x'] \downarrow \qquad x'y' \downarrow$$

**“filled” zig-zag**

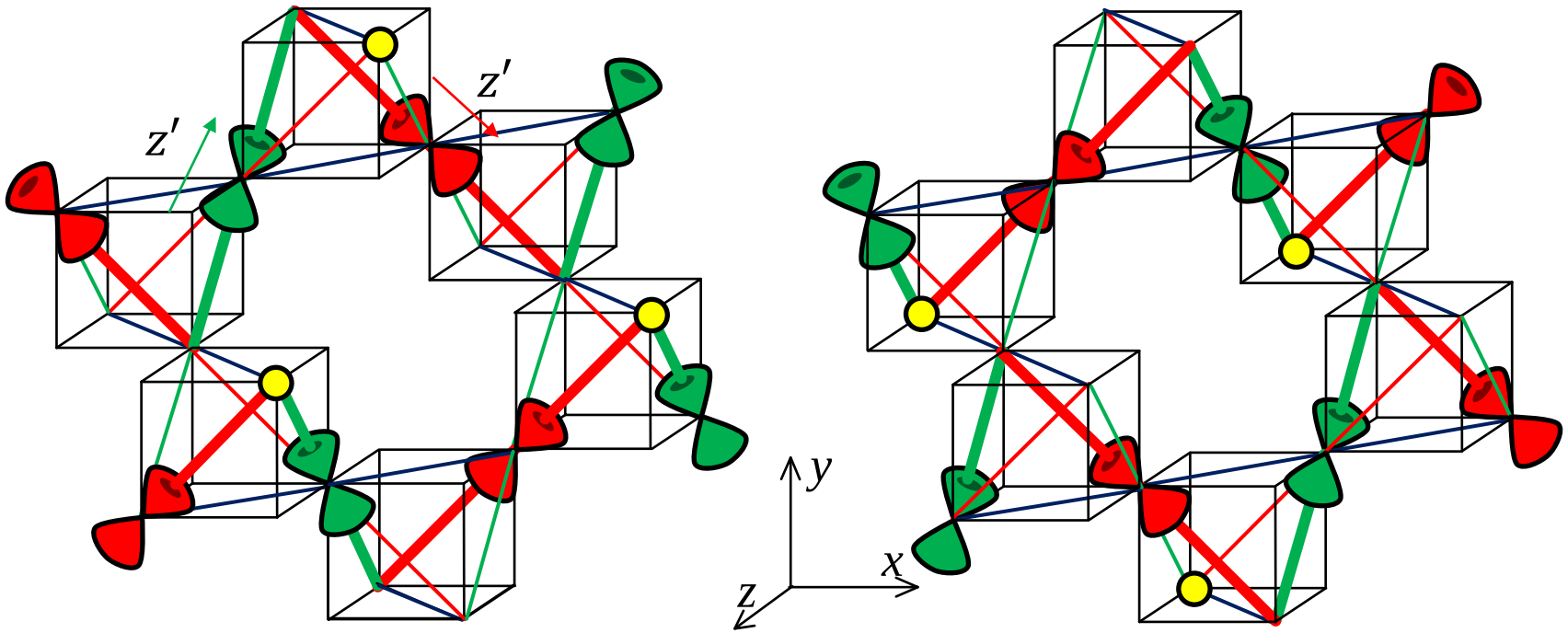

# Outline

1. Electron-phonon interaction and Peierls transition
   (not in the text, for undergraduate)

2. Orbitally induced Peierls transition: Case study on $CuIr_2S_4$ (section 2.1)

3. Toy models on square/triangular lattice (sections 2.2 and 2.3)

4. Application to Spinel and Pyrochlore materials (sections 3.1 and 3.2)

5. Application to triangular/honeycomb/kagome lattice systems (3.3/3.4/3.5)

6. Summary

# Transition-metal oxides with edge-sharing octahedra

**Rutile(1D)**

$VO_2$: $V^{4+}$ $d^1$ $T_{MI}$=340 K M-NMI

**Hollandite(1D)**

$K_2V_8O_{16}$: $V^{4+}$,$V^{3+}$ $d^1$,$d^2$ $T_{MI}$=210 K M-NMI

$K_2Cr_8O_{16}$: $Cr^{4+}$,$Cr^{3+}$ $d^2$,$d^3$ $T_{MI}$=95 K FM-FMI

**triangular lattice (2D)**

$NaTiO_2$ $Ti^{3+}$ $d^1$ $T_{NM}$ = 260 K I-NMI

$LiVO_2$ $V^{3+}$ $d^2$ $T_{NM}$ = 500 K I-NMI

$BaV_{10}O_{15}$ $V^{3+}$ ,$V^{2+}$ $d^2$,$d^3$ $T_{MI}$=130 K M-AFI

$Na_xCoO_2$ $Co^{4+}$,$Co^{3+}$ $d^5$,$d^6$

**honeycomb lattice (2D)**

$Li_2RuO_3$ $Ru^{4+}$ $d^4$ $T_{MI}$ = 540 K M-NMI

$Na_2IrO_3$ $Ir^{4+}$ $d^5$

**Spinel (3D)**

$MgTi_2O_4$ $Ti^{3+}$ $d^1$ $T_{MI}$ = 260 K M-NMI

$ZnV_2O_4$ $V^{3+}$ $d^2$

$AlV_2O_4$ $V^{3+}$, $V^{2+}$ $d^2$,$d^3$

$LiRh_2O_4$ $Rh^{4+}$,$Rh^{3+}$ $d^5$,$d^6$ $T_{MI}$=170 K M-NMI

# Transition-metal chalcogenides/pnictides

| | | | | |
|---|---|---|---|---|
| **q-1D** | | | | |
| $(TaSe_4)_2I$ | $Ta^{5+}$, $Ta^{4+}$ | $d^0$, $d^1$ | $T_{MI}$=260 K | M-NMI |
| $BaVS_3$ | $V^{4+}$ | $d^1$ | $T_{MI}$=74 K, $T_N$=35 K | |
| $BaFe_2S_3$ | $Fe^{2+}$ | $d^6$ | $T_S$=200 K, $T_N$=120 K | |
| $Ta_2NiSe_5$ | $Ni^{0+}$, $Ta^{5+}$ | $d^{10}$ , $d^0$ | $T_S$=328 K | NMI-NMI |
| **q-2D** | | | | |
| $TiSe_2$ | $Ti^{4+}$ | $d^0$ | $T_S$=200 K | M-M |
| $VSe_2$ | $V^{4+}$ | $d^1$ | $T_S$=110 K | M-M |
| $TaS_2$ | $Ta^{4+}$ | $d^1$ | $T_S$=200-350 K | M-M |
| $LiVS_2$ | $V^{3+}$ | $d^2$ | $T_{MI}$=305 K | M-NMI |
| $CrSe_2$ | $Cr^{4+}$ | $d^2$ | $T_{MI}$=165-180 K | M-AFI |
| $IrTe_2$ | $Ir^{4+}$ | $d^5$ | $T_S$=180-280 K | M-M |
| FeSe | $Fe^{2+}$ | $d^6$ | $T_S$=90 K | M-M |
| $BaFe_2As_2$ | $Fe^{2+}$ | $d^6$ | $T_S$=$T_N$=143 K | M-AFM |
| $BaNi_2As_2$ | $Ni^{2+}$ | $d^8$ | $T_S$=130 K | M-M |
| **3D** | | | | |
| RuP | $Ru^{3+}$ | $d^5$ | $T_{MI}$=270 K | M-NMI |
| $CuIr_2S_4$ | $Ir^{4+}$, $Ir^{3+}$ | $d^5$, $d^6$ | $T_{MI}$=226 K | M-NMI |
| NiS | $Ni^{2+}$ | $d^8$ | $T_S$=$T_N$=200 K | M-AFM |

# Structural transition and superconductivity of $IrTe_2$

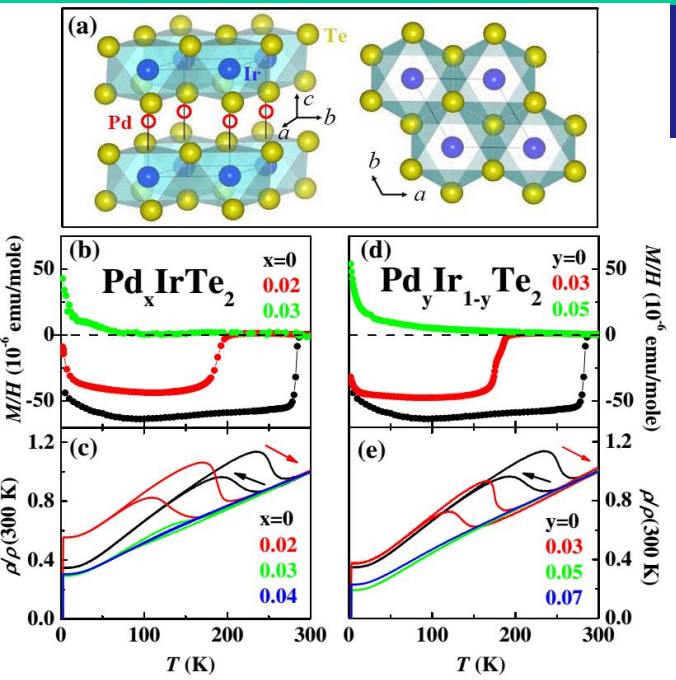


## Structural transition at 280 K

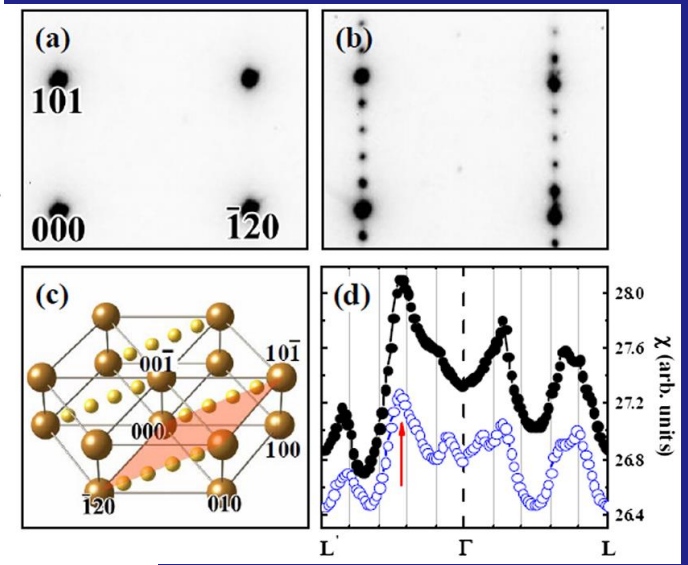


## Pt doping induces superconductivity

S. Pyon *et al.*, J. Phys. Soc. Jpn. **81**, 053701 (2012).

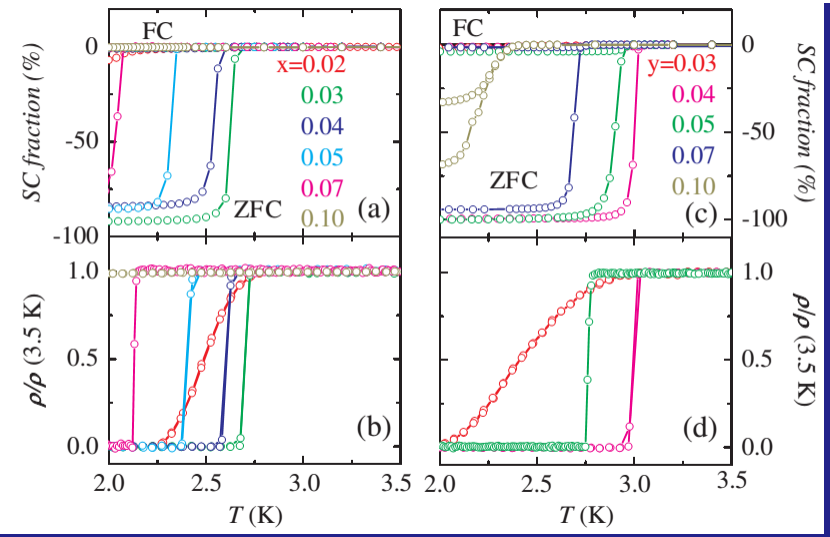


## Charge density wave and superconductivity

J. J. Yang *et al.*, Phys. Rev. Lett. **108**, 116402 (2012).

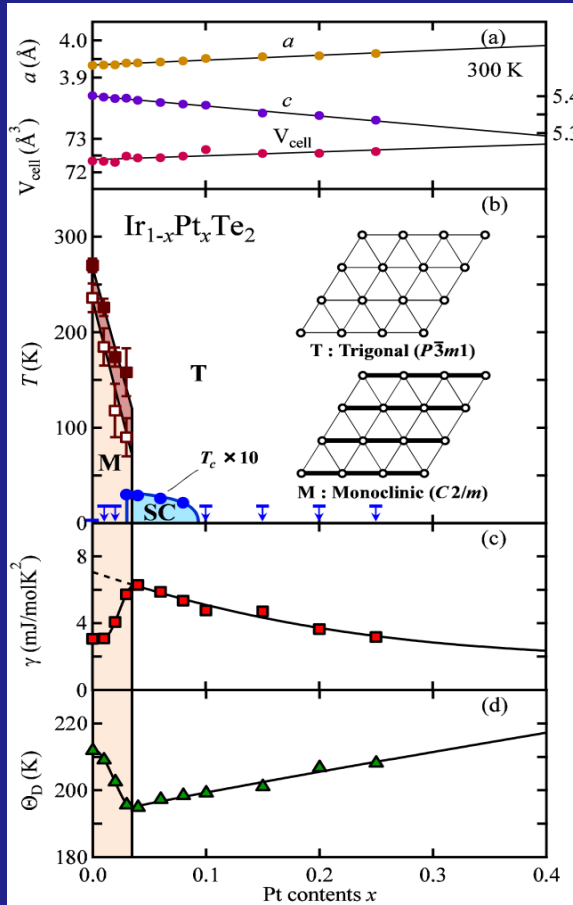

# Charge stripe phase at the low temperature phase

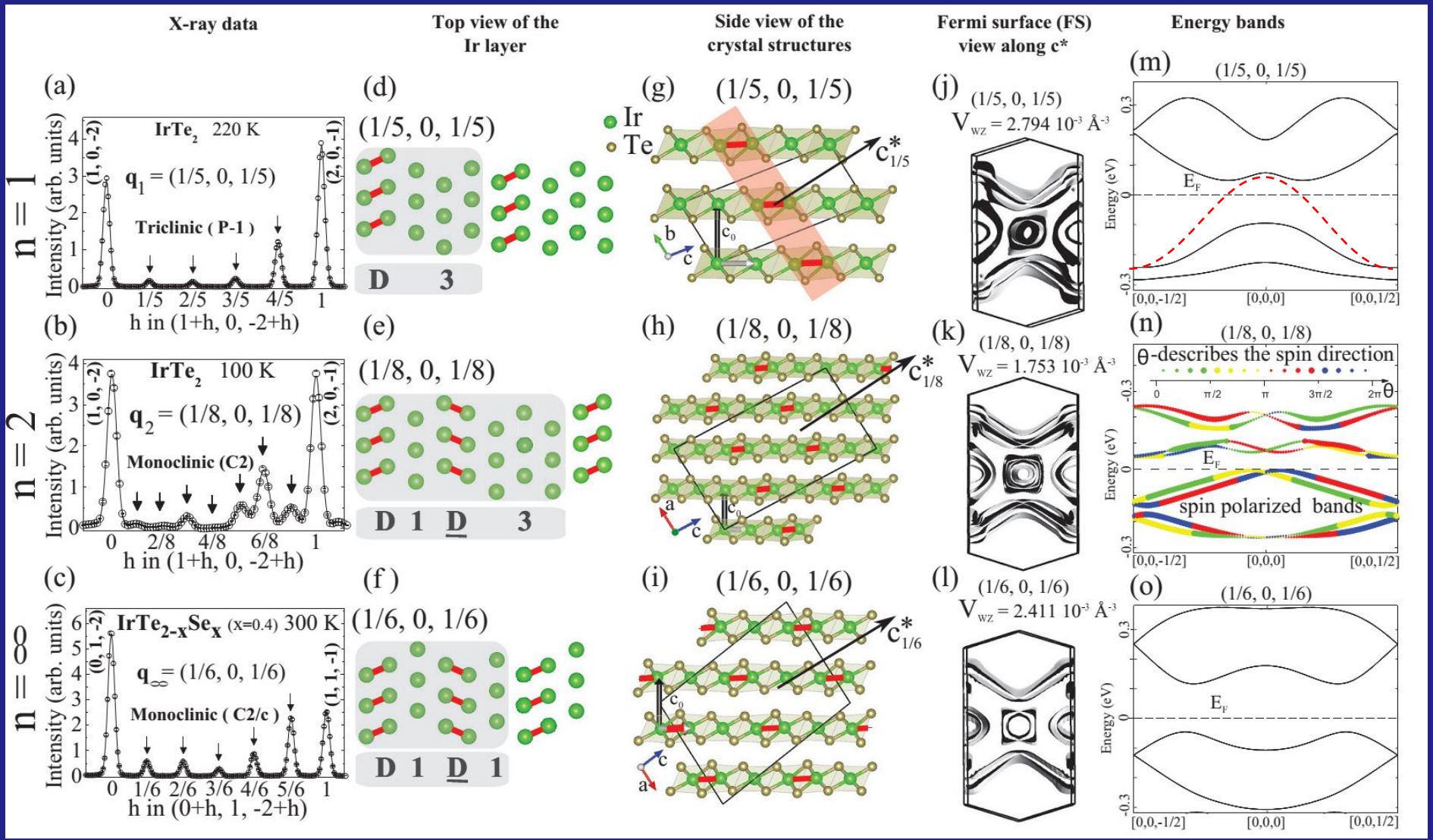


G. L. Pascut *et al.*, Phys. Rev. Lett. **112**, 86402 (2014); Phys. Rev. B **90**, 195122 (2014).
T. Toriyama *et al.*, J. Phys. Soc. Jpn. **83**, 033701 (2014).

# Small but finite charge modulation in $IrTe_2$

**Ir 4*f* XPS close to $Ir^{3+}$**

D. Ootsuki *et al.*, Phys. Rev. B **86**, 014519 (2012).

**Importance of Te 5p hole and p-d hybridization**

**similar to $CaFeO_3$?**

**However, no change in Te 3d XPS**

**Te 3d XAS should be done to detect Te 5p holes!**

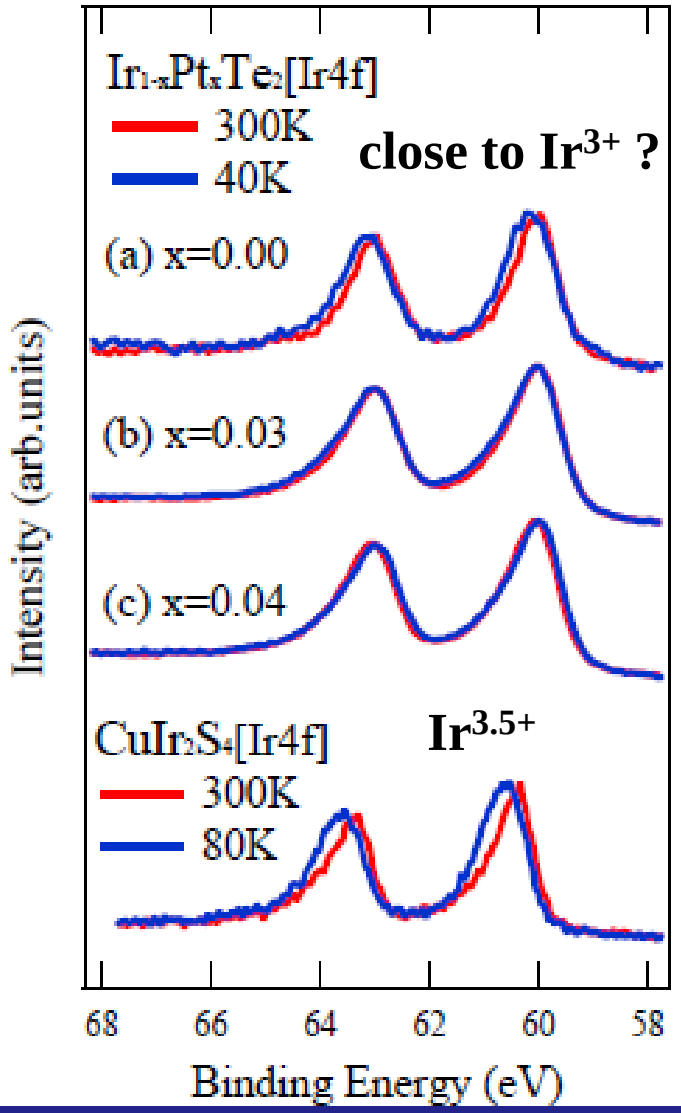


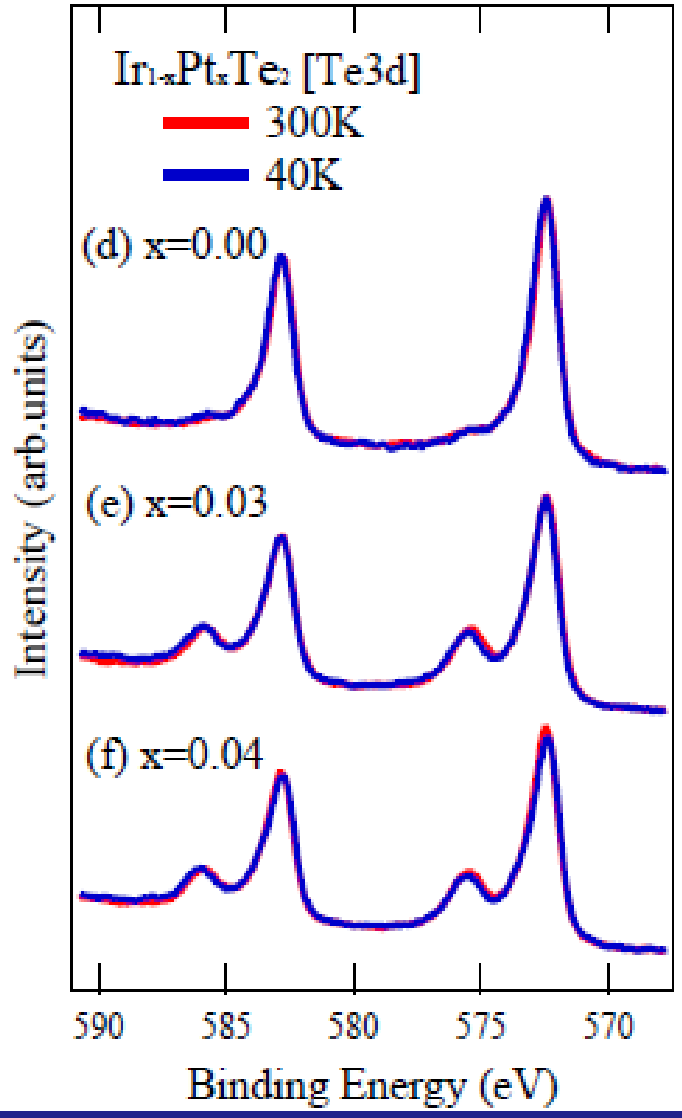

# Te 3d XAS and REXS of $IrTe_2$

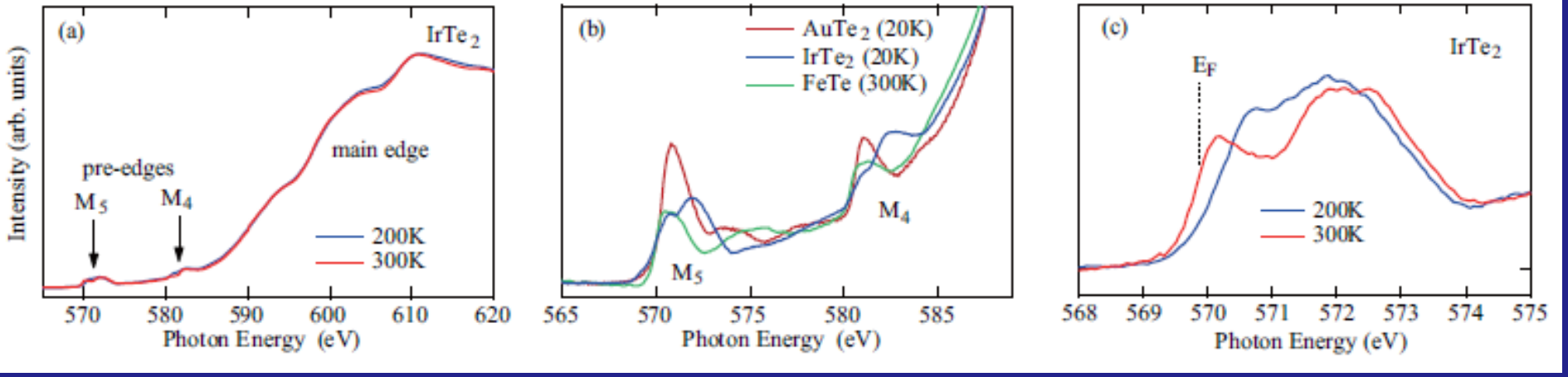


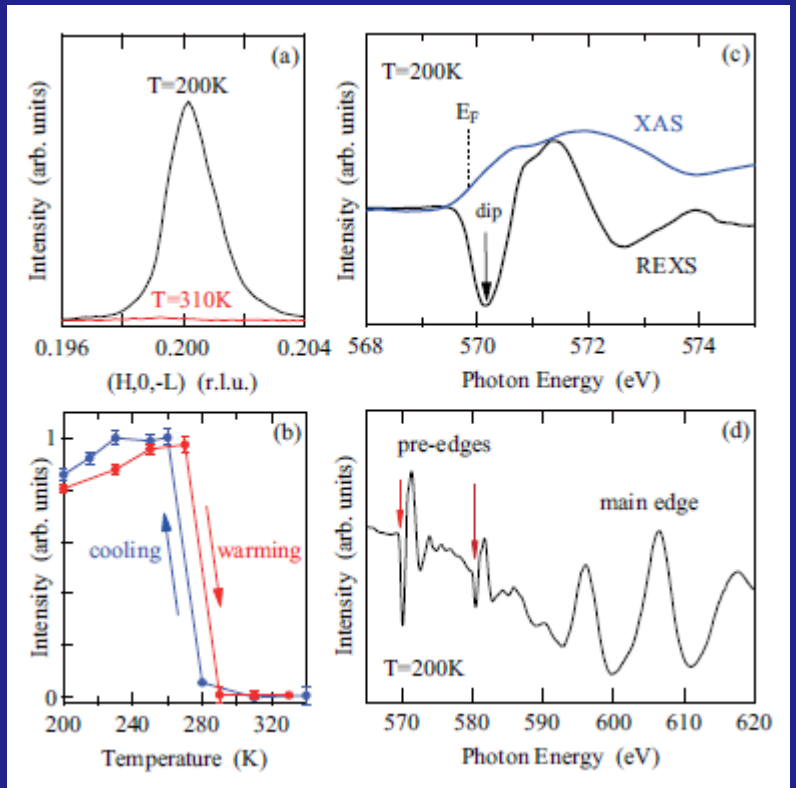


**Te 3d → Te 5p transition**
**Te 5p hole**

**Te 5p band changes across the transition**

**Resonant x-ray scattering at Te 3d**
**Q=(1/5, 0, -1/5)**
**stripe of Te 5p hole**

K. Takubo *et al.*,
Phys. Rev. B **90**, 081104(R) (2014).

# Charge-transfer from Te to Ir

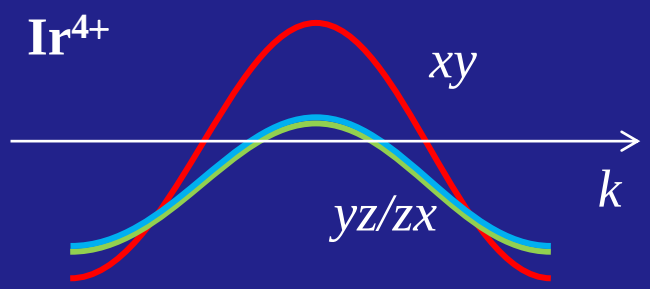


1/2 filled band is difficult

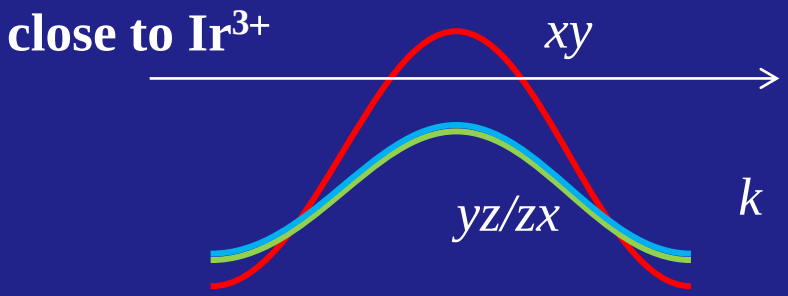


1/5 or 1/6 or 1/8 filled band

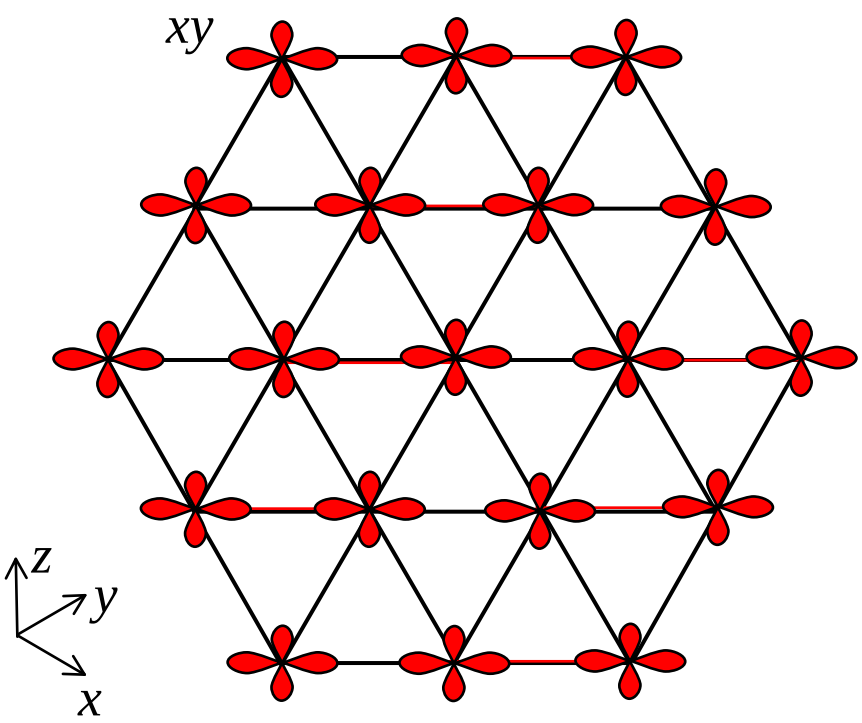


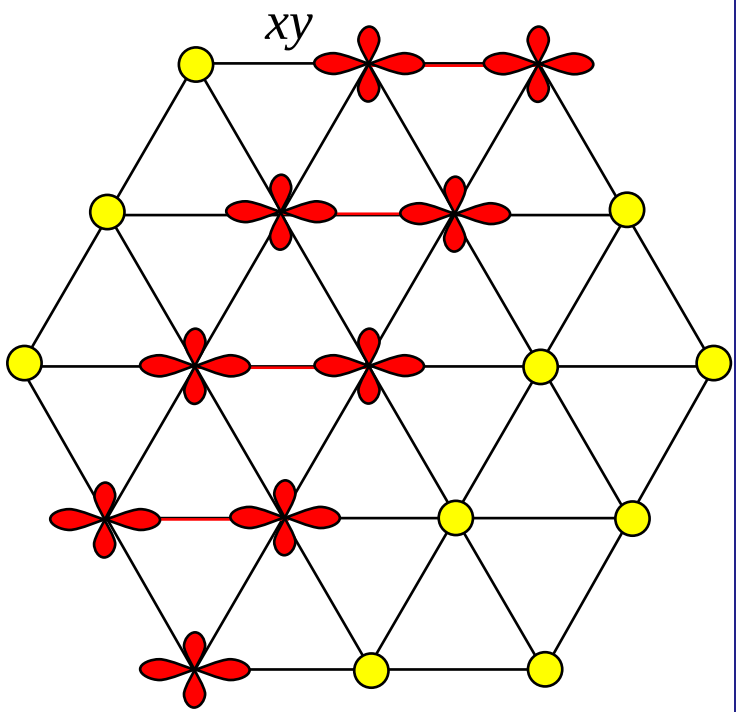

# Spin singlet in $NaTiO_2$ and $NaVO_2$

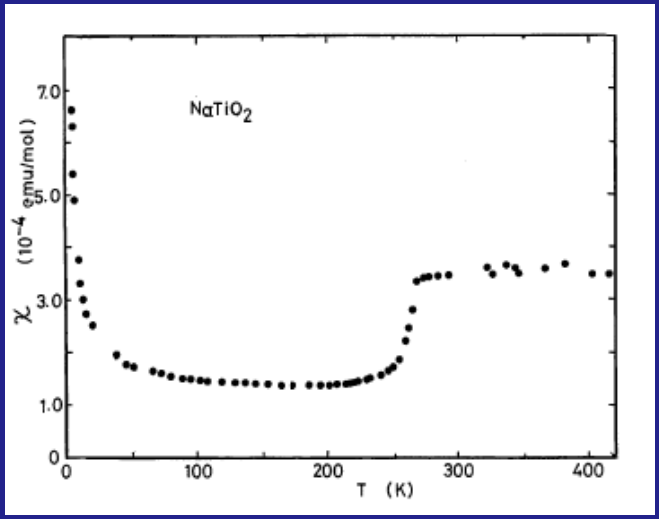


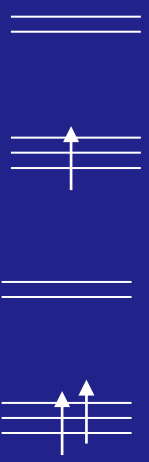


K. Takeda, K. Miyake, K. Takeda, K. Hirakawa, J. Phys. Soc. Jpn. **61**, 2156 (1992).

**nonmagenetic insulator < 260 K**

S. J. Clarke, A. J. Fowkes, A. Harrison, R. M. Ibberson, and M. J. Rosseinsky, Chem. Mater. 10, 372 (1998).

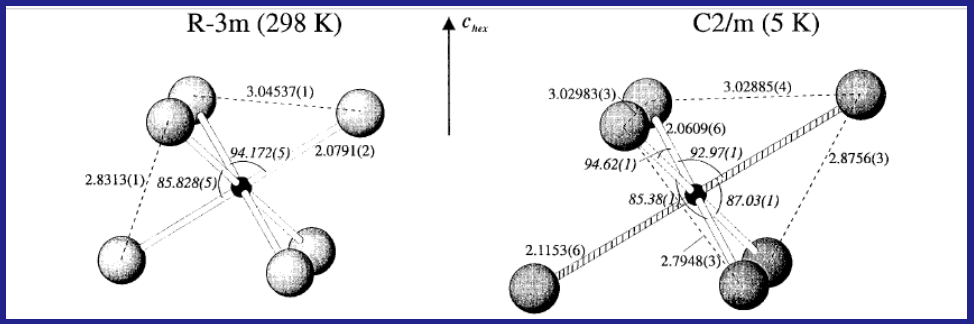


**Jahn-Teller rather than dimerization**

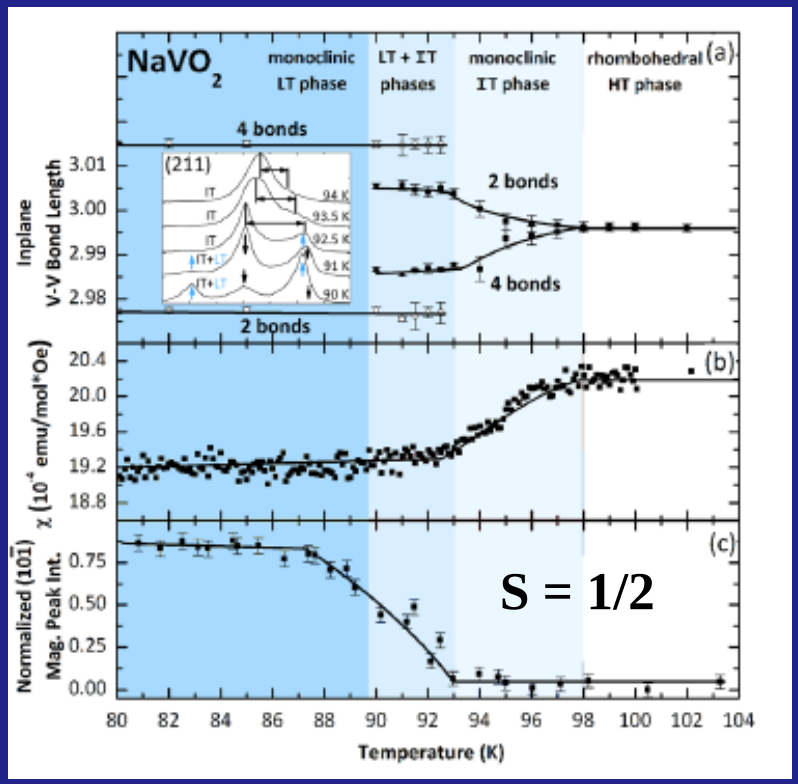


T. M. McQueen *et al.*, Phys. Rev. Lett. **101**, 166402 (2008)

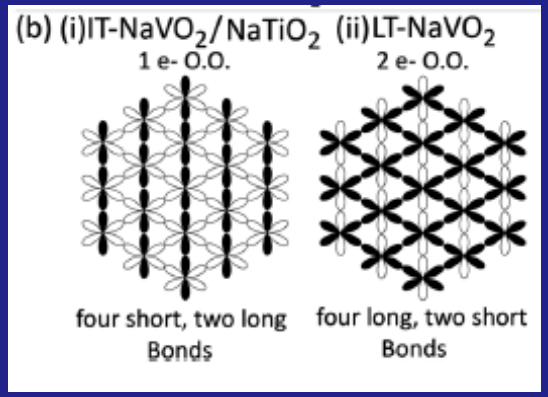


**partial singlet bond**

# Dimerization in $NaTiO_2$ and $NaVO_2$(triangular lattice)

It is difficult to describe the singlet bond by LDA(GGA)+*U*.

**$NaTiO_2$** **$LiVO_2$**

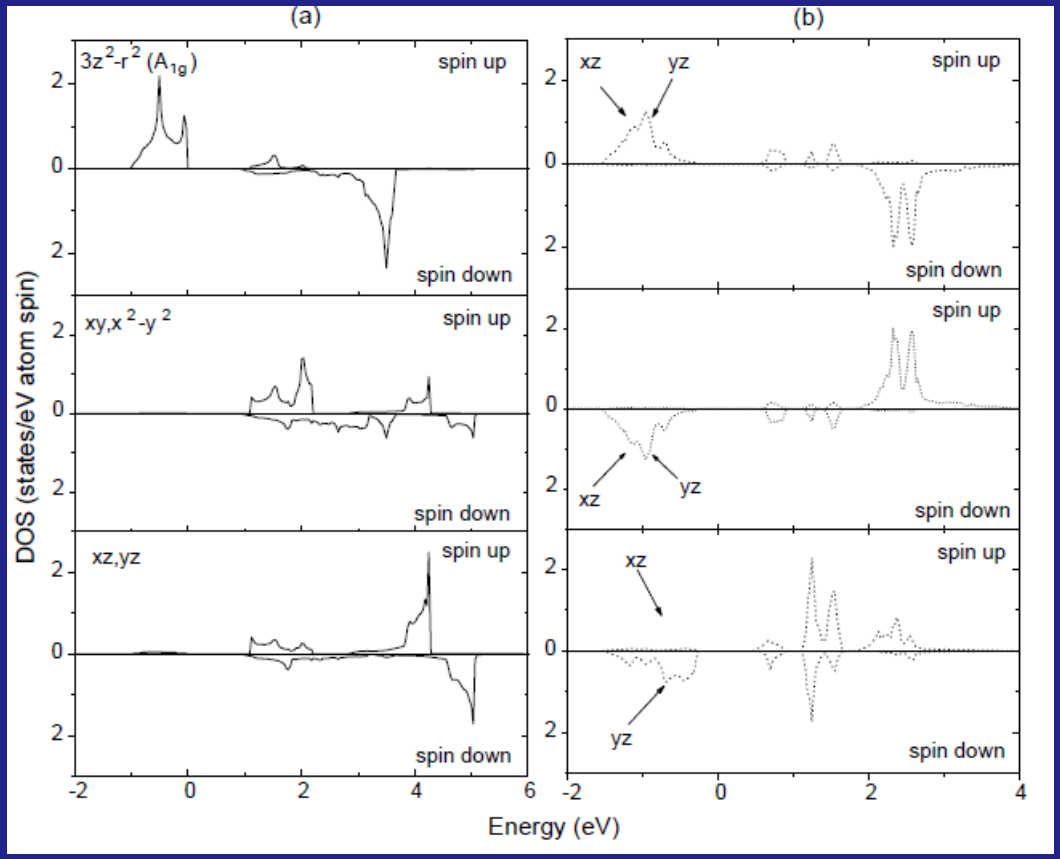


**$NaVO_2$**

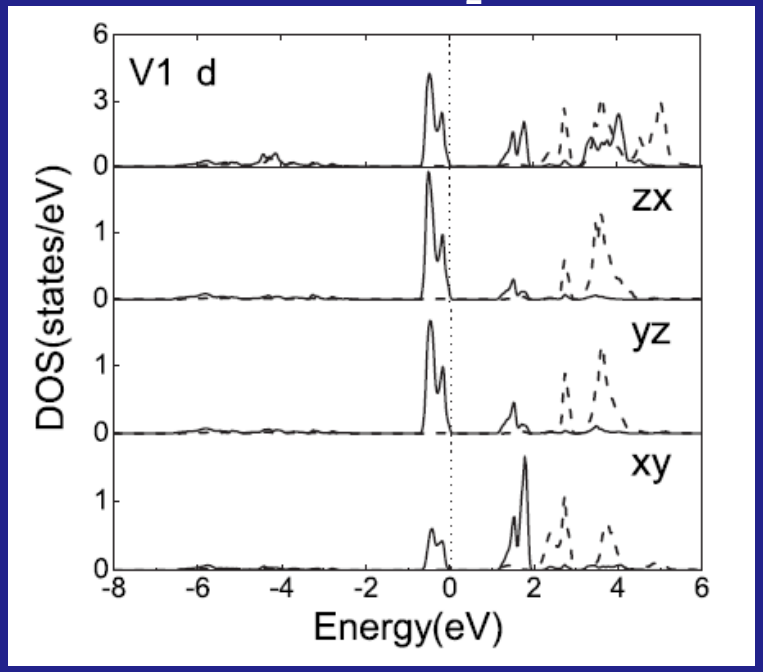


Ting Jia, Guoren Zhang, Zhi Zeng,
H. Q. Lin, Phys. Rev. B 80, 045103 (2009).

S. Yu. Ezhov, V. I. Anisimov, H. F. Pen, D. I. Khomskii,
G. A. Sawatzky, Europhys. Lett. 44, 491 (1998).

# Possible orbital order in $NaTiO_2$

**$NaTiO_2$**

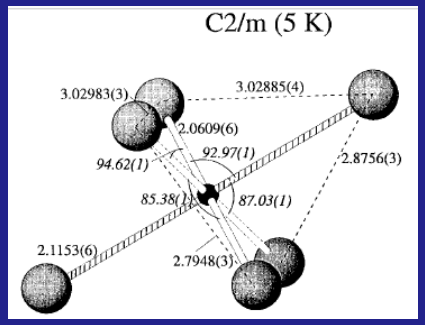


**band picture**

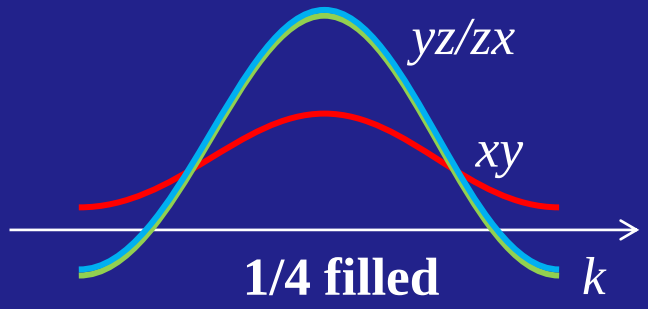


**localized picture**

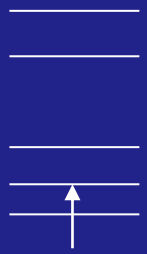

$$\frac{1}{\sqrt{6}}(-2|xy\rangle + |zx\rangle + |yz\rangle)$$

$$\frac{1}{\sqrt{3}}(|xy\rangle + |zx\rangle + |yz\rangle)$$

$$\frac{1}{\sqrt{2}}(|zx\rangle - |yz\rangle)$$

**similar to $MgTi_2O_4$**

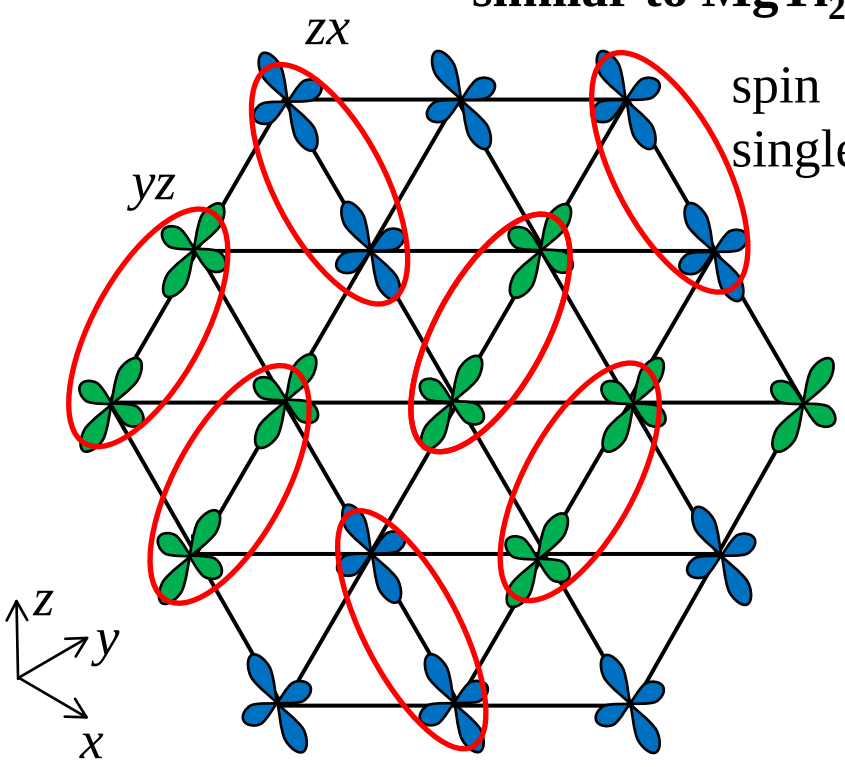


$$\frac{1}{\sqrt{2}}(zx - yz)$$

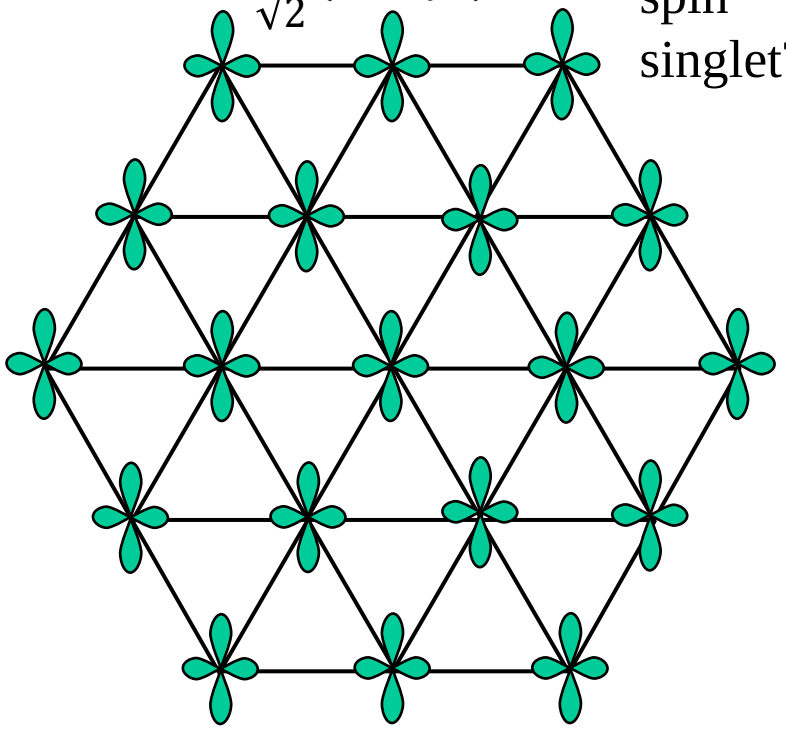

# Possible orbital order in $NaVO_2$

## $NaVO_2$

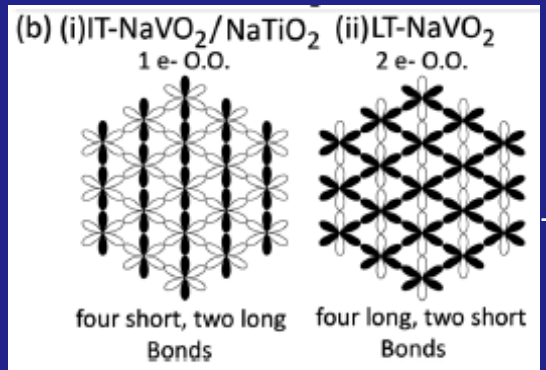


## band picture

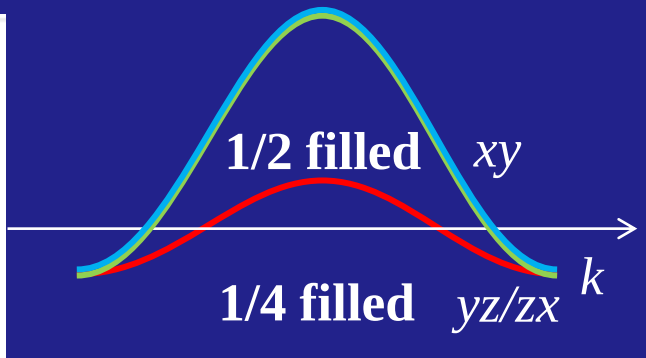


## localized picture

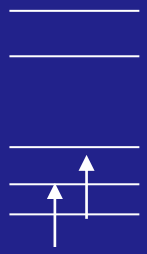

$$\frac{1}{\sqrt{2}}(|zx\rangle - |yz\rangle)$$

$$\frac{1}{\sqrt{6}}(-2|xy\rangle + |zx\rangle + |yz\rangle)$$

$$\frac{1}{\sqrt{3}}(|xy\rangle + |zx\rangle + |yz\rangle)$$

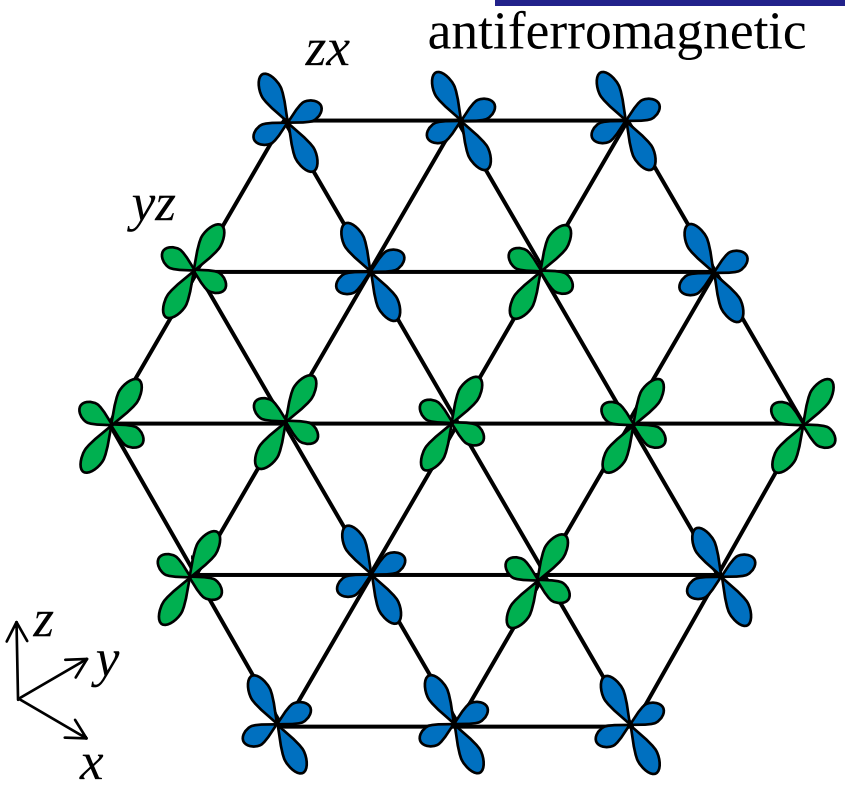


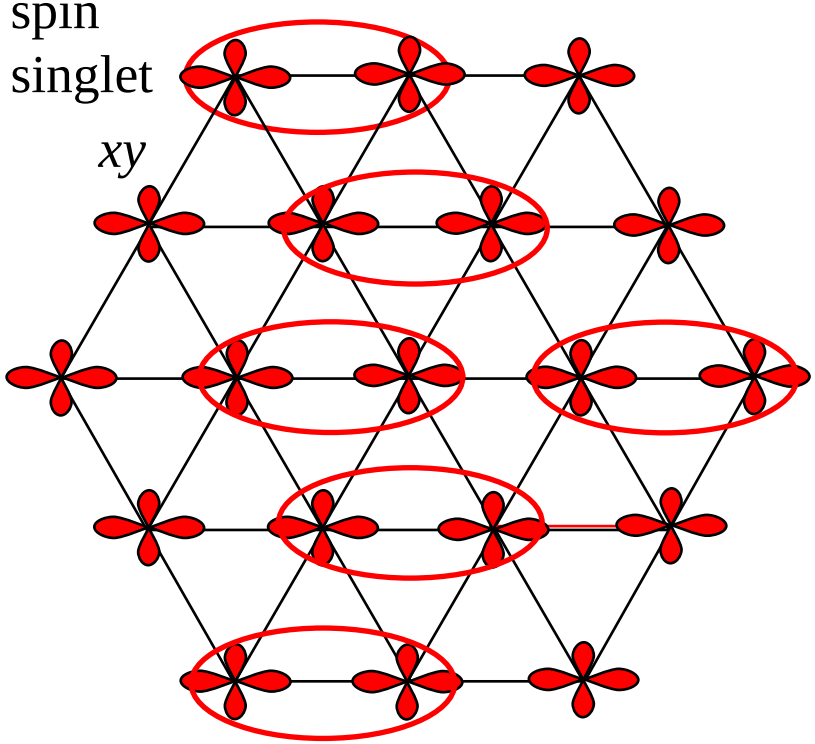

# Trimerization in $LiVO_2$

M. Onoda, T. Naka, and H. Nagasawa,
J. Phys. Soc. Jpn. **60**, 2550 (1991).

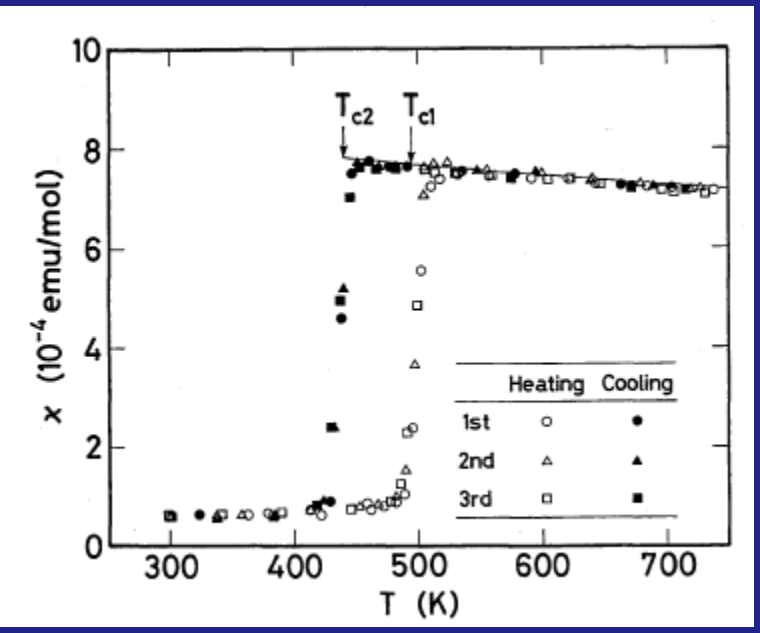


**nonmagenetic insulator < 450 K**

$V^{3+}$ ($d^2$)

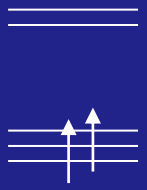

V 2*p* XAS
H. F. Pen *et al.*,
Phys. Rev. B **55**, 15500 (1997).

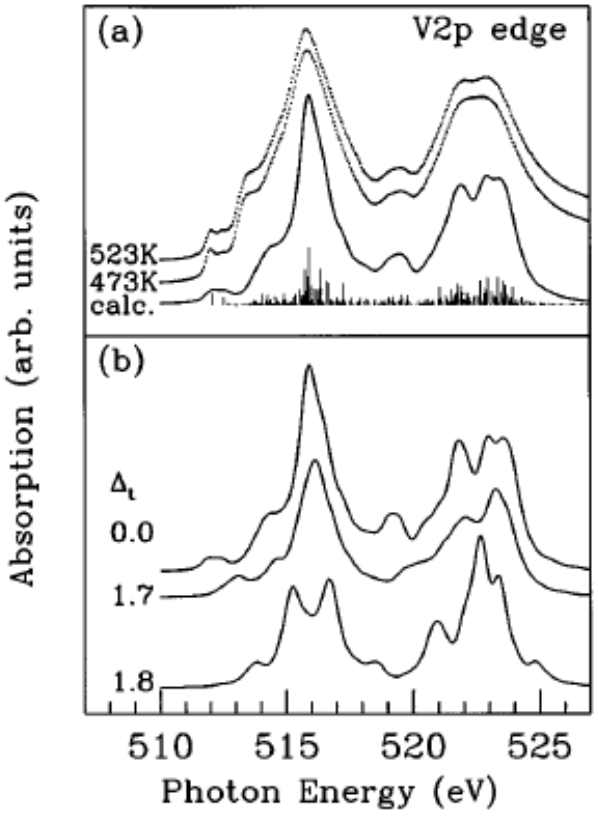


**Multiplet structure**
**→ Hund coupling!**

**V trimerization**

H. F. Pen *et al.*,
Phys. Rev. Lett. **78**, 1323 (1997).

**$V^{3+}$ ($d^2$)- $V^{3+}$ ($d^2$) trimerization is inconsistent with the Hund coupling?**

# Trimerization in $LiVS_2$ (triangular lattice)

N. Katayama *et al.*, Phys. Rev. Lett. 103, 146405 (2009).

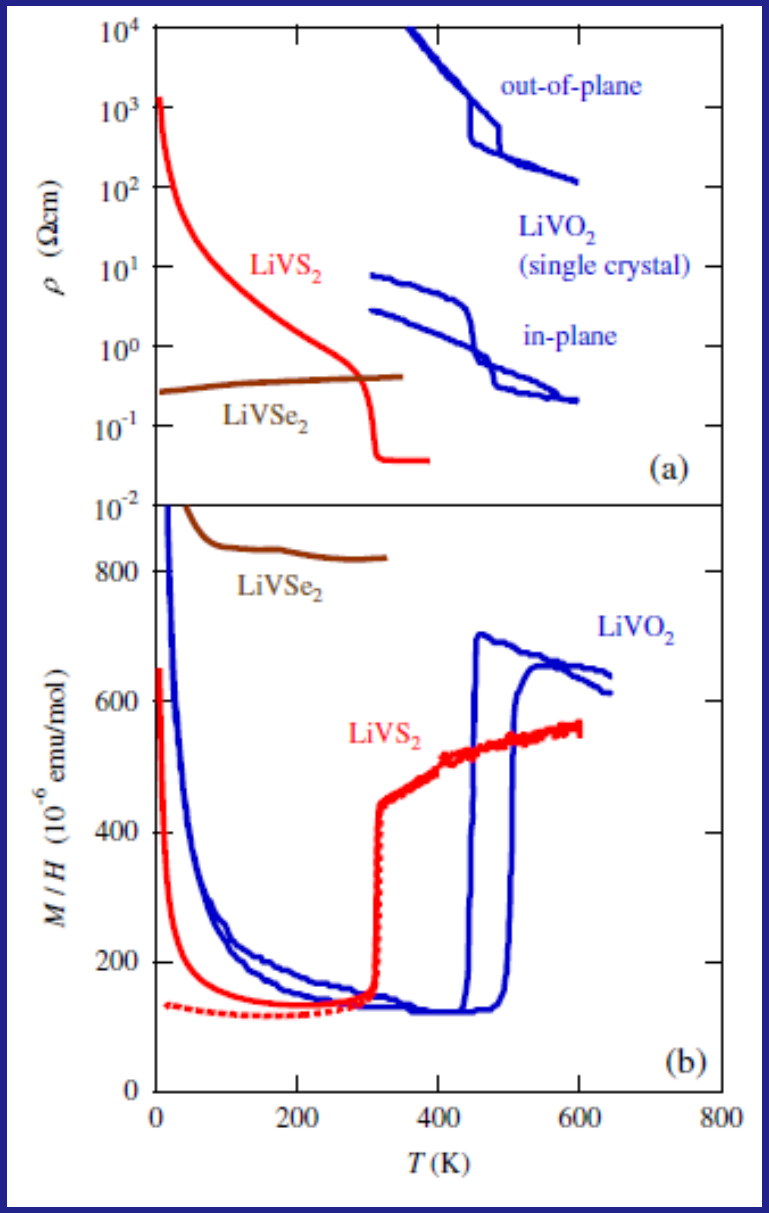


N. Katayama *et al.*,
npj Quantum Mater. 6, 16 (2021)

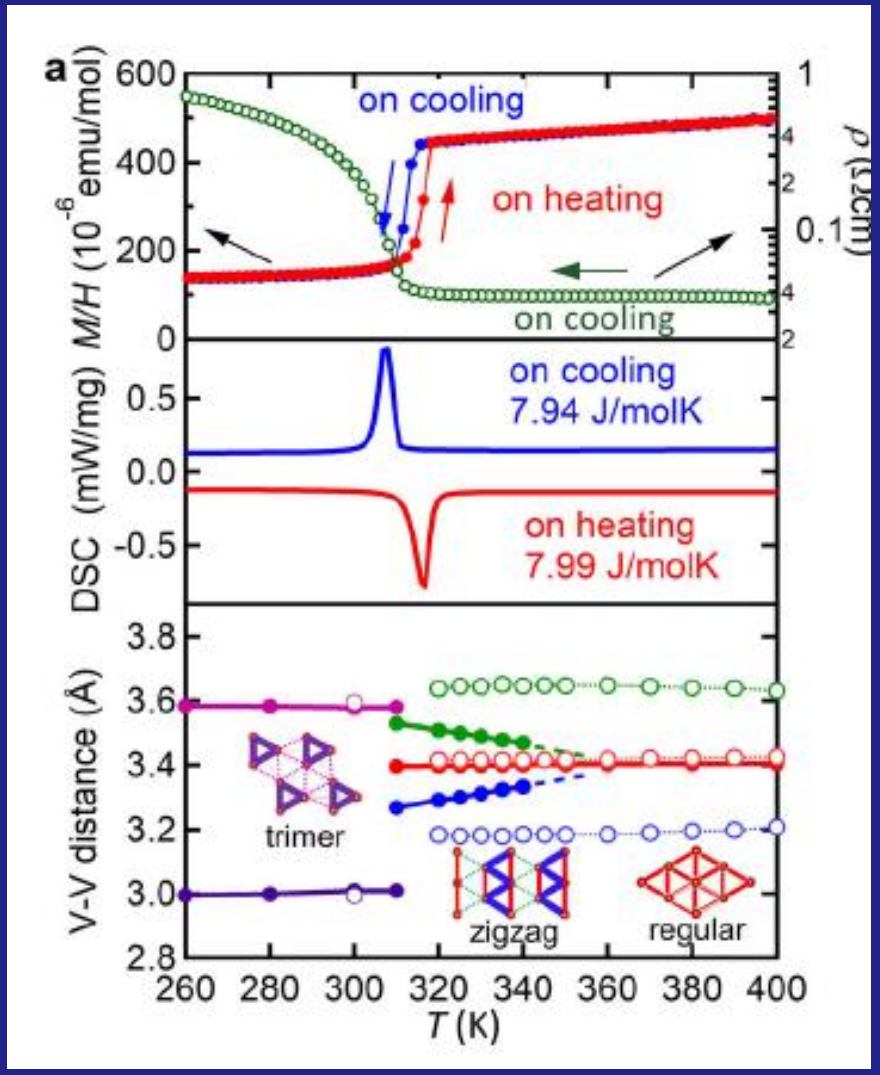

# Orbitally induced Peierls description of trimerization

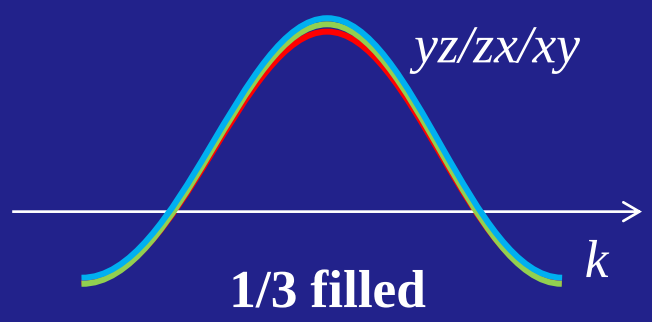


**$yz$ → 1/3 fillled 1D band along $(1/2,\sqrt{3}/2)$**

**$zx$ → 1/3 fillled 1D band along $(1/2,-\sqrt{3}/2)$**

**$xy$ → 1/3 fillled 1D band along (1,0)**

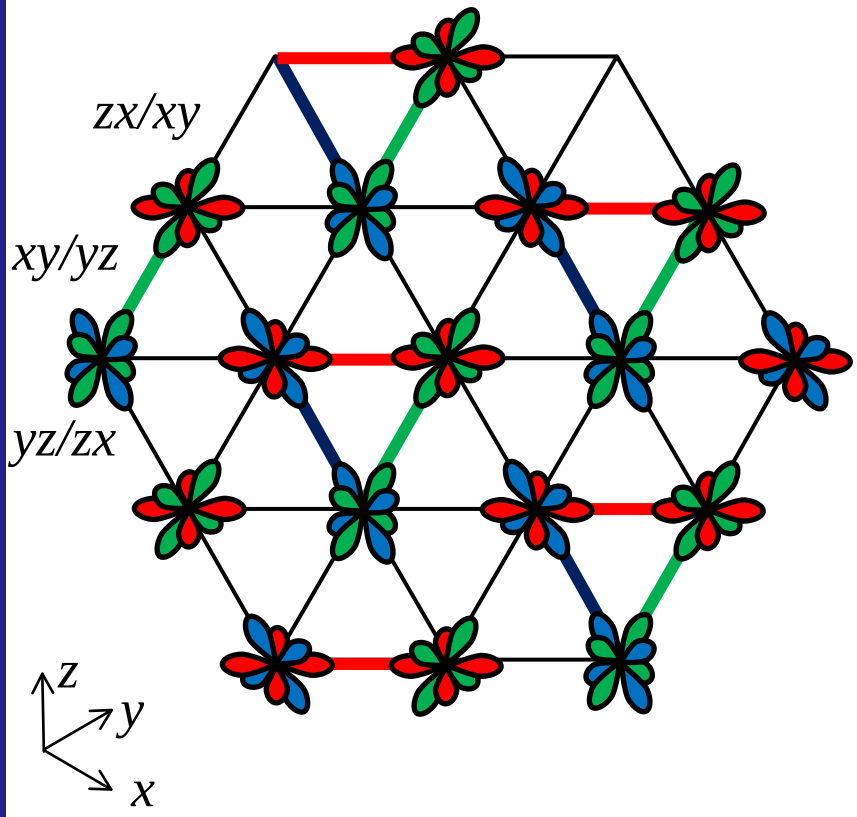


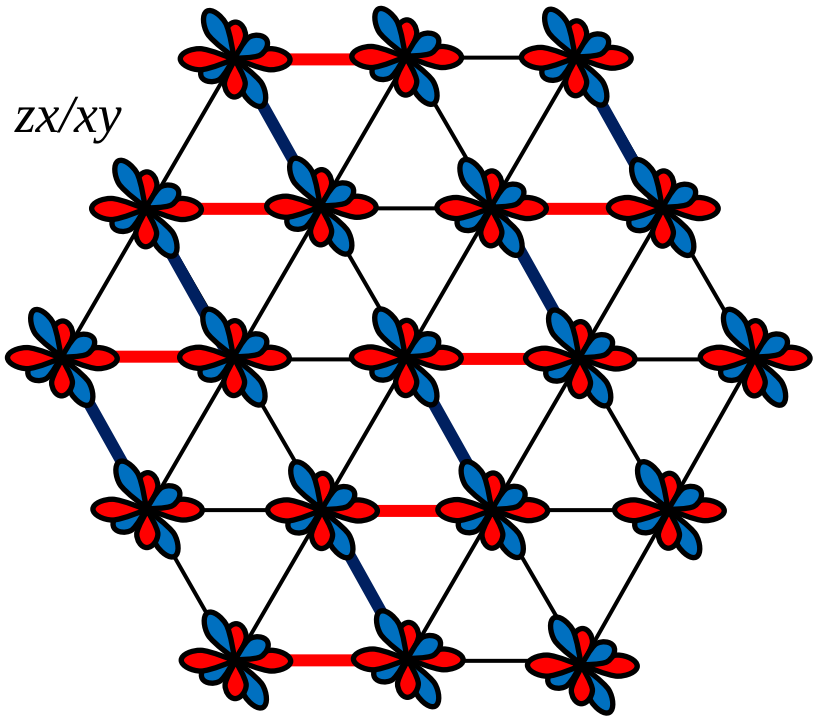

# $Li_2RuO_3$ (Honeycomb lattice)

Y. Miura *et al.*, J. Phys. Soc. Jpn. **76**, 033705 (2007).

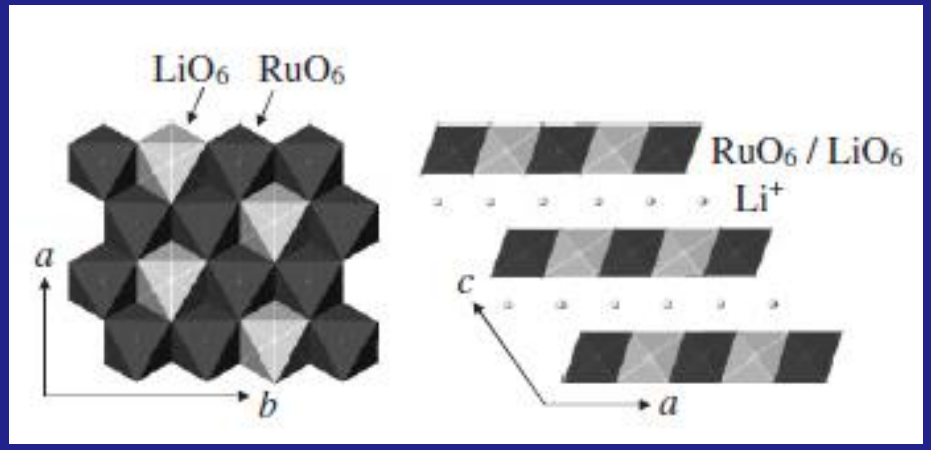


$Ru^{4+}$ ($d^4$)

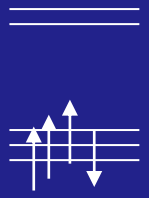

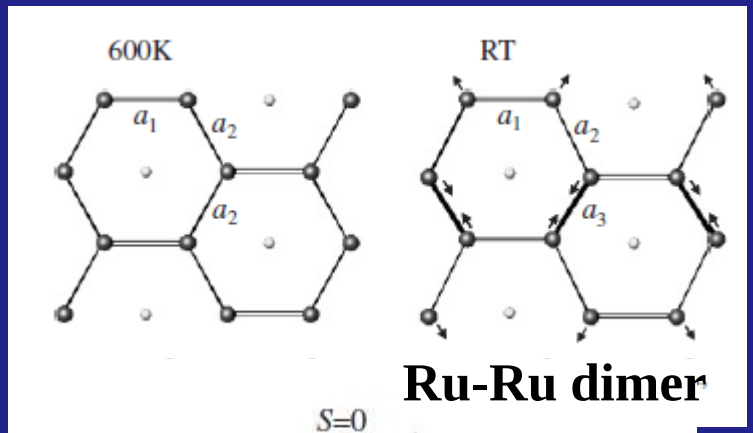


**Ru-Ru dimer**

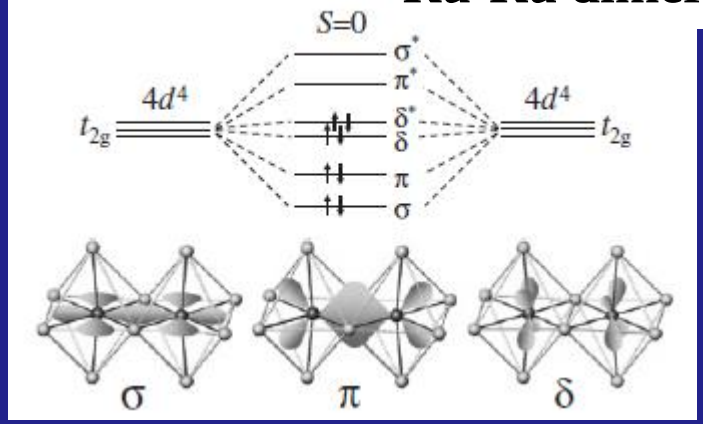


**nonmagnetic insulator** < 540 K

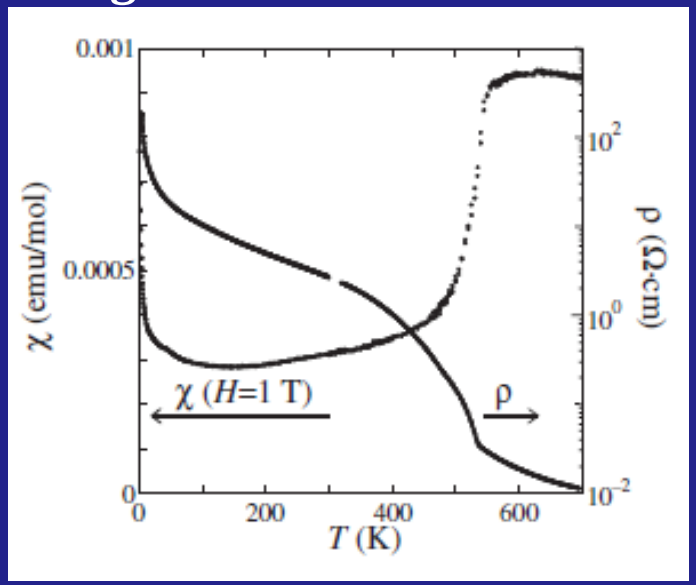


S.V. Streltsov and D.I. Khomskii, PNAS. 113, 10491 (2016)

# Orbitally induced dimerization

$MgVO_3$

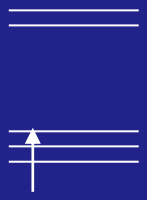

H. Yamamoto *et al.*,
J. Am. Chem. Soc. 144, 1082 (2022).

$RuCl_3$ (under pressure)

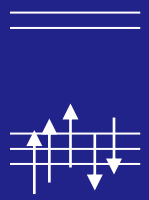

G. Bastien *et al.*,
Phys. Rev. B 97, 241108(R) (2018).

$Li_2RuO_3$

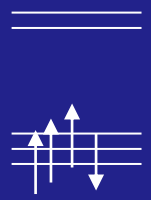

Y. Miura *et al.*,
J. Phys. Soc. Jpn. **76**, 033705 (2007).

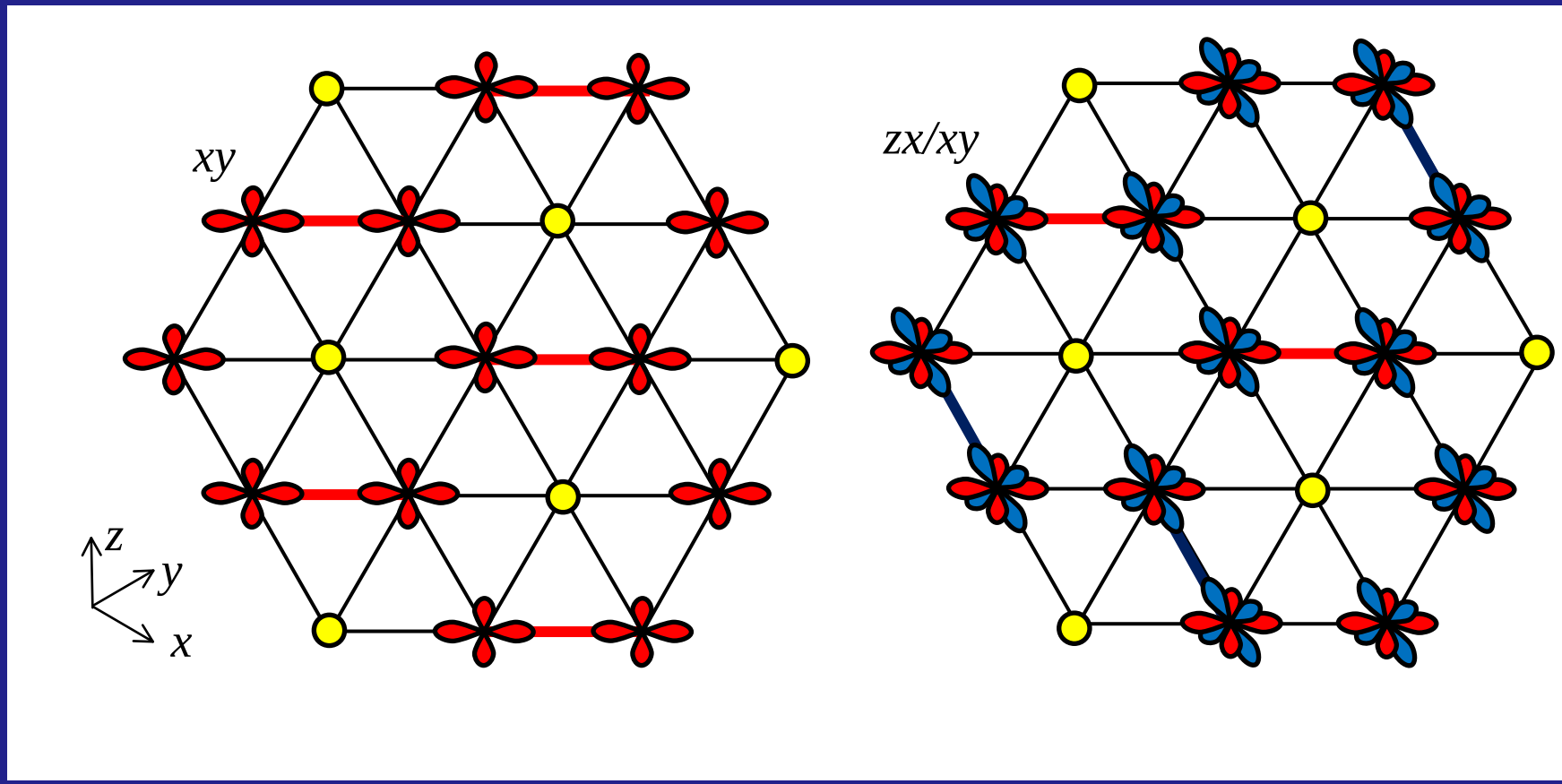

# Orbitally induced trimerization

$Li_2RuO_3$

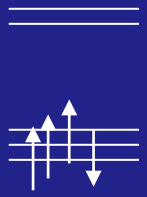

Y. Miura *et al.*,
J. Phys. Soc. Jpn. **76**, 033705 (2007).

$TcCl_3$

F. Poineau *et al.*,
Inorg. Chem. 51, 4915 (2012).

$MoCl_3$

H. Schäfer ae al.,
Z. Anorg. Allgem. Chem. 353, 281 (1967).

double bond

triple bond

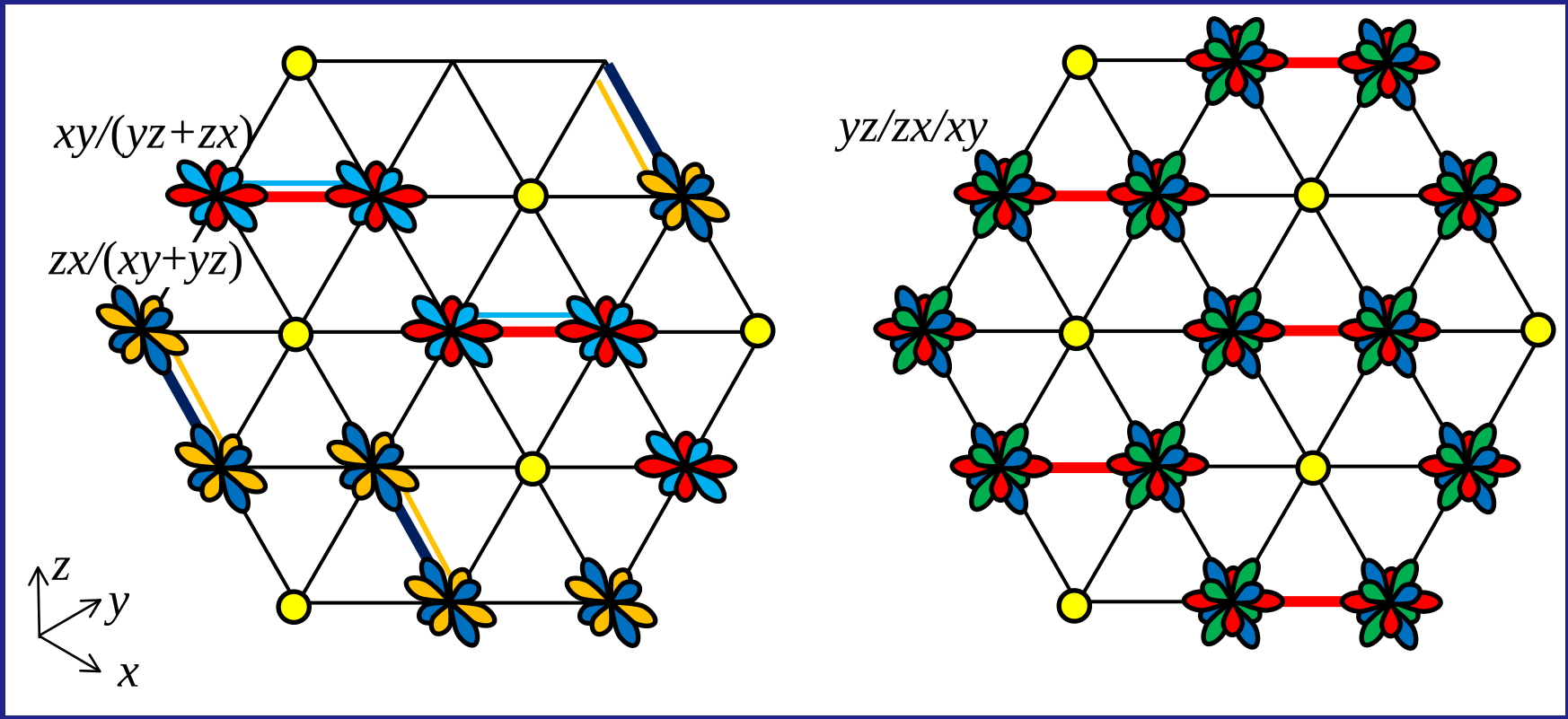

# $Na_2Ti_3Cl_8$ (kagome lattice)

D.J. Hinz, G. Meyer, T. Dedecke, and W. Urland, Angew. Chem., Int. Ed. Engl. 34, 71 (1995).

$Ti^{2+}$

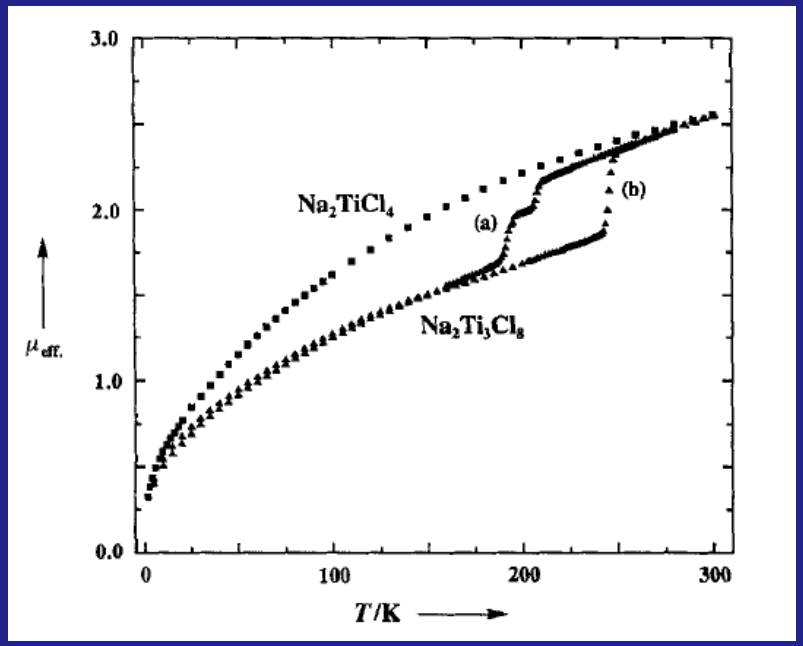


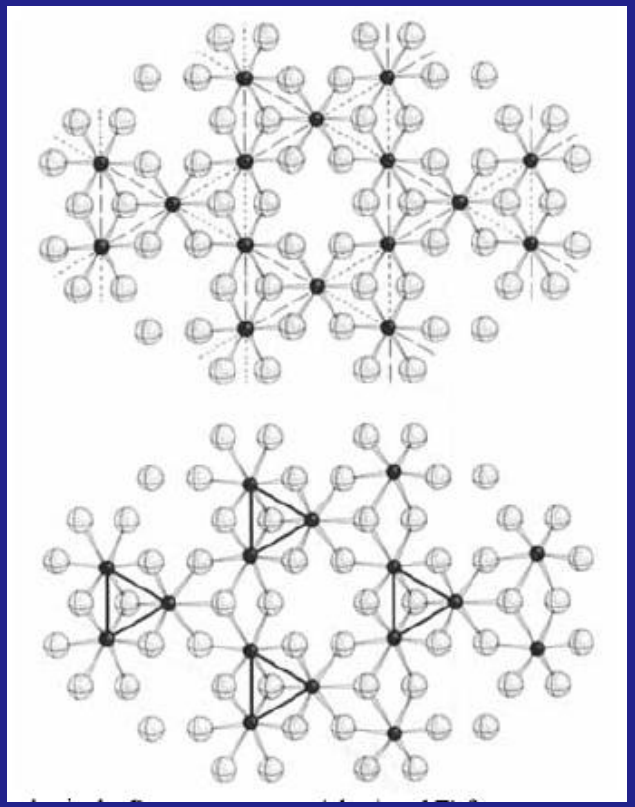

Ti-Ti bond length 3.7 Å →3.0 Å

Spin-lattice coupling theory

A. Paul, C.M. Chung, T. Birol, and H.J. Changlani, Phys. Rev. Lett. 124, 167203 (2020)

Orbital induced trimerization

D.I. Khomskii, TM, and S.V. Streltsov, Phys. Rev. Lett. 127, 049701 (2021)

# $Zn_2Mo_3O_8$ and Li $Zn_2Mo_3O_8$ (kagome lattice)

J.P. Sheckelton, J.R. Neilson, D.G. Soltan, and T.M. McQueen, Nat. Mater. 11, 493 (2012).

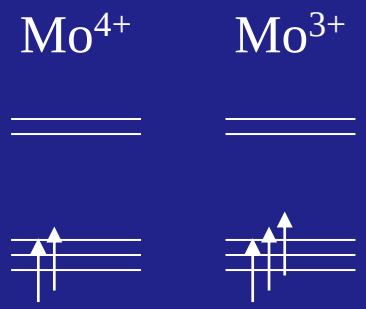


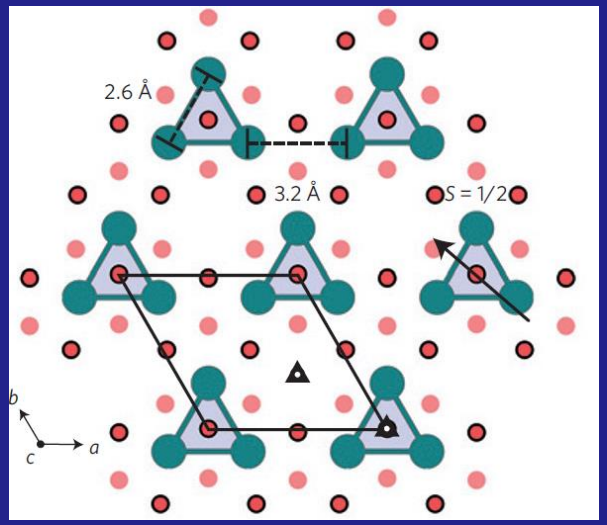


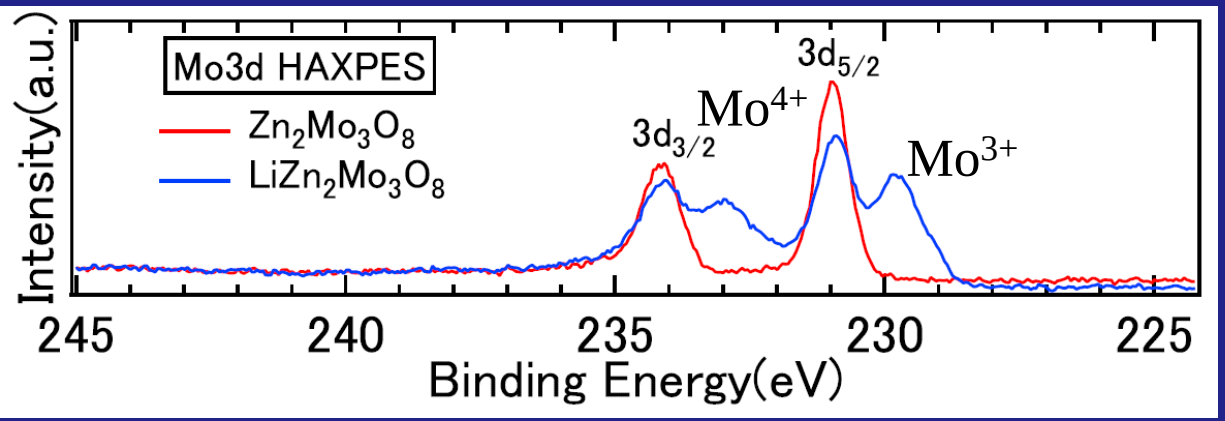


R. Nakamura *et al.*, unpublished.

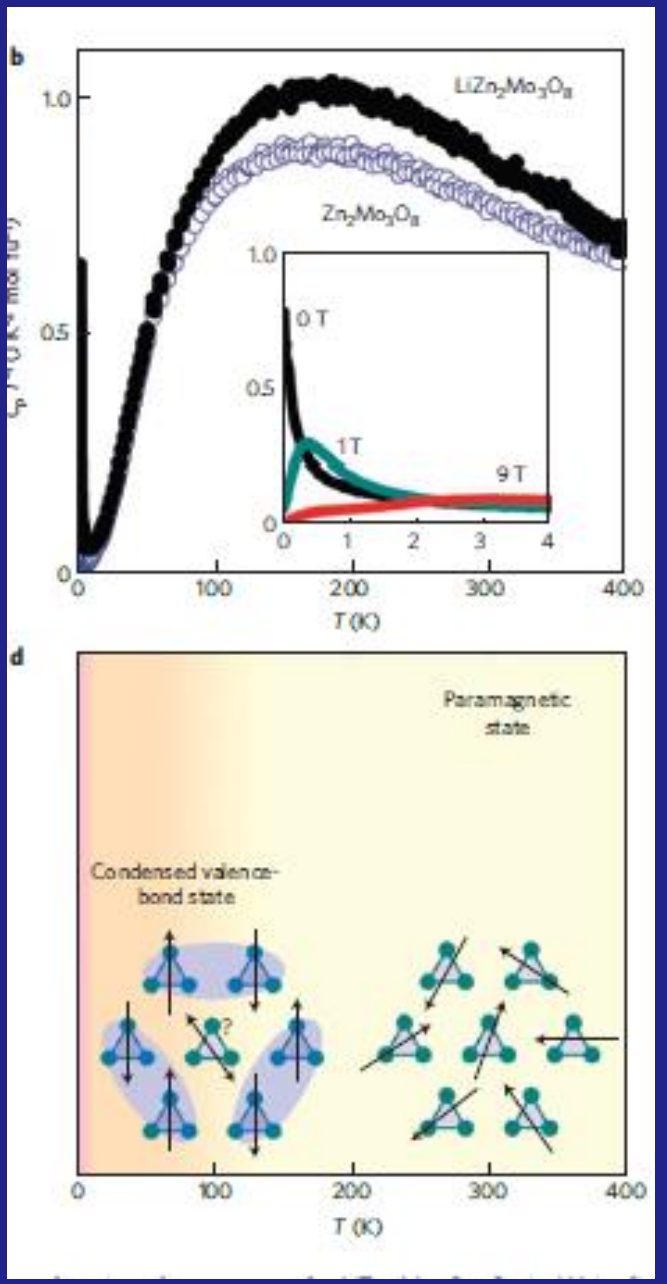

# Orbitally induced trimerization

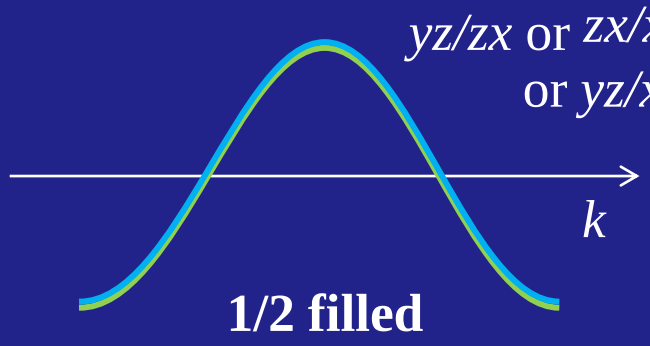


**yz → 1/2 fillled 1D band along** $(1/2,\sqrt{3}/2)$

**zx → 1/2 fillled 1D band along** $(1/2,-\sqrt{3}/2)$

**xy → 1/2 fillled 1D band along (1,0)**

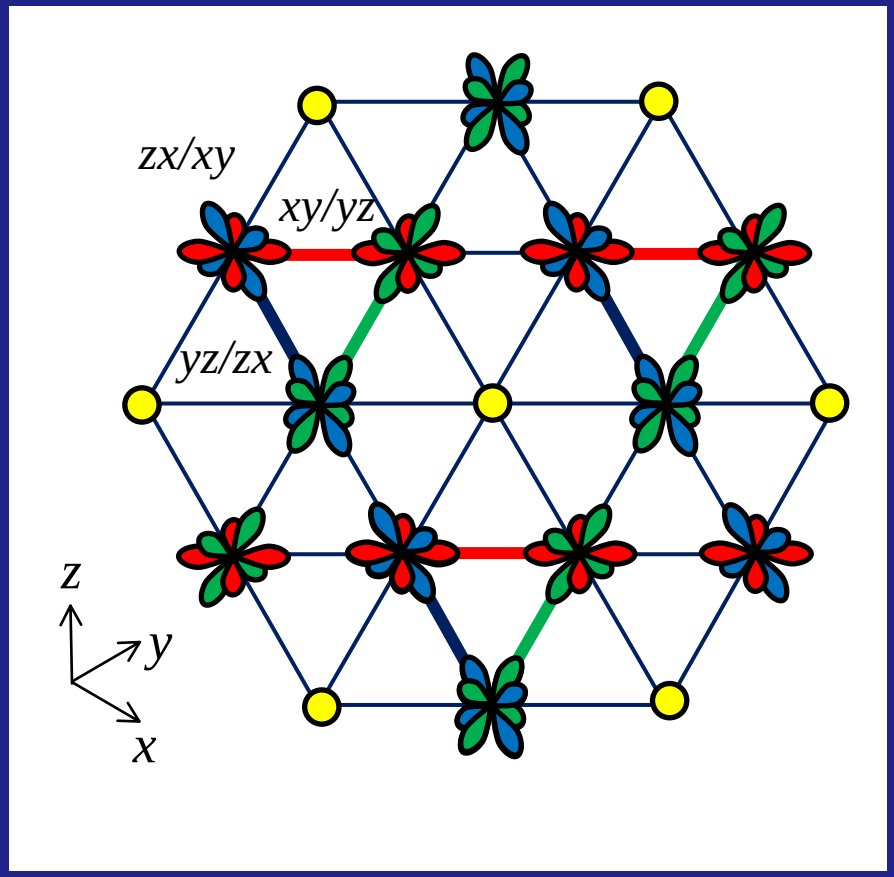

# Summary

**Orbitally induced Peierls transition for $t_{2g}$ electron system:**
**Band Jahn-Teller effect (or local orbital order)**
**Peierls transition (or local singlet bond formation)**

**pyrochlore lattice: $CuIr_2S_4$, $LiRh_2O_4$, $AlV_2O_4$, $MgTi_2O_4$**
**triangular lattice: $IrTe_2$, $LiVS_2$, $LiVO_2$, $NaTiO_2$**
**honeycomb lattice: $MgVO_3$, $Li_2RuO_3$, $TcCl_3$, $MoCl_3$**
**kagome lattice: $Na_2Ti_3Cl_8$, $Zn_2Mo_3O_8$**

**orbital restrictive case: charge order follows orbital order only $LiRh_2O_4$ ?**
**orbital selective: orbital order is selected to optimize charge order**

**Acknowledgement: Prof. D. I. Khomskii, Prof. S. V. Streltsov, Prof. L. H. Tjeng, Prof. S. Nagata, Prof. H. Takagi, Prof. M. Nohara, Prof. Y. Okamoto**

Thank you very much for your attention!

**Future prospect:**
**Construction/Destruction of the multimers magnetic and/or optical control**
**Order/Disorder of the multimers bipolaron/tripolaron, pseudogap**
**Charge fluctuation in the multimer $Ti^{3+}$-$Ti^{4+}$, $Mo^{3+}$-$Mo^{4+}$-$Mo^{3+}$, multiferroics**